(69)

# I. SYNTHESIS OF BETA-LACTONES

# II. USE OF TEMPLATED HELICES TO DETERMINE ZIMM-BRAGG PARAMETERS

by

Janette H. Lee

B.A., Cornell University

(1989)

Submitted in Partial Fulfillment

of the Requirements for the

Degree of

Doctor of Philosophy

at the

Massachusetts Institute of Technology

September, 1997



Signature of Author_____
Department of Chemistry
July 22, 1997

Certified by_____
Professor Daniel S. Kemp
Thesis Supervisor

Accepted by_____
Professor Dietmar Seyferth
Chairman, Departmental Committee on Graduate Students

This doctoral thesis has been examined by a Committee of the Department of Chemistry as follows:

Professor Rick L. Danheiser_____
Chairman

Professor Daniel S. Kemp_____
Thesis Supervisor

Professor Scott C. Virgil_____

# I. SYNTHESIS OF BETA-LACTONES

# II. USE OF TEMPLATED HELICES TO DETERMINE ZIMM-BRAGG PARAMETERS

by

JANETTE H. LEE

Submitted to the Department of Chemistry
at the Massachusetts Institute of Technology on July 23, 1997
in partial fulfillment of the requirements for the degree of Doctor of Philosophy

## ABSTRACT

A procedure for the synthesis of beta-lactones from thioesters and the conversion of beta-lactones to the corresponding olefins on a large scale has been investigated, showing that the reactions occur in good yield.

Three simple N-terminal templated derivatives using AcHel(1) have been studied for potential intramolecular hydrogen bonding capacity. AcHel(1)Val-OH and the reduced template thiol corresponding to the Ac-Hel(1) template show no exceptional hydrogen bonding capacity. The derivative Ac-Hel(1)-NHMe shows intramolecular hydrogen bonding by NMR studies.

Three templated oligopeptides containing multiple contiguous lysines at the C-terminus (AcHel(1)Ala(5)LysAla(4)Lys(n)-NH2, n = 2 to 4) show that the charge effect of proximal lysines offset the stabilizing effect of a terminal lysine in alpha helices. Circular dichroism studies of Ac-Hel(1)Ala(4)LysAla(4)LysAla(n)-NH2, n = 2, 3 show per residue ellipticities within ranges reported in the literature.

The s-value of glycine has been determined from a series of short templated peptides (Ac-Hel(1)Ala(n-1)GlyAla(5-n)-NH2, n=2 to 5 to be ca. 0.22. The temperature dependent s-value of lysine and the passive role of alanine in stabilizing helices were determined from an independent analysis of AcHel(1)Ala(7)Lys-NH2 and AcHel(1)Ala(n-1)Gly(7-n)Lys-NH2, n = 1 to 7. The s-value of glycine from t/c ratios for this series at 25 deg C is ca. 0.20 to 0.35; the s-value of alanine was determined to be 1.00.

AcHel(1)Ala(7)Lys-NH2 and AcHel(1)Ala(n-1)Gly(7-n)Lys-NH2, n = 1 to 7 were also studied by circular dichroism.

Thesis Supervisor: Professor Daniel S. Kemp

Title: Professor of Chemistry

Acknowledgements

Prof. Rick Danheiser taught me some interesting modern synthetic chemistry both on the bench and on paper, some not mentioned in this thesis. His understanding of the art of organic synthesis is respected and to be emulated. I thank Prof. Danheiser for research assistantships (1990-1993) and the Department of Chemistry for teaching assistantships (1989-1990).

Prof. Daniel Kemp provided me with the opportunity to work on the alpha helix project. It is always a privilege to work for someone who is inspired. As a chemist of the Woodwardian era once said to me, Prof. Kemp is a chemist's chemist. I thank Prof. Kemp for research assistantships (1994-1997) and for his illuminating tangents and discussions.

I thank the MIT Spectroscopy Laboratory and the Biemann group for mass spec analyses.

Many graduate students and post-docs deserve gratitude: James Nowick of the Danheiser laboratory for his advice and discovery; Fari Firooznia, Kathy Lee (Sis), and other members of the Danheiser group for their support; Dave Chalfoun and Robert Carey for good advice; Z.Q. Li for his integrity and friendship ; Kim McClure and Peter Renold for incredible improvements in the Ac-Hel(1) synthesis; Evan Powers (Mr. E) for the things that will preclude his nomination to the Supreme Court; Peter R. for his friendship and translations; Jeff Rothman for being on our side of the thin line; Linda Szabo Shimizu for her friendship and support; Sam Tsang for helpful peptide advice; Tom Allen, Robert Bieganski, Katrin Groebke, Gene Hickey, Sherri Oslick, and Jonny Z. for group solidarity; Larry Williams for *sans papier* synthetic discussions on reserpine and other natural products; Kristian Kather for his *Herzlichkeit*; and Peter Wallimann for his singularity. I wish Evan and the newest line of offense (no pun intended) - Songpon 'Ace' Deechongkit , Kristian, Robert Kennedy, Peter W., and Larry - results, papers, personal happiness and good fortune.

Thanks to Bob K., Evan, Kristian, Peter W., Sam, and Larry (and Prof. Kemp) for proofreading parts of this thesis.

I cannot thank Prof. Jon C. Clardy of Cornell University - enough. The years spent in your laboratory were priceless. Thanks. I am also mindful of the counsel and friendship of many of the graduate students of that era, though there are too many to name. But the scoundrels know who they are.

A knowing glance is cast to Lisa 'Sunshine' Wang, a fine adventurer and friend, whose unswerving dedication to chemistry is admirable.

I appreciate the support of my brother, Michael, and I thank him for not getting himself killed riding his donorcycle or while skydiving.

Kit Sheung Lee, my Mom, has given me more love, care and support than I could ever qualify for. I am very grateful to her for my sound, yet unfettered, upbringing. Until I raise a 'demure' daughter of my own, I am sure that I shall not fully appreciate her sacrifices and her wisdom. Thanks, Mom. See the next page.

The last four people mentioned have each been like a Rock of Gibraltar, but there is yet another and that is chemistry itself.

To

Mom

and

C., M.N. and A.,

*the Untouchables*

## Table of Contents

Part I



Part II

# Chapter 1

## Synthesis of β-Lactones and Alkenes via Thiol Esters

## Introduction

The susceptibility of the 2-oxetanone system to ring opening by nucleophiles contributes to the biological activity of many β-lactone natural products. By the same token this lability is responsible for the scarcity of such examples in the literature until the 1980s.[1] Anisatin and neoanisatin are the two most powerful neurotoxins of plant origin.[2] The trans disubstituted β-lactones ebelactones A and B,[3] esterastin,[4] L-659,699 (Antibiotic 1233A),[5] lipstatin, tetrahydrolipstatin (Orlistat®),[6] panclicin D,[7] and valilactone[8] irreversibly inhibit various enzymes in the cholesterol biosynthetic and fatty acid metabolic pathways.

---

[1] a) Lowe, C.; Vederas, J. C. *Org. Prep. Proced. Int.* **1995**, *27*, 305. b) Pommier, A.; Pons, J.-M. *Synthesis* **1995**, 729. c) Pmmier, A.; Pons, J.-M. *Synthesis* **1990**, 441.

[2] (a) Yang, C.-S.; Hashimoto, M.; Baba, N.; Takahashi, M.; Kaneto, H.; Kawano, N.; Kuono, I. *Chem. Pharm. Bull.* **1990**, *38*, 291. (b) Niwa, H.; Nisiwaki, M.; Tsukada, I.; Ishigaki, T.; Ito, S.; Wakamatsu, K.; Mori, T.; Ikagawa, M.; Yamada, K. *J. Am. Chem. Soc.* **1990**, *112*, 9001. (c) Kouno, I.; Mori, K.; Akiyama, T.; Hashimoto, M. *Phytochemistry* **1991**, *30*, 351. (d) Niwa, H.; Yamada, K. *Chem. Lett.* **1991**, 639. (e) Kouno, I.; Hashimoto, M.; Enjoji, S.; Takahashi, M.; Kaneto, H.; Yang, C.-S. *Chem. Pharm. Bull.* **1991**, *39*, 1773.

[3] (a) Umezawa, H.; Aoyagi, T.; Uotani, K.; Hamada, M.; Takeuchi, T.; Takahashi, S. *J. Antibiot.* **1980**, *33*, 1594. (b) Uotani, K.; Naganawa, H.; Kondo, S.; Aoyagi, T.; Umezawa, H. *J. Antibiot.* **1982**, *35*, 1495. (c) Total synthesis of ebelactone A: Paterson, I; Hulme, A. N. *Tetrahedron Lett.* **1990**, *31*, 7513.

[4] (a) Umezawa, H.; Aoyagi, T.; Hazato, T.; Uotani, K.; Kojima, F.; Hamada, M.; Takeuchi, T. *J. Antibiot.* **1978**, *31*, 639. (b) Kondo, S.; Uotani, K.; Miyamoto, M.; Hazato, T.; Naganawa, N.; Aoyagi, T.; Umezawa, H. *J. Antibiot.* **1978**, *31*, 797.

[5] (a) Aldridge, C. C.; Giles, D.; Turner, W. B. *J. Chem. Soc. C* 1971, 3888. (b) Greenspan, M. D.; Lo, C. L.; Chen, J. S.; Alberts, A. W.; Hunt, V. M.; Chang, M. N.; Yang, S. S.; Thompson, K. L.; Chiang, Y. P.; Chabala, J. C.; Monaghan, R.L.; Schwartz, R. E.. *Proc. natl. Acad. Sci. U.S.A.* , **1987**, *84*, 7488. (c) Omura, S.; Toma, H.; Kumagai, H.; Greenspan, M. D.; Yodkovitz, J.B.; Chen, J. S.; Alberts, A. W.; Martin, I; Mochales, S.; Monaghan, R.L.; Chabala, J. C.; Schwartz, J. C.; Patchett, A. A. *J. Antibiot.* **1987**, *40*, 1356. (d) Chaing, Y. P.; Chang, M. N.; Yang, S. S.; Chabala, J. C.; Heck, J. V. *J. Org. Chem.* **1988**, *53*, 4599. (e) Mori, K.; Takahashi, Y. *Liebigs Ann. Chem.* **1991**, 1057.

[6] (a) Weibel, E. K.; Hadvary, P.; Hochuli, E.; Kupfer, E.; Lengsfeld, H. *J. Antibiot.* **1987**, *40*, 1081. (b) Hochuli, E.; Kupfer, E.; Maurer, R.; Meister, W.; Mercadal, Y.; Schmidt, K. *J. Antibiot.* **1987**, *40*, 1086. (c) Barbier, P.; Schneider, F.; Widmer, U. *Helv. Chim. Acta* **1987**, *70*, 1412. (d) Barbier, P.; Schneider, F. *J. Org. Chem.* **1988**, *53*, 1218. (e) Synthesis of (-)-tetrahydrolipstatin: Pons, J.-M.; Kocienski, P. *Tetrahedron Lett.* **1989**, *30*, 1833. (f) Fleming, I.; Lawrence, N. J. *Tetrahedron Lett.* **1990**, *31*, 3645.

[7] Yoshinarik, K.; Aoki, N.; Ohtsuka, T.; Nakayama, N.; Itezono, Y.; Mutoh, M.; Watanabe, J.; Yokose, K.; *J. Antibiot.* **1994**, *47*, 1376.

[8] (a) Kitahara, M.; Asano, M.; Naganawa, H.; Maeda, K.; Hamada, M.; Aoyagi, T.; Umezawa, H.; Iitaka, Y.; Nakamura, H. *J. Antibiot.* **1987**, *40*, 1647. (b) Bates, R. W.; Fernandez-Moro, R.; Ley, S. V. *Tetrahedron Lett.*, **1991**, *32*, 2651.

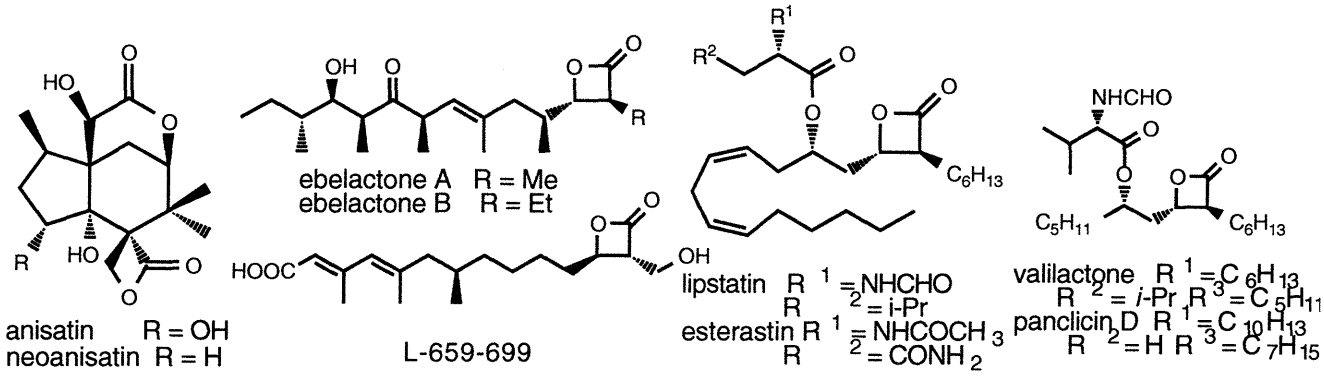


The cis disubstituted N-acylated α-amino β-lactones oxazolomycin,[9] curromycins (triedimycins) A and B,[10] obafluorin[11], and SQ 26,517[12] are antibacterial agents. In addition, the last four compounds display antitumor activity. The fused β-lactone lupeolactone[13] shows anticholesteremic activity. Though three other natural products with fused β-lactone rings have been isolated, their biological activities have not been reported.[1]

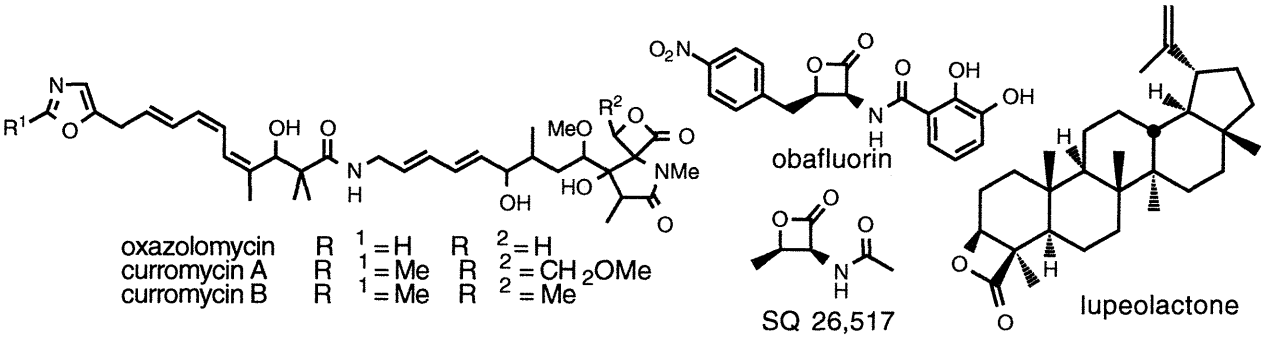


9 Mori, T.; Takahashi, K.; Kashiwabara, M.; Uemura, D.; Katayama, C.; Iwadare, S.; Shizuri, Y.; Mitomo, R.; Nakano, F.; Matasuzaki, A. *Tetrahedron Lett.* **1985**, *26*, 1073.

10 Ikeda, Y.; Kondo, S.; Naganawa, H.; Hattori, S.; Hamada, M.; Takeuchi, T. *J. Antibiot.* **1991**, *44*, 453.

11 (a) Wells, J. S.; Trejo, W. H.; Principe, P. A.; Sykes, R. B. *J. Antibiot.* **1984**, *37*, 802. (b) Tymiak, A. A.; Culver, C. A.; Malley, M. F.; Gougoutas, J. A. *J. Org. Chem.* **1985**, *50*, 5491.

12 Synthesis of SQ 26,517: (a) Parker, W. L.; Rathnum, M. L.; Liu, W.-C. *J. Antibiot.* **1982**, *35*, 900. (b) Pu, Y.; Martin, F. M.; Vederas, J. C. *J. Org. Chem.* **1991**, *56*, 1280. (c) Rao, M. N.; Holkar, A. G.; Ayyangar, N. R. *Chem. Commun.*, **1991**, 1007.

13 Kikuchi, H.; Tensho, A.; Shimizu, I.; Shiokawa, H.; Kuno, A.; yamada, S.; Fujiwara, T.; Tomita, K. *Chem. Lett.* **1983**, 603.

β-Lactones are also useful synthetic intermediates, mainly by ring opening, decarboxylation, and substitution via the enolate. The β-lactone ring is strained and can be opened by nucleophiles either at the acyl carbon or at the β-carbon (C4). Alkylations occur with soft nucleophiles. Alkylations and acylations occur with hard nucleophiles and are dependent on the substitution of the β-lactone. Ring opening of β-lactones with organocopper reagents or with Grignard reagents in the presence of a copper (I) catalyst[14] gives β-substituted propionic acids that have found applicability in terpene synthesis.[15] Ring opening with organocadmium[16] and organoaluminum reagents are also known, with the latter method having been utilized in the synthesis of a prostacyclin analog.[17] Vederas and coworkers have used organometallic reagents to open N-protected α-amino β -lactones and obtain useful rare amino acids.[18] Corey *et al.* have used the thiol group of a cysteine derivative to open a β-lactone intermediate in his improved synthesis of lactacystin.[19] Lithium enolates of β-lactones with only β-substituents react with electrophiles from the less sterically hindered side to form mainly trans substituted β-lactones.[20] Lithium enolates of trisubstituted β-lactones react with electrophiles to form mixtures containing predominantly cis products.[21] In addition to modifications of the ring itself, β-lactones can be

[14] (a) Normant, J. F.; Alexakis, A.; Cahiez, G. *Tetrahedron Lett.* **1980**, *21*, 935. (b) Sato, T.; Kawara, T.; Kawashima, M.; Fujisawa, T. *Chem. Lett.* **1980**, 571. (c) Kawashima, M.; Sato, T.; Fujisawa, T. *Tetrahedron* **1989**, *45*, 403.

[15] Fujisawa, T.; Sato, T.; Kawara, T.; Noda, A.; Obinata, T. *Tetrahedron Lett.* **1980**, *21*, 2553.

[16] Stuckwisch, C. G.; Bailey, J. V. *J. Org. Chem.* **1963**, *28*, 2362.

[17] Shinoda, M.; Iseki, K.; Oguri, T.; Hayasi, Y.; Yamada, S.-I.; Shibasaki, M. *Tetrahedron Lett.* **1986**, *27*, 87.

[18] (a) Arnold. L. D.; Kalantar, T. H.; Vederas, J. C. *J. Am. Chem. Soc.* **1985**, *107*, 7105. (b) Arnold, L. D.; Driver, J. C. G.; Vederas, J. C. *J. Am. Chem. Soc.*, **1987**, *109*, 4649. (c) Arnold, L. D.; May, R. G.; Vederas, J. C. *J. Am. Chem. Soc.* **1988**, *110*, 2237. (d) Pansare, S. V.; Vederas, J. C. *J. Org. Chem.* **1989**, *54*, 2311.

[19] Corey, E. J.; Reichard, G. A.; Kania, R. *Tetrahedron Lett.* **1993**, *34*, 6977.

[20] Mulzer, J.; de Lasalle, P.; Chucholowski, A.; Blaschek, U.; Brüntrup, G. *Tetrahedron* **1984**, *40*, 2211.

[21] Danheiser, R. L.; Nowick, J. S. *J. Org. Chem.* **1991**, *56*, 1176.

decarboxylated either thermally or under acidic conditions in high yield.[22] The thermal [2+2] cycloreversion occurs at 80 - 160 °C and is stereospecific, which is particularly useful for the preparation of highly substituted olefins. Electron-donating groups at the β-position promote the reaction while electron-withdrawing groups decrease the rate. A minimal effect is seen for substituents at the α-position. The reaction also proceeds faster in polar solvents. These observations support an intermediate with a partial positive charge at the C4 carbon. With 0.1 to 1.0 weight equiv silica gel as catalyst, decarboxylation proceeds below 100 °C with high stereospecificity. Acid-catalyzed decarboxylations lead not only to an increase in rate but to a greater proportion of trans olefins.[23] This non-stereospecific reaction proceeds via a zwitterionic intermediate in which the O-C4 bond is heterolytically cleaved and rotation about the C3-C4 bond occurs.[24] Due to the versatility of β-lactones as intermediates and their occurrence in biologically active natural products, many methods of synthesizing β-lactones have been reported. Dr. Nowick of the Danheiser laboratory discovered that β-lactones could be formed by the reaction of thiol esters and ketones or aldehydes. This chapter will utilize the method discovered in the Danheiser group and the known stereospecific thermal decarboxylation of β-lactones to provide a generally applicable *Organic Syntheses* procedure for the large scale synthesis of olefins. Before this new method of β-lactone synthesis is discussed, a brief presentation of earlier methods of β-lactone formation is appropriate.

---

[22] (a) Noyce, D. S.; Banitt, E. H. *J. Org. Chem.* **1966**, *31*, 4043. (b) Sultanbawa, M. U. S. *Tetrahedron Lett.* **1968**, 4569. (c) Tanabe, M.; Peters, R. H. *J. Org. Chem.* **1971**, *36*, 2403. (d) Adam, W.; Baeza, J.; Liu, J.-C. *J. Am. Chem. Soc.* **1972**, *94*, 2000. (e) Mageswaran, S.; Sultanbawa, M. U. S. *J. Chem. Soc., Perkin Trans. I* **1976**, 884. (f) Marshall, J. A.; Karas, L. J. *J. Am. Chem. Soc.* **1978**, *100*, 3615. (g) Mulzer, J.; Pointer, A.; Chucholowski, A; Bruntrup, G. *J. Chem. Soc., Chem. Commun,* **1979**, 52. (h) Luengo, J. I.; Koreeda, M. *Tetrahedron Lett.* **1984**, *25*, 4881.

[23] Mulzer, J.; Zippel, M. *Chem. Commun.* **1981**, 891.

[24] Mulzer, J.; Zippel, M. *Tetrahedron Lett.* **1980**, *21*, 751.

Perhaps the most widely used method of preparing β-lactones today is that by Adam *et al.*,[25] in which a carboxylic acid dianion reacts with an aldehyde or a ketone to form a β -hydroxy acid. The carboxylic acid is treated with an arenesulfonyl chloride and pyridine to form the mixed anhydride, which then undergoes lactonization.

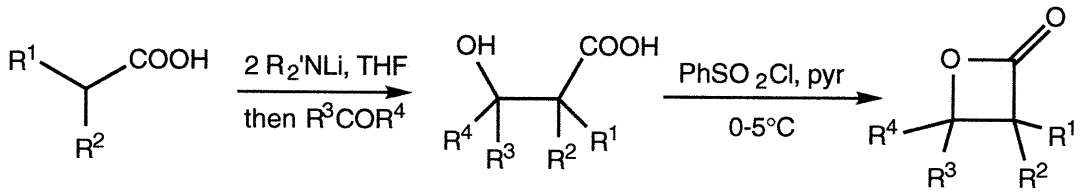


A variation from the Vederas group uses Seebach's imidazolidinone[26] titanium enolate to react with an aldehyde in the synthesis of (+)-obafluorin.[27] The resulting β-hydroxy acid is activated via the 4-bromophenylsulfonate of the carboxyl group and cyclized to form the cis substituted α-amino β-lactone, albeit in low yield.

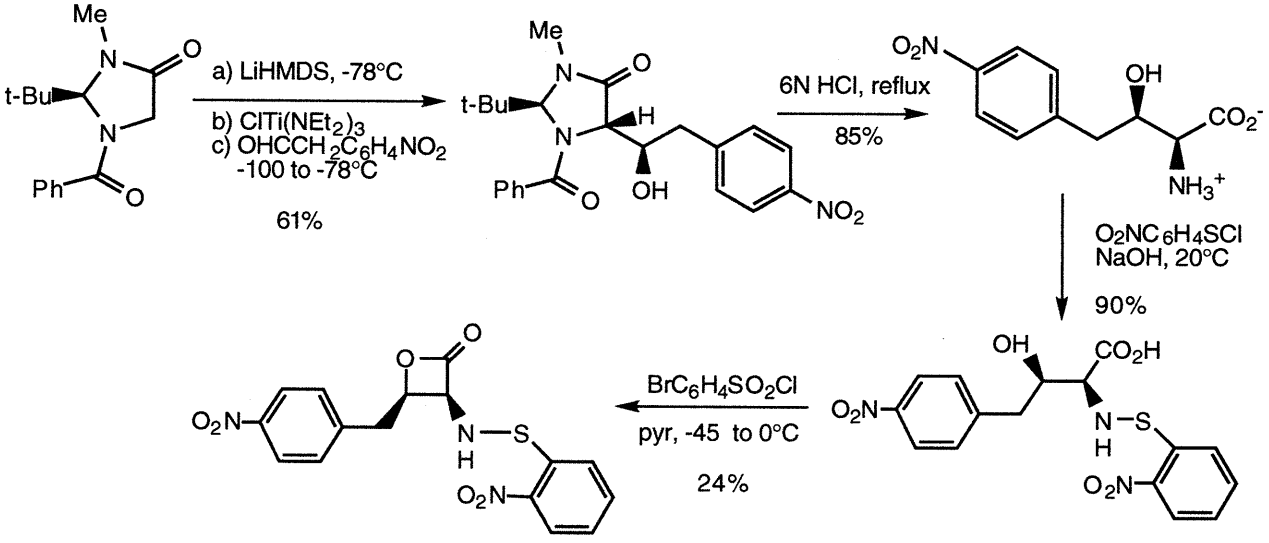


[25] Adam, W.; Baeza, J.; Liu, J.-C. *J. Am. Chem. Soc.* **1972**, *94*, 2000.
[26] Seebach, D.; Juaristi, E.; Miller, D. D.; Schickli, C.; Weber, T. *Helv. Chim. Acta* **1987**, *70*, 237.
[27] Lowe, C.; Pu, Y.; Vederas, J. C. *J. Org. Chem.*, **1992**, *57*, 10.

Cyclization of a carboxylic acid with various leaving groups positioned at the β-carbon include the use of halogens,[28] diazonium salts,[29] and activated hydroxyl groups (Mitsunobu-type cyclization)[30] as leaving groups. Other intramolecular routes to β-lactones include halolactonization of β,γ-unsaturated carboxylic acids,[31] photochemical cyclization of α, β-unsaturated carboxylic acids,[32] thermal Wolff rearrangements of carbenes derived from methyl trimethylsilyldiazoacetate,[33] and rhodium-catalyzed decomposition of methyl esters of α-diazo-β-keto carboxylic acids.[34]

Annulation routes to β-lactones include the addition of ketenes to carbonyl compounds under catalytic conditions,[35] and the reaction of lithium ynolates with carbonyl compounds.[36]

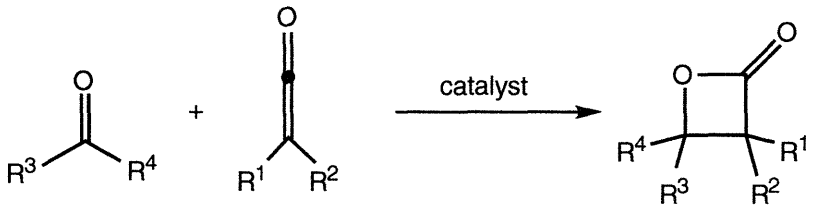


28 Einhorn, A. *Chem. Ber.* **1883**, *16*, 2208.

29 Testa, E.; Fontanella, L.; Cristiani, G. F.; Fava, F. *Liebigs Ann. Chem.* **1958**, *619*, 47. (b) Testa, E.; Fontanella, L.; Cristiani, G. F. *Liebigs Ann. Chem.* **1959**, *626*, 121. (c) Testa, E.; Fontanella, L.; Cristiani, G. F.; Gallo, G. *J. Org. Chem.* **1959**, *24*, 1928. (d) Testa, E.; Fontanella, L.; Cristiani, G. F.; Mariani, L. *Liebigs Ann. Chem.* **1961**, *639*, 166.

30 Mitsunobu, O. *Synthesis*, **1981**, 1.

*31 Comp. Org. Syn.*; Trost, B. M. Ed.; Pergamon Press, Inc.: New York, 1991; Volume 4; p. 368ff.

32 Chapman, O. L.; Adams, W. R. *J. Am. Chem. Soc.* **1968**, *90*, 2333.

33 Ando, W.; Sekiguchi, A.; Migita, T.; Kammula, S.; Green, M.; Jones, M., Jr. *J. Am. Chem. Soc.* **1975**, *97*, 3818.

34 Lee, E. ; Jung, K. W.; Kim, Y. S. *Tetrahedron Lett.* **1990**, *31*, 1023.

35 For reviews, see: a) Zaugg, H. E. *Org. React.* **1954**, *8*, 305. b) Kröper, H. In *Methoden der Organischen Chemie*; Müller, E., Ed.; Verlag: Stuttgart, 1963; Volume 6/2; pp 511-599. c) Etienne, Y.; Fisher, N. In *The Chemistry of Heterocyclic Compounds;* Weissberger, A., Ed.; Interscience: New York, 1964; Part 2; Chapter 6; pp 729-884. d) Searles, G. In *Comprehensive Heterocyclic Chemistry;* Katritsky, A. R. and Rees C. W. Eds.; Pergamon: Oxford, 1984; Volume 7; Chapter 5.13. e) *Ketenes*; Tidwell, T. T.; Wiley and Sons, Inc.: New York, 1995. f) Hyatt, J.; Raynolds, P. W. *Org. Reactions* **1994**, 45, 159.

36 (a) Schollkopf, U.; Hoppe, I. *Angew. Chem. Int. Ed. Engl.* **1975**, *14*, 765, (b) Hoppe, I.; Schöllkopf, U. *Liebigs Ann. Chem.* **1979**, 219. (c) Kowalski, C. J.; Fields, K. W. *J. Am. Chem. Soc.* **1982**, *104*, 321.

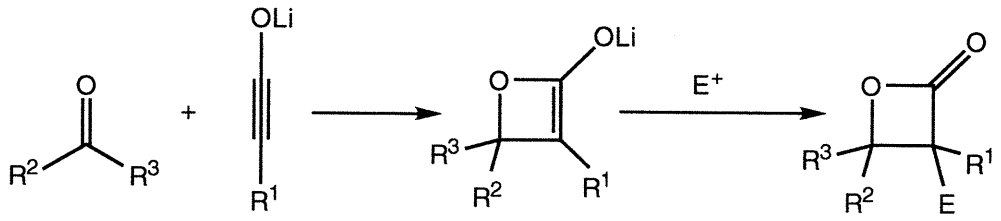


The palladium-catalyzed carbonylation has also been used to make α–vinyl and α-phenyl β-lactones.[37] Hydroxypalladation of ethylene and subsequent insertion of carbon monoxide has provided β-propiolactone.[38] The transformation[39] of alkenyl epoxides to α-alkenyl- β-lactones using $Fe_2(CO)_9$ has been utilized in Ley's synthesis of (-)-valilactone in good yield.[40] Davies has used an iron acyl complex in an aldol condensation, furnishing the β-lactone upon decomplexation.[41]

Other means to β-lactones include ruthenium-catalyzed oxidation of oxetanes,[42] photooxidation of 2-alkoxyoxetanes,[43] and derivatization of diketene.[23]

Several syntheses of α-alkylidene β-lactones have been reported recently: including reaction of an α, β-unsaturated carboxylic acid and singlet oxygen followed by treatment with triphenylphosphine;[44] rhodium-catalyzed carbonylation of propargyl alcohols;[45] reaction of cumulenones (generated by flash vapor pyrolysis of Meldrum's acid derivatives) with chloral;[46]

---

37 Cowell, A.; Stille, J. K. *J. Am. Chem. Soc.* **1980**, *102*, 4193.
38 Stille, J. K.; Divakaruni, R. *J. Am. Chem. Soc.* **1978**, *100*, 1303.
39 Annis, G. D.; Ley, S. V.; Self, C. R.; Sivaramakrishnan, R. *J. Chem. Soc., Perkin Trans. I* **1981**, 270.
40 Bates, R. W.; Fernandez-Moro, R. ; Ley, S. V. *Tetrahedron*, **1991**, *47*, 9929.
41 Case-Green, S. C.; Davies, S. B.; Hedgecock, C. J. R. *Synlett* **1991**, 781.
42 Renzoni, G. E.; Yin, T.-K.; Miyake, F.; Borden, W. T. *Tetrahedron* **1986**, *42*, 1581.
43 Schroeter, S. H. *Tetrahedron Lett.* **1969**, 1591.
44 (a) Adam, W.; Hasemann, L.; Prechtl, F. *Angew. Chem. Int. Ed. Engl.* **1988**, *27*, 1536. (b) Adam, W.; Hasemann, L. *Chem. Ber.* **1990**, *25*, 1697.
45 Matsuda, I; Ogiso, A.; Sata, S. *J. Am. Chem. Soc.* **1990**, *112*, 6120.
46 (a) Chickh, A. B.; Pommelet, J.-C.; Chuche, J. *J. Chem. Soc., Chem. Commun.* **1990**, 615.

and from α-alkylidene-β-hydroxy carboxylic acids via more conventional means.[47]

Masamune has used thiol esters and aldehydes or ketones to form β-hydroxy thiol esters, followed by treatment with 2 equiv mercury (II) methanesulfonate and $Na_2HPO_4$ to effect cyclization.[48]

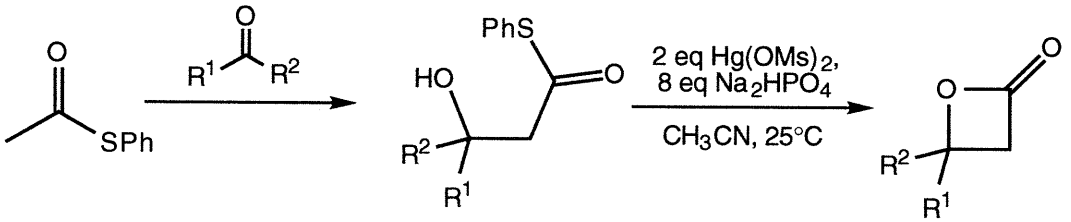


The route investigated in the Danheiser laboratory, and first reported in 1991,[21] involves the condensation of a thiol ester enolate with an aldehyde or ketone to form a β-hydroxy thiol ester alkoxide intermediate, which cyclizes to the β-lactone upon warming.

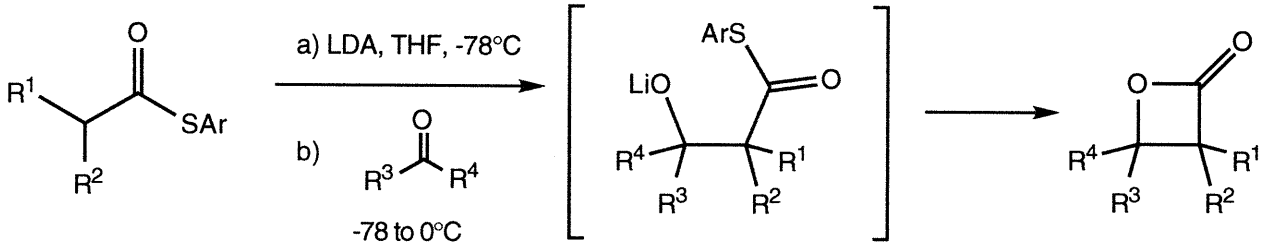


Thiol esters are easily prepared from acid chlorides in high yield.[49] Treatment of thiol esters with 1 equiv of LDA in THF at -78 °C gives the corresponding enolates, which can react with ketones or aldehydes at -78 °C. Wemple and coworkers observed that only β-hydroxy thiol esters were isolated from the reaction mixture, due to quenching at low temperature.[50] Dr. Nowick

[47] Campi, E. M.; Dyall, K.; Fallon, G.; Jackson, W. R.; Perlmutter, P.; Smallridge, A. J. *Synthesis*, **1990**, 855.
[48] Masamune, S.; Hayase, Y.; Chan, W. K.; Sobczak, R. L. *J. Am. Chem. Soc.* **1976**, *98*, 7874.
[49] a) Reißig, H.-U.; Scherer, B. *Tetrahedron Lett.* **1980**, *21*, 4259. b) Dellaria, Jr., J. F.; Nordeen, C.; Swett, L. R. *Syn. Commun.* **1986**, *16*, 1043.
[50] Wemple, J. *Tetrahedron Lett.* **1975**, 3255.

discovered, however, that the aldolate could be cyclized by warming the reaction mixture to *ca.* 0 °C. Although closely related to the route of Masamune, our method is a one-pot reaction that also occurs in high yield, but avoids the use of toxic mercury salts.

In the new β-lactone synthesis, it has been found that cyclization occurs best if the thiol ester is a thiophenol (or substituted thiophenol) ester. Reactions using S-ethyl ethanethioate fail to cyclize. In addition, it has been found that β-branching in the thiol ester leads to lower yields with ketones, though not with aldehydes. The lower yield, however, may be increased in these cases by utilizing the 2,6-dimethylbenzenethiol ester (see Table 1.1, entry 3).

With regard to the ketone or aldehyde component, ketones may be added to the thiol ester enolates neat, whereas aldehydes must be added as a precooled solution in THF due to reaction of aldolate with unreacted aldehyde. Also, α, β-unsaturated ketones cannot be used in this procedure due to extensive polymerization and other side reactions.

Stereochemically, the trans substituted β-lactones are favored, due most likely to the rapid reversibility of the aldol condensation and to the faster cyclization rate of the aldolate that leads to the less sterically hindered trans substituted tetrahedral intermediate, relative to the diastereomeric aldolate. Only one anomalous case has been observed, in which S-phenyl 3-methylbutanethioate and *n*-octanal react to give the β-lactone with a cis to trans ratio of 3 : 1, however, this preference can be reversed by using the 2,6-dimethylphenyl thiol ester (Table 1.1, entry 8).

β-Lactones with up to three or four substituents can be obtained in fair to excellent yields, including heteroatom substitutents. Although some sterically encumbered β-lactones form only in low yield, this problem can be circumvented by synthesis of a less substituted β-lactone followed by reaction of the corresponding β-lactone enolate and various electrophiles. In our procedure

alkenes with high boiling points are formed from the corresponding β-lactones by refluxing in benzene or cyclohexane in the presence of 1 weight equiv silica gel. Alkenes with lower boiling points (< 200 °C) are obtained by kugelrohr distillation of the β-lactone in the presence of 0.1 weight equiv silica gel, distilling the alkene as it forms.

The overall procedure provides a convenient synthesis of substituted alkenes, comparing favorably with even the classic Wittig and Julia-Lythgoe reactions in terms of yield, stereoselectivity, cost, and ease of byproduct removal.[51]

[51] For related work from the Danheiser group see a) Danheiser, R. L.; Choi, Y. M.; Menichincheri, M.; Stoner, E. J. *J. Org. Chem.* **1993**, *58*, 322. b) Danheiser, R. L.; Lee, T. W.; Menichincheri, M.; Brunelli, S.; Nishiuchi, M. Synlett **1997**, 469.

Table 1.1 Preparation of β-Lactones via Thiol Esters

| entry | carbonyl compound | thiol ester | β-lactone | % isolated yield |
|---|---|---|---|---|
| 1 | cyclohexanone | $CH_3COSPh$ | 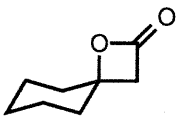 | 86 |
| 2 | cyclohexanone | $CH_3CH_2COSPh$ | 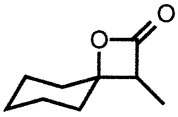 | 92 |
| 3 | cyclohexanone | $(CH_3)_3CHCH_2COSPh$ | 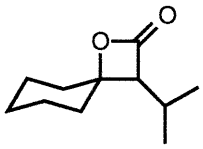 | 48, 72 [a] |
| 4 | 6-methyl-5-hepten-2-one | $CH_3CH_2CH_2COSPh$ | 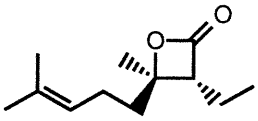 | 84 |
| 5 | benzaldehyde | $t\text{-}BuCH_2COSPh$ | 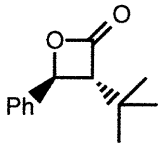 34 : 1 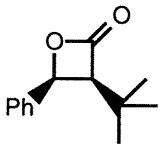 | 85 |
| 6 | n-octanal | $(CH_3)_2CHCOSPh$ | 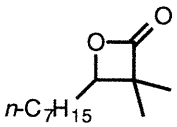 | 54 |
| 7 | n-octanal | $CH_3CH_2COSPh$ | 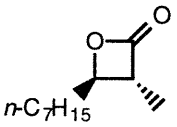 2.5 : 1 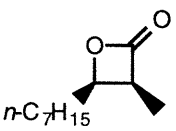 | 42 |
| 8 | n-octanal | $(CH_3)_2CHCH_2COSPh$ | 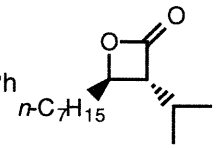 1 : 3 (5 : 1)[a] 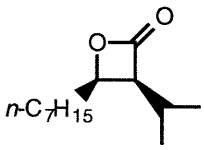 | 66 |

[a] obtained using the 2,6-dimethylphenyl thiol ester

## Results

The method discovered in the Danheiser group of preparing β-lactones and alkenes is applicable to a variety of substrates, and was adapted into an *Organic Syntheses* procedure. Such a procedure would be checked, and thus more attractive to organic chemists interested in synthesizing β-lactones or alkenes. Such a procedure would also demonstrate the applicability of our method on a large (*ca.* 0.1 mol) scale. The desired qualities of the thiol ester, β-lactone, and alkene that would be used were that they be non-volatile and easy to purify. Optimization studies were performed first on a small scale (*ca.* 2.5 mmol), and later on a larger scale.

Three different cases will be discussed: S-phenyl 3-phenyl-propanethioate, S-phenyl dodecanethioate, and S-phenyl decanethioate, each with 3-methyl-2-butanone. The three thiol esters were each prepared from the acid chloride in good yield and easily purified by distillation or recrystallization.

The general procedure for preparing the β-lactone involves formation of the thiol ester enolate at -78 °C for 30 min, neat addition of the ketone dropwise to the reaction mixture, stirring at -78 °C for 30 min, gradual warming of the reaction mixture to 0 °C over a period of 1.5 h, and then quenching with half-saturated ammonium chloride and workup with aqueous $K_2CO_3$. The yield of β-lactones using this procedure has typically been fair to excellent, and a yield of *ca.* 80-90% was desired while developing the *Organic Syntheses* procedure. The general procedure for preparing the alkene from pure β-lactone involves refluxing the β-lactone with one weight equiv silica gel in cyclohexane for 45 min. The yield of alkene using this procedure is typically very high, *ca.* 90%, and future decarboxylations were expected to occur in high yield as well.

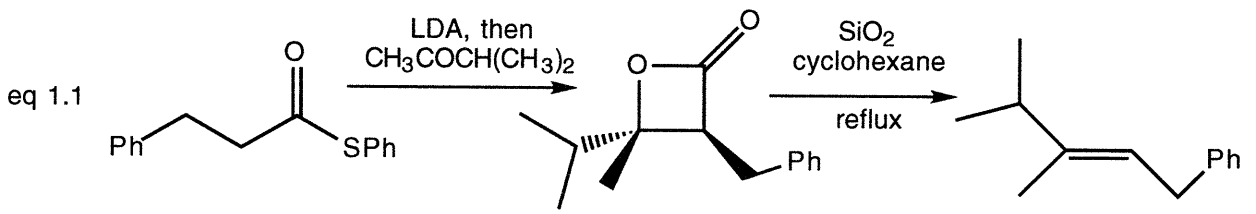


Initially, the reaction of S-phenyl 3-phenyl-propanethioate with 3-methyl-2-butanone (eq 1.1) was chosen as a suitable case. The thiol ester was available from commercially available hydrocinnamic acid in two steps via the acid chloride and purified by recrystallization from pentane. Purification of the β-lactone was complicated by a) the coelution of β-lactone with what we believe to be self-condensation product of the thiol ester (vide infra) during chromatography and b) the codistillation of β-lactone and self-condensation product upon kugelrohr distillation. An NOE experiment done on impure β-lactone showed the expected trans stereochemistry; the impurities did not interfere with the experiment. However, serendipitous but irreproducible formation of β-lactone crystals did occur after column chromatography and kugelrohr distillations. Although the β-lactone was crystalline in its pure state at room temperature, preferential crystallization of the thiol ester typically complicated purification by this method. Hence, subsequent small samples were obtained by column chromatography to remove most of the impurities followed by kugelrohr distillation and/or recrystallization.

Neither excess LDA nor use of lithium hexamethyldisilazide instead of LDA increased the purity of the product mixture. Slow addition of the thiol ester resulted in an insignificant difference. Reaction of the thiol ester enolate with 5 equiv of methyl iodide resulted in a *ca.* 9 : 1 ratio of methylated thiol ester to self-condensation product as determined by $^1$H NMR analysis. Little or no thiol ester remained, indicating relatively complete enolate formation. Carrying out the reaction at 0.5 M, rather than at 0.1 M, 0.25 M, 0.75 M or 1.0 M, resulted in less unreacted thiol

ester. Use of a slight excess of ketone did not change the composition of the product mixture. Use of cyclohexanone as the ketone component gave similar results, implying that 3-methyl-2-butanone was not an unusually problematic substrate.

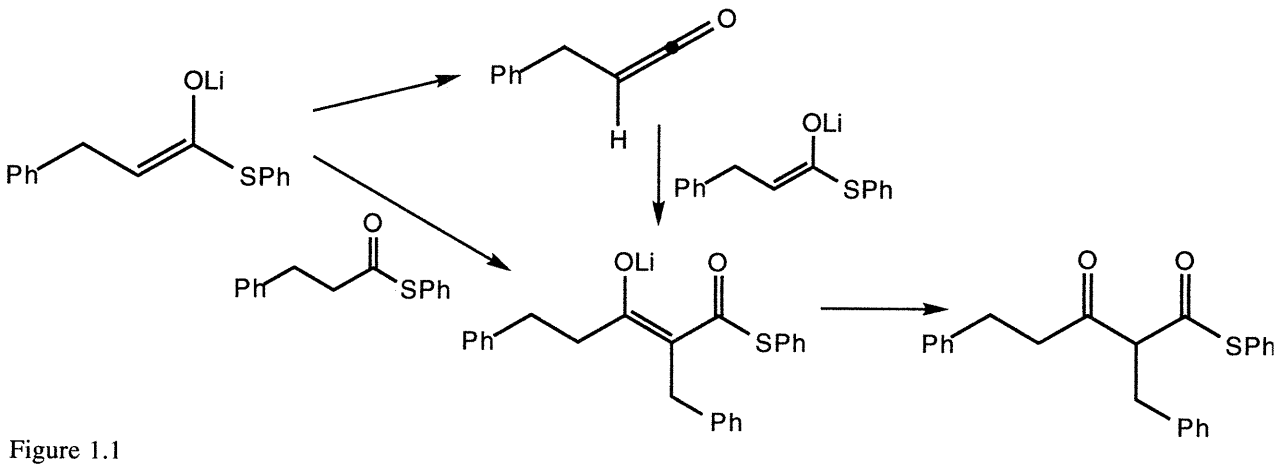


Figure 1.1

The troubleshooting process was obscured by the incapability to monitor amounts of purported self-condensation product due to formation of it on the tlc plate, via a ketene intermediate and/or a Claisen-like condensation (Fig. 1.1). Efforts to synthesize the self-condensation product itself were also complicated by separation problems.

Nevertheless using crystals of pure β-lactone, it was determined that the yield of the decarboxylation step using one weight equiv silica gel and refluxing in cyclohexane for 1 h was *ca.* 78%.

Thus, with no practical method of purification, the β-lactone was carried on to the alkene in crude form. An NOE experiment on crude alkene confirmed the expected trans stereochemistry of the major product. Several experiments were carried out to determine the time necessary for decarboxylation of crude β-lactone using various amounts of silica gel. Decreasing the amount of silica gel required increased reaction times and in some cases use of 0.1 weight equiv of $SiO_2$ resulted in incomplete decarboxylation even after 3 h of reflux. A convenient reaction time for

completion (1h) was achieved with one weight equiv silica gel. Yields of alkene ranged from *ca.* 40 to 60% from the thiol ester.

The modest yields and formation of significant amounts of self-condensation product was confirmed by Dr. Nowick. From his experiments, it was determined that: a) the alkene forms in 53% yield from the thiol ester with a 97:3 E:Z stereoselectivity; b) although previous cases have shown a small degree of self-condensation product (< 5%), the extent of its formation *(ca.* 20% yield) in this case is unprecedented.

eq 1.2

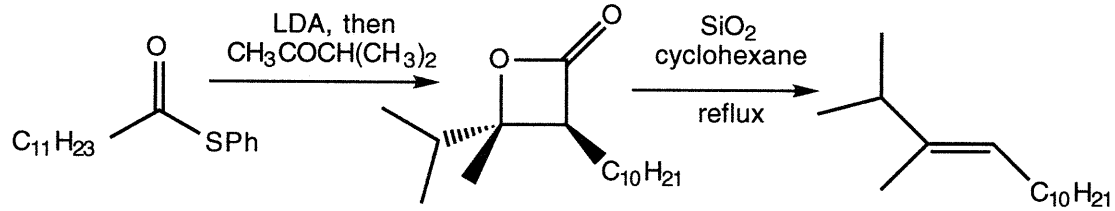


The second case investigated the reaction of S-phenyl dodecanethioate with 3-methyl-2-butanone (eq 1.2). It was necessary to add the thiol ester to the reaction mixture as a solution in THF due to crystallization at low temperature, a problem not seen in the 3-phenyl-propanethioate case. The $^1$H NMR of the crude β-lactone showed a ratio of *ca.* 5:1 of β-lactone to purported self-condensation product. The yield of alkene was 52% from the thiol ester. The significant amount of self-condensation product and the low temperature characteristics of the thiol ester rendered this specific case unsuitable for an *Organic Syntheses* procedure.

eq 1.3

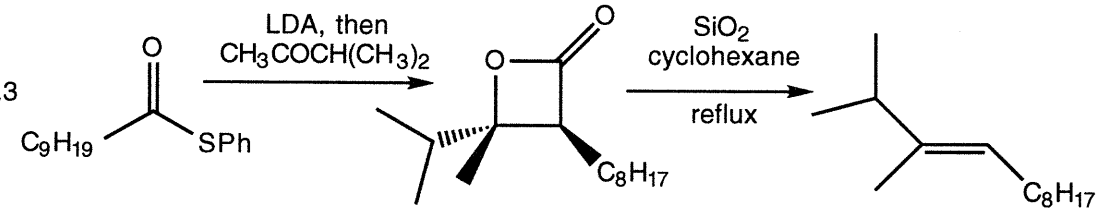


The third case involved the reaction of S-phenyl decanethioate with 3-methyl-2-butanone (eq 1.3). S-Phenyl decanethioate was formed from thionyl chloride, distilled pyridine, and commercially available decanoyl chloride in high yield after distillation (92-98%) on up to a 97 g scale. The yields of alkene ranged from 48 to 59% from the thiol ester with 96 - 97% of the alkene

as the trans isomer. The trans stereochemistry of the major product was confirmed by NOE experiment. The alkene was typically purified by high vacuum distillation. To mitigate the extensive foaming that accompanied the distillations, shredded glass wool was placed in the distillation flask, enough to cover the material in the distillation flask. Substitution of ether as solvent resulted in greater amount of impurities in the crude β-lactone than usual. Addition of the ketone as a THF solution down the side of the reaction flask to precool the solution before reaching the bulk of the reaction mixture did not improve the yield significantly.

A sample of pure β-lactone for characterization purposes was obtained by kugelrohr distillation and flash column chromatography. An NOE experiment on this material confirmed the trans stereochemistry.

We next turned our attention to the slightly variable yields of alkene obtained in the decanoyl case. We considered the possibility that the variance might be due to the method of purification, especially the temperature and pressure at which the alkene was distilled. However, experiments which varied the distillation conditions did not support this.

The *Organic Syntheses* checkers who were assigned to our proposed procedure encountered problems making synthesizing S-phenyl decanethioate: formation of *ca.* 10-15% decanoyl anhydride and yields of thiol ester in the range of 71-88%. Consequently, we were obliged to propose hypotheses for their results. S-Phenyl decanethioate is a known compound with two syntheses with yields appearing in the literature: Anderson *et al.* prepared the thiol ester in quantitative yield from the acid chloride, pyridine, and thionyl chloride;[52] Cainelli *et al.* prepared the thiol ester from the acid chloride in 90% yield using an anion exchanger.[53] Decanoyl anhydride was undetectable in our acid chloride, in our crude thiol ester, and in our distilled thiol ester. Only after performing the reaction with undistilled pyridine, in contradiction to the instructions in our procedure, were we able to induce significant anhydride formation. The anhydride conspicuously

[52] Anderson, R. J.; Henrick, C. A.; Rosenblum, L. D. *J. Am. Chem. Soc.* **1974**, *96*, 3654.
[53] Cainelli, G.; Contento, M.; Manescalchi, F.; Plessi, L.; Panunzio, M. *Gazz. Chim. Ital.* **1983**, *113*, 523.

presents itself by codistilling with the thiol ester and condensing into a clear, colorless, crystalline material in the condenser.

In the β-lactone formation step, the *Organic Syntheses* checkers also encountered byproducts which we usually did not, specifically diphenyl disulfide and dinonyl ketone. In order to determine the extent of β-lactone formation, the reaction was monitored by $^1$H NMR using an internal standard. In this case, dibenzyl ether proved to be a suitable standard, being non-volatile, inert to the reaction conditions, and exhibiting signals that did not interfere with $^1$H NMR interpretation. With this tool, we were able to conduct experiments and conclude that on a large scale (*ca.* 0.1 M) a) the $^1$H NMR yield of β-lactone is 53 to 68%; b) the levels of thiol ester remaining are 9 to 12%; c) self-condensation product does not occur to any significant extent (0-3%); and d) the thiol ester enolate by itself forms no $^1$H NMR detectable amounts of self-condensation product, even at 0 °C. Very little diphenyl disulfide was observed by either $^1$H NMR or thin layer chromatography in the crude β-lactone. Little or no dinonyl ketone was observed in the crude β-lactone by $^1$H NMR. The checkers postulate that the appearance of this material may be due to the thermal decomposition of an enolate molecule to the corresponding ketene, reaction with another enolate molecule, followed by hydrolysis and decarboxylation (Fig. 1.2).

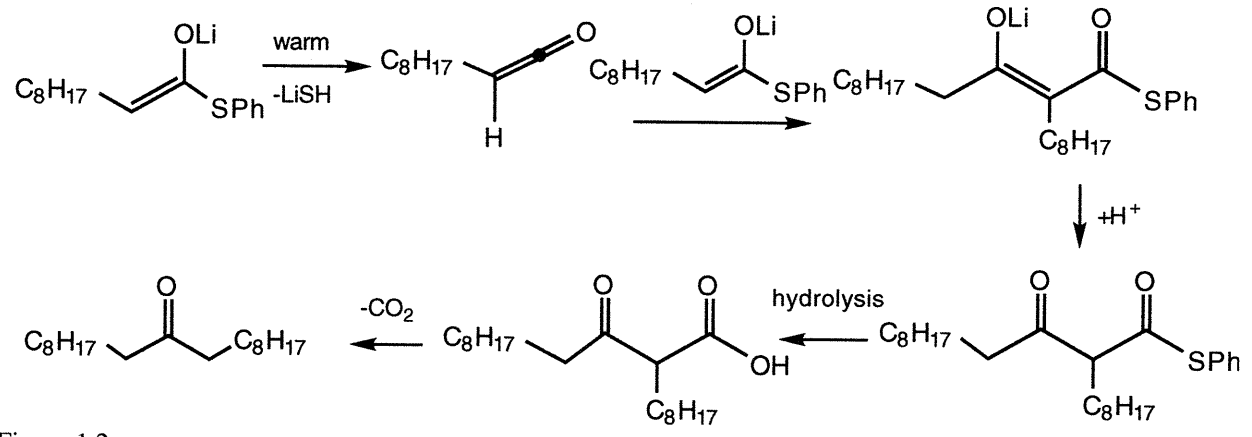


Figure 1.2

In light of the aforementioned enolate stability and the stability of thiol esters to hydrolysis in general, it is difficult to explain the appearance of dinonyl ketone in the crude β-lactone obtained by the checkers. From our experiments with S-phenyl decanethioate, thiol esters are stable to the procedure for the β-lactone workup, to prolonged contact with aqueous sodium carbonate, and to overnight storage in an ethereal solution over $MgSO_4$. It may be that the adventitious decanoyl anhydride in the checker's thiol ester was not removed, since the boiling points of the two are very close. The anhydride might then be deprotonated and react with thiol ester, perhaps via the ketene intermediate above.

We also conducted tests on the stability of the β-lactone, tests instigated by problems encountered by the *Organic Syntheses* checkers and despite an internal check within the Danheiser group. We found that the β-lactone was surprisingly stable (± 3 %) to various workup and storage malpractices, such as prolonged workup times, overnight storage in ether over $MgSO_4$ at room temperature, overnight storage in concentrated form at room temperature, and concentration by rotary evaporation using a 40 °C bath. The robustness of the β-lactone to these tests led us to concentrate on the decarboxylation step. Unfortunately, the internal standard that had served us so

well could not be used to determine the yield of the decarboxylation step, due to adsorption of the dibenzyl ether onto the silica gel used in the reaction.

We also considered the possibility that the low yields of alkene obtained by the checkers (32-36% from the thiol ester) might be due to side reactions of the alkene. One plausible side reaction would be polymerization of the alkene, initiated by thiophenol radical addition to an alkene molecule; the thiophenol radical might be produced from the diphenyl disulfide found in the checkers' crude β-lactone. This can probably be prevented by thorough, but expedient, washing of the crude β-lactone with sodium carbonate during workup.

It is our conclusion that for the S-phenyl decanethioate case, when our procedure[54] is followed exactly, variations in alkene yield are most likely due to variations in temperature control that facilitate proton transfer from 3-methyl-2-butanone to the thiol ester enolate. Several related methods have appeared since the publication of our procedure. An asymmetric version of our method has been explored by Cossío and coworkers.[55] Schick *et al.* have reported the reaction of lithium enolates of phenyl esters on aldehydes[56] as well as the use of lithium enolates of 1-acylbenzotriazoles with aldehydes or ketones to give di- and trisubstituted β-lactones.[57] A Mukaiyama aldol-lactonization using ketene thiopyridylacetals and aldehydes provides α-unsubstituted and α, β-disubstituted β-lactones.[58]

---

54 Danheiser, R.L.; Nowick, J. S.; Lee, J. H.; Miller, R. F.; Huboux, A. *Organic Syntheses* **1995**, *73*, 61.
55 Arrastia, I.; Begoña, L.; Cossío, F. P. *Tetrahedron Lett.* **1996**, *37*, 245.
56 Wedler, C.; Kunath, A.; Schick, H. *J. Org. Chem.* **1995**, *60*, 758.
57 Wedler, C.; Kleiner, K.; Kunath, A.; Schick, H. *Liebigs Ann.* **1996**, 881.
58 Yang, H. W.; Romo, D. *J. Org. Chem.* **1997**, *62*, 4.

# Chapter 2

## Investigative Methods for Understanding and Predicting Helicity

## Introduction

In 1989 Marqusee, Robbins, and Baldwin reported the unusually high helicity exhibited in water near 0 °C by polypeptides of the sequence $(Ala_4Lys)_n$ where n = 3 to 6, and since that time close structural relatives of these peptides have found many applications, both as helical scaffolds for probing a variety of bioorganic issues and as host platforms for probing the detailed energetics of polypeptide helix formation.[59] Coincidentally a year earlier, Kemp and Curran had introduced an N-terminal templating principle for inducing and studying helicity in short peptides.[60] This section of this thesis focuses on applications of the Curran helical template Ac-$Hel_1$ to probe a variety of questions concerning the structure and stability of alanine-rich, lysine-containing polypeptides, such as those studied by Baldwin and coworkers. Beginning with a discussion of helical structure, this chapter introduces issues that are fundamental to the work reported in Chapters 3, 4, and 5.

## The Structures of α and $3_{10}$ Helices

What structural features define a peptide helix? Pauling and Corey first introduced what we now know as the α-helix to explain the X-ray fiber diffraction patterns exhibited by the keratins, a broad class of insoluble structural proteins that includes hair and horn.[61] Relying on atomic parameters derived from X-ray crystallographic analysis of small polypeptides, Pauling noted that if the relatively freely rotating ϕ and ψ peptide dihedral angles[62] are assigned respective values of -57° and -46°, a regular helical structure shown in Fig. 2.1 is generated that contains 3.6 amino acid residues per helical turn and that allows hydrogen bond formation between carbonyl oxygen

---

[59] Marqusee, S.; Robbins, V. H.; Baldwin, R. L. *Proc. Natl. Acad. Sci. USA* **1989**, *86*, 5286.

[60] a) Kemp, D.S.; Curran, T. P. *Tetrahedron Lett.* **1988**, *29*, 4931. b) Kemp, D.S.; Curran, T. P. *Tetrahedron Lett.* **1988**, *29*, 4935.

[61] Pauling, L.; Corey, R. B.; Branson, H. R. *Proc. Natl. Acad. Sci. U.S.A.* **1951**, *37*, 205.

[62] The ϕ and ψ angles refer to the dihedral angles about the N-$C_\alpha$ and $C_\alpha$-C' bond, respectively.

and amide hydrogen four residues apart along the peptide backbone (*i, i+4*).[63] (Since the resulting ring contains 13 atoms, the α-helix can also be termed $3.6_{13}$.) Subsequent X-ray diffraction analysis of crystalline globular proteins confirmed the relevance of Pauling's α-helix as one of three major architectural elements of proteins, but also demonstrated that a tighter $3_{10}$ helix can be formed with dihedral angles of ϕ, ψ *ca.* -54°, -28°. From an analysis of the protein database, Thornton has found that 3.4% of all helical residues are of the $3_{10}$ type and likely to be found in short helices (*ca.* 3-4 residues) or at the ends of α-helices.[64] X-ray studies by Karle,[65] Toniolo,[66] and their associates of simple helical peptides have shown that formation of a $3_{10}$ helix is favored by the presence within the peptide sequence of unnatural amino acids bearing two α-alkyl groups; within this general class, Aib = α-aminoisobutyric acid (α-methylalanine) is the most frequently encountered. Helices in solution must be viewed as manifolds of nearly isoenergetic molecules that contain helical regions, and the available evidence leaves unresolved the question of whether a given peptide might exist as a rapidly equilibrating mixture of these two types of helices, or whether hybrid conformations containing bifurcated hydrogen bonds may under some conditions be isoenergetic with the pure α and $3_{10}$ states.

---

[63] This standard terminology refers to amino acid residue units NH-CHR-C(O) in the N-terminus to C-terminus direction.

[64] Barlow, D. J.; Thornton, J. M. *J. Mol. Biol.* **1988**, *201*, 601.

[65] a) Karle, I. L.; Flippen-Anderson, J.; Sukumar, M.; Balaram, P. *Proc. Natl. Acad. Sci. USA* **1987**, *84*, 5087. b) Karle, I. L.; Flippen-Anderson, J.; Sukumar, M.; Balaram, P. Int. J. Peptide Protein Res. **1988**, *31*, 567. c) Karle, I. L. Biopolymers **1989**, *28*, 1. d) Karle, I. L.; Gurunath, R.; Prasad, S.; Rao, R. B.; Balaram, P. *Int. J. Peptide Protein Res.* **1996**, *47*, 376. e) Karle, I. L.; Flippen-Anderson, J. L.; Uma, K.; Balaram, P. *Biopolymers* **1993**, *33*, 401.

[66] a) Pavone, V.; DiBlasio, B.; Santini, A.; Benedetti, E.; Pedone, C.; Toniolo, C.; Crisma, M. *J. Mol. Biol.* **1990**, *214*, 633. b) Benedetti, E.; DiBlasio, B.; Pavone, V.; Pedone, C.; Toniolo, C.; Crisma, M. *Biopolymers* **1992**, *32*, 453.

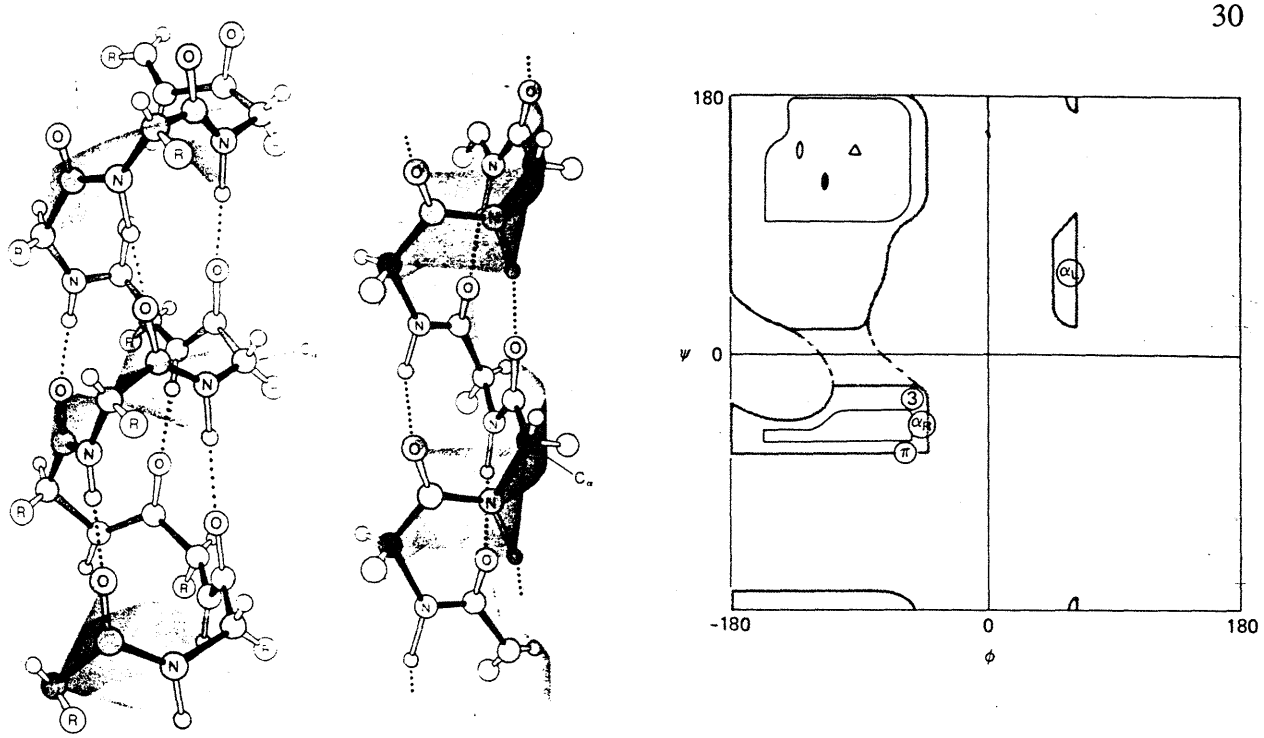


a b

Fig. 2.1 a) α vs. $3_{10}$ helix; b) Ramachandran diagram. $\alpha_R$ = right-handed alpha-helix, 3 = $3_{10}$-helix.

How can the structures of α and $3_{10}$ helices be assigned? For crystalline materials, the evidence of X-ray diffraction is usually unambiguous, but much less confidence attends assignment of these structures in solution. The conformations of polypeptides are usually assigned by applying evidence from a series of different physical methods. Circular dichroism (CD) spectroscopy reflects the contributions of a series of chirally perturbed chromophores within the overall molecule. Provided suitable distinctive reference spectra are available, CD spectroscopy can often establish with some confidence that a given conformation contributes significantly to the conformational manifold of a particular peptide in solution. (A more detailed discussion of this process is found in Chapter 4.) Although the CD spectra of helices are both intense and distinctive, the literature contains conflicting reports on the use of CD to distinguish between α and

$3_{10}$ helices.[67] NOE interactions derived from high field $^1$H NMR solution spectra of a peptide usually provide the most compelling evidence for the presence of a helix, and the relative intensities of a series of these interactions have been used to draw the $\alpha/3_{10}$ structural distinction.[68] From these studies it is clear that α-helices are the predominant conformations formed from natural peptide sequences in solution. However, recently Millhauser and coworkers have introduced a novel double spin labeling electron spin resonance (ESR) technique for making this distinction and has argued that the shorter $A_4K$ sequence polymers contain substantial $3_{10}$ structure.[69] Although the interpretation of his results has been questioned and his method requires significant structural perturbation of the system, for all its faults, Millhauser's labor-intensive double spin labeling may be the best $3_{10}$ structural test that is currently available.

**The Energetics of Helix Formation**

A solution to the protein folding problem for the simple case of unaggregated peptide helices in aqueous solution would mean that one could predict quantitatively the dependence of helical stability on amino acid composition and sequence for any random peptide sequence. This important problem has received much attention over the past 25 years, and although some recently have expressed confidence that it is nearing solution,[70] major unresolved conflicts with both the data and the interpretations offered by different workers must be addressed before the form of a solution can be envisaged. A very brief description of the major approaches is necessary to understand the scope and objectives of our studies with Ac-$Hel_1$ derivatives and the results to be presented in later chapters.

---

[67] a) Toniolo, C.; Polese, A.; Formaggio, F.; Crisman, M.; Kamphius, J. *J. Am. Chem. Soc.* **1996**, *118*, 2744. b) Sudha, T. S.; Vijayakumar, E. K. S.; Balaram, P. *Int. J. Pept. Prot. Res.* **1983**, *22*, 464.

[68] Millhauser, G. L.; Stenland, C. J.; Hanson, P.; Bolin, K. A.; van de Ven, F. J. M. *J. Mol. Biol.* **1997**, *267*, 963.

[69] a) Fiori, W. R.; Miick, S. M.; Millhauser, G. L. *Biochemistry* **1993**, *32*, 11957. b) Miick, S. M.; Martinez, G. V.; Fiori, W. R.; Todd, A. P.; Millhauser, G. L. *Nature* **1992**, *359*, 653.

[70] Chakrabartty, A.; Baldwin, R. L. *Adv. Prot. Chem.* **1995**, *46*, 141.

The simplest of all helicity algorithms does not address the question of energetics at all. In 1974 working from a statistical analysis of 15 proteins of known conformation, Chou and Fasman assigned probabilities for each of the 20 natural amino acids of being in an α-helix, β-sheet, or random coil.[71] Using these probabilities, they defined a predictive algorithm for identifying regions of proteins that are likely to be helical, working from only the amino acid primary sequence. At its best, this approach gives predictions in the 70-80% confidence range, but even with input from a much larger database, it is clear that further improvements in prediction accuracy are unlikely. Moreover, the assumptions of the analysis have been criticized, and the overall approach can give no insight into cause-effect relationships or detailed energetics.

If a peptide amino acid composition and sequence are regarded as a helical code, then one obvious approach to cracking it is to examine the natural amino acids one by one in a context that is helix-supportive but free of unexpected interactions. The stabilizing features of each that is measured in this minimally interactive context can then be corrected by context dependent interactions with pairs of precisely spaced amino acid residues. This host-guest analysis was pioneered by Scheraga and coworkers, who over a 15 year period studied the melting behavior of helices formed by poly(N-hydroxybutyl-L-glutamine) containing up to 5% of each of the natural amino acids.[72] The data were interpreted using a statistical mechanical model introduced by Zimm and Bragg[73] to explain the melting behavior of related helices first prepared and studied by Doty and coworkers.[74] Three parameters appear in this model: n, which is the peptide length; σ, a

[71] Chou, P.Y.; Fasman, G.D. *Biochemistry* **1974**, *13*, 222.

[72] a) von Dreele, P. H.; Poland, D.; Scheraga, H. A. *Macromolecules* **1971**, *4*, 396. b) von Dreele, P. H.; Lotan, N.; Ananthanarayanan, V. S.; Andreatta, R. H.; Poland, D.; Scheraga, H. A. *Macromolecules* **1971**, *4*, 408. c)Platzer, K.E.B.; Ananthanarayanan, V. S.; Andreatta, R.H.; Scheraga, H.A. *Macromolecules* **1972**, *5*, 177. d) Kidera, A.; Mochizuki, M.; Hasegawa, R.; Hayashi, T.; Sato, H.; Nakajima, A.; Frederickson, R. A.; Powers, S. P.; Lee, S.; Scheraga, H. A. *Macromolecules* **1983**, *16*, 162. e) Sueki, M.; Lee, S.; Powers, S. P.; Denton, J. B.; Konishi, Y.; Scheraga, H. A. *Macromolecules* **1984**, *17*, 148.

[73] a) Zimm, B. H.; Bragg, J. K. *J. Chem. Phys.* **1959**, *31*, 526. b) Zimm, B. H. in Polyamino Acids, Polypeptides, and Proteins ed. Stahmann, M.A., 1961, p.229.

[74] a) Doty, P.; Holtzer, A. M.; Bradbury, J.H.; Blout, E.R. *J. Am. Chem. Sci.* **1954**, *76*, 4493. c) Doty, P.; Bradbury, J. H.; Holtzer, A. M. *J. Am. Chem. Soc.* **1956**, *78*, 947. c) Doty, P.; Bradbury, J. H.; Holtzer, A. M. *J. Am. Chem. Soc.* **1956**, *78*, 947. d) Doty, P.; Yang, J. T. *J. Am. Chem. Soc.* **1956**, *78*, 498. e) Doty, P.;

temperature-independent parameter that measures the difficulty of initiating a helix; and s, a propagation parameter that can be viewed as an equilibrium constant that measures the tendency of a given amino acid to join a preexisting helix to which it is linked (Fig. 2.2). Scheraga has reported s values from this study, but these reflect no context-sensitive effects, since the copolymers studied were random in sequence.

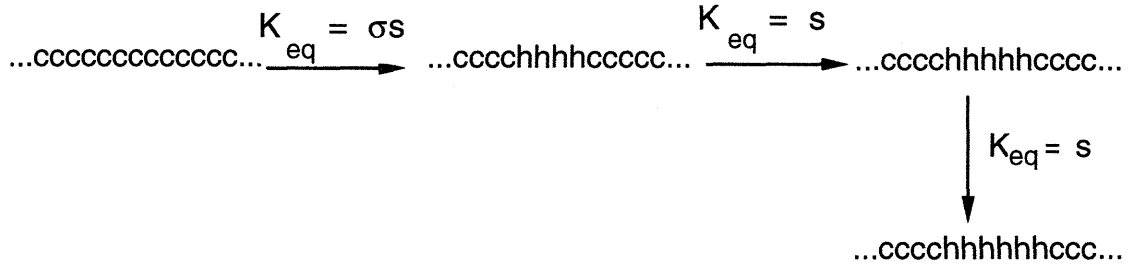


Fig. 2.2 Nucleation and propagation of helical structure shown for a homopolymer of unspecified length. A heteropolymer would require different s-values depending on the specific residue assuming helical structure. (c = amino acid residue with random coil $\phi$ and $\psi$ angles; h = amino acid residue with $\alpha$-helical $\phi$ and $\psi$ angles.)

An important prediction of the Zimm-Bragg model, taken with the Scheraga data, is that no short isolated helix made up of natural amino acids should be stable enough to be detectable in water. Although for more than a decade this prediction agreed with all experimental findings, in 1982 Bierzynski, Kim, and Baldwin[75] reported a thorough reinvestigation of an earlier report of Brown and Klee[76] that short peptides clipped from the N-terminus of bovine pancreatic ribonuclease showed substantial helicity near 0 °C in water. A series of studies by the Baldwin group aimed at identifying the key stabilizing interactions that characterize this unusual helix culminated in the remarkable finding alluded to in the first paragraph of this chapter. Alanine sequences containing solubilizing amino acids such as Lys, Arg, Gln, or Gly[77] at every fifth residue were shown to exhibit the high temperature dependence and an even higher fractional

Wada, A.; Yang, J. T.; Blout, E. R. *J. Polymer Sci.* **1957**, *23*, 851. f) Gratzer, W. B.; Doty, P. *J. Am. Chem. Soc.* **1962**, *85*, 1193.

[75] a) Bierzynski, A.; Kim, P.S.; Baldwin, R.L. *Proc. Natl. Acad. Sci. USA* **1982**, *79*, 2470. b) Shoemaker, K.R.; Kim, P.S.; Brems, D.N.; Marqusee, S.; York, E.J.; Chaiken, I.M.; Stewart, J. M.; Baldwin, R.L. *Proc. Natl. Acad. Sci. USA* **1985**, *82*, 2349.

[76] Brown, J.E.; Klee, W. A. *Biochemistry* **1971**, *10*, 470.

[77] The following standard abbreviations will be used in the remainder of this thesis: A, Ala, L-alanine; R, Arg, L-arginine; Q, Gln, L-glutamine; G, Gly, L-glycine; H, His, L-histidine; K, Lys, L-lysine; O, Orn, L-ornithine.

helicity than that showed by the ribonuclease fragments.[78] Since that time the Baldwin group and others have used the $Ala_4Lys$ motif as a host context for deriving s values and context sensitivities,[79] and others have reported s value measurements in a variety of peptide,[80] protein,[81] and designer protein [82] contexts. These values are only moderately well-correlated, although most agree with Baldwin's finding that alanine is the most helix-stabilizing of the natural amino acids ($s_{Ala} = 1.5$).

A key assumption of the Baldwin analysis is that the $(Ala_4Lys)_n$ host context is essentially non-interactive. Specifically, this means that replacement of an Ala residue by a guest amino acid at the (*i, i-3*) site with respect to Lys results in no context-dependent interactions between the side chain of the Lys and the guest. This assumption has been challenged on theoretical grounds by Scheraga,[83] and in a series of papers published in 1995-1996 on experimental grounds by Kemp and coworkers,[84] who have used peptide conjugates of the N-terminal reporting template as the substrates for their studies. The helicity values required for s value assignments by the Baldwin group have been obtained by CD measurements. During the past year Dr. Shimizu[85] and more

[78] a) Scholtz, J.M.; York, E. J.; Stewart, J. M.; Baldwin, R. L. *J. Am. Chem. Soc.* **1991**, *113*, 5102. b) Padmanabhan, S.; Baldwin, R. L. *J. Mol. Biol.* **1991**, *219*, 135. c) Scholtz, J. M.; Qian, H.; York, E. J.; Stewart, J. M.; Baldwin, R. L. *Biopolymers* **1991**, *31*, 1463.

[79] Chakrabartty, A.; Kortemme, T.; Baldwin, R.L. *Protein Science* **1994**, *3*, 843.

[80] a) Merutka, G.; Lipton, W.; Shalongo, W.; Park, S.-H.; Stellwagen, E. *Biochem* **1990**, *29*, 511. b) Shalongo, W.; Dugad, L.; Stellwagen, E. *J. Am. Chem. Soc. 1994*, *116*, 8288. c) Lyu, P.C.; Liff, M. I.; Marky, L. A.; Kallenbach, N. R. *Science* **1990**, *250*, 669.

[81] a) Serrano, L.; Sancho, J.; Hirshberg, M.; Fersht, A.R. *J. Mol. Biol.* **1992**, *227*, 544. b) Horovitz, A.; Matthews, J.M.; Fersht, A.R. *J. Mol. Biol.* **1992**, *227*, 560. c) Blaber, M.; Zhang, X.- J.; Matthews, B.W. *Science* **1993**, *260*, 1637. d) Nicholson, H.; Anderson, D.E.; Dao-pin, S.; Matthews, B.W. *Biochemistry* **1991**, *30*, 9816.

[82] a) O'Neil, K.T.; DeGrado, W. F. *Science* **1990**, *250*, 646. b) Ho, S.P.; DeGrado, W.F. *J. Am. Chem. Soc.* **1987**, *109*, 6751.

[83] Vila, J.; Williams, R.L.; Grant, J.A.; Wojcik, J.; Scheraga, H.A. *Proc. Natl. Acad. Sci. USA* **1992**, *89*, 7821.

[84] a) Kemp, D.S.; Allen, T. J.; Oslick, S. L. *J. Am. Chem. Soc.* **1995**, *117*, 6641. b) Cammers-Goodwin, A.; Allen, T. J.; Oslick, S. L.; McClure, K. F.; Lee, J. H.; Kemp, D. S. *J. Am. Chem. Soc.* **1996**, *118*, 3082. c) Kemp, D. S.; Allen, T. J.; Oslick, S. L.; Boyd, J. G. *J. Am. Chem. Soc.* **1996**, *118*, 4240. d) Kemp, D. S.; Oslick, S. L.; Allen, T. J. *J. Am. Chem. Soc.* **1996**, *118*, 4249.e) Groebke, K.; Renold, P.; Tsang, K. Y.; Allen, T. J.; McClure, K. F.; Kemp, D. S. *Proc. Natl. Acad. Sci. USA* **1996**, *93*, 4025. f) Renold, P.; Tsang, K. Y.; Shimizu, L. S.; Kemp, D. S. *J. Am. Chem. Soc.* **1996**, *118*, 12234.

[85] Shimizu, L. S., Ph.D. Thesis, Massachusetts Institute of Technology, 1997.

recently Dr. Wallimann in the Kemp group used the reporter feature of the Ac-$Hel_1$ template to recalibrate the correlation equation that links measured CD ellipticity with fractional helicity. They have found that for high mean residue ellipticities, the equation seriously overestimates helicity. The circular dichroism studies reported in this thesis are part of an ongoing process of defining a database of N-templated helical peptides for which both CD and NMR-based correlations of ellipticity are available.

## The Reporting Conformational Template Ac-$Hel_1$: Calculation of the Helical State Sum

The Ac-$Hel_1$ template, introduced by Curran and Kemp in 1988, is an acetyl-diprolyl derivative designed with a methylene sulfur bridge between the two prolines to favor the alignment of its three carbonyl groups necessary for helicity in its peptide conjugates (Fig 2.3). The template not only imparts solubility without interactions with side chains, but nucleates and reports helicity.

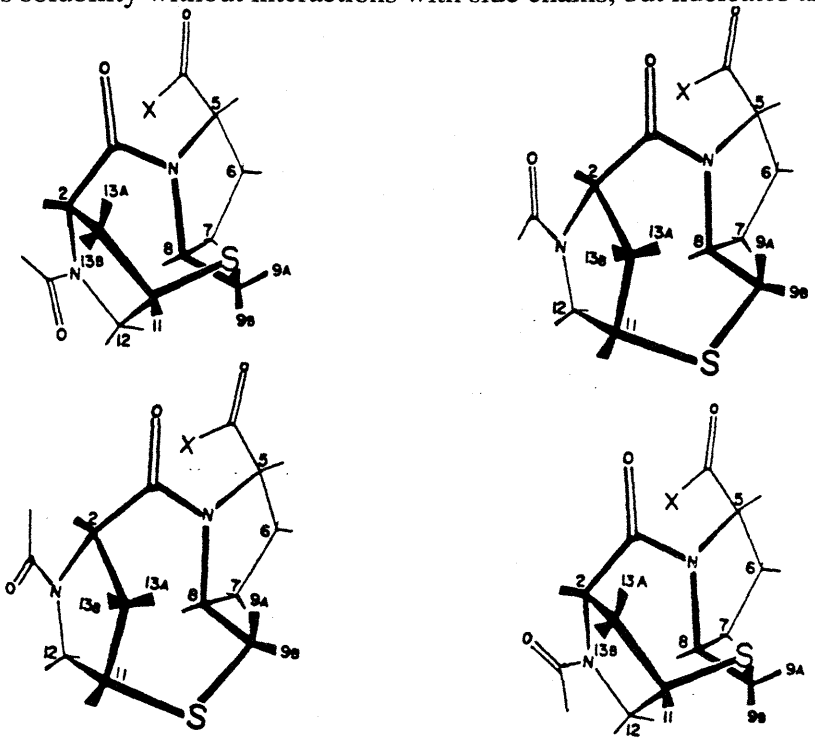

Fig. 2.3 Top left, cs conformation; top right, te conformation; bottom left ce conformation; bottom right, ts conformation. X = peptide. (adapted from reference 60a)

The measured quantity that is a function of helical propensities of the amino acid residues in the peptide conjugate is the trans/cis (t/c) ratio of the acetyl group ( Figures 2.4 and 2.5 and Eq. 2.1).

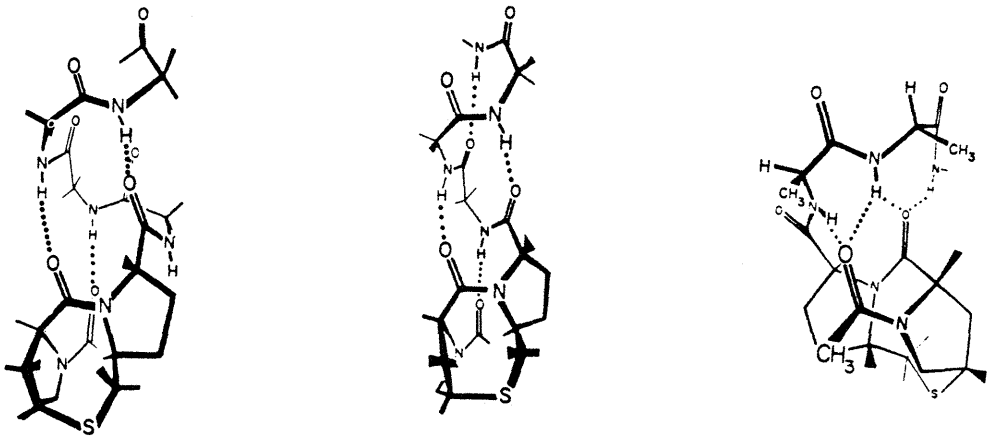

a) b) c)

Fig. 2.4 Ac-Hel$_1$ peptide conjugate. a) α-helix configuration; b) $3_{10}$ configuration; c) bifurcated configuration. (from reference 60b)

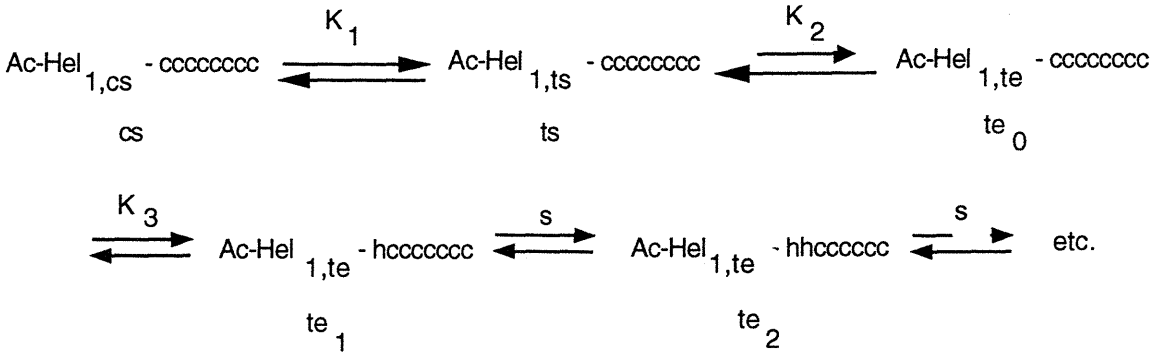


Fig. 2.5 Propagation of helical structure of a templated homooctapeptide.

$$
\begin{aligned}
t/c &= \frac{ts+te_0+te_1+te_2+\ldots+te_8}{cs} = \frac{ts}{cs}+\frac{te_0}{cs}+\frac{te_1}{cs}+\frac{te_2}{cs}+\ldots\frac{te_8}{cs} \\
&= K_1+K_1K_2+K_1K_2K_3+K_1K_2K_3s+\ldots+K_1K_2K_3s^8 \\
&= A+B(1+s+s^2+\ldots+s^8), \text{ where } A=K_1+K_1K_2 \text{ and } B=K_1K_2K_3 \\
&= A+B(1+s+s^2+\ldots+s^8)(s-1)/(s-1) \\
&= A+B\,\frac{s^9-1}{s-1}
\end{aligned}
$$

Eq. 2.1 Representative mass action equations for the propagation of helical structure of an unspecified templated homooctapeptide.

The methylene bridge limits the lactam ring to two conformations, a staggered (s) and an eclipsed (e) orientation about the C8-C9 bond. Although there are four possible combinations resulting from the t/c and s/e options, experiments have shown that the ce state is undetectable, and that the peptide conjugates of the cs and ts states have random coil characteristics. Only the te state is capable of nucleating helical structure in any conjugated peptide (Fig. 2.4). As the t/c equilibrium is slow on the NMR time scale, and the s/e equilibrium fast on the same scale, the resonances corresponding to the t state are an abundance weighted average of the limiting resonances of the te and ts states.[84a] The mole fractions of the cs, ts, and te states are related to the t/c ratio and $K_1$ by Equations 2.2 to 2.4.

Eq. 2.2
$$\chi_{cs} = \frac{cs}{cs+ts+te} = \frac{1}{1+\frac{ts}{cs}+\frac{te}{cs}} = \frac{1}{1+\frac{t}{c}}$$

Eq. 2.3
$$\chi_{ts} = \frac{ts}{cs+ts+te} = \frac{\frac{ts}{cs}}{1+\frac{ts}{cs}+\frac{te}{cs}} = \frac{K_1}{1+\frac{t}{c}}$$

Eq. 2.4
$$\chi_{te} = \frac{te}{cs+ts+te} = \frac{\frac{te}{cs}+\frac{ts}{cs}-\frac{ts}{cs}}{1+\frac{ts}{cs}+\frac{te}{cs}} = \frac{\frac{t}{c}-K_1}{1+\frac{t}{c}}$$

The equation for the observed chemical shift for the t state as a weighted average of the limiting chemical shifts for the ts and te states can be rewritten in terms of $K_1$ and c/t (Eq. 2.5). From a linear regression analysis of the chemical shifts of over 30 template derivatives of varying t/c character, $K_1$ has been found to be 0.79, independent of the nature of the peptide conjugate.[84a]

$$\delta_{obs,\,t} = \delta_{te}\frac{te}{ts+te} + \delta_{ts}\frac{ts}{ts+te}$$

$$= \delta_{te}\frac{\frac{te}{cs}+\frac{ts}{cs}-\frac{ts}{cs}}{\frac{ts}{cs}+\frac{te}{cs}} + \delta_{ts}\frac{\frac{ts}{cs}}{\frac{ts}{cs}+\frac{te}{cs}}$$

$$= \delta_{te}\frac{\frac{t}{c}-K_1}{\frac{t}{c}} + \delta_{ts}\frac{K_1}{\frac{t}{c}}$$

$$= \delta_{te} - \delta_{te}K_1\frac{c}{t} + \delta_{ts}K_1\frac{c}{t}$$

$$= \delta_{te} + (\delta_{ts}-\delta_{te})K_1\frac{c}{t}$$

$$= A' + B'\frac{c}{t}\ ;\ \text{where } A' = \delta_{te} \text{ and } B' = (\delta_{ts}-\delta_{te})K_1$$

Eq. 2.5 Relation of observed chemical shift for the t state and limiting ts and te chemical shifts.

In the absence of an attached peptide or moiety capable of intramolecularly hydrogen-bonding with the acetyl group, the template shows no te character. The ability of the template to nucleate helices ($\sigma$ = 0.12 to 0.18) from the N-terminus allows for simpler models,[84d] since fraying occurs only at the C-terminus, in contrast to the Baldwin peptides and similar hosts. Within the helical manifold supported by the te state, helical structure advances from the N-terminus, and helical structure separated from the template by random coil residues is unlikely for short peptides.

The Ac-Hel$_1$ tool has been used to investigate the subtle effects of residue composition and sequence on helicity both structurally and energetically. NMR and circular dichroism (CD) spectroscopy are the primary instruments used to determine the conformations of conjugated peptides and their relative populations. The necessary deconvolutions of CD spectra will be discussed in Chapter 4. The following chapters will begin with the formation of the first hydrogen bond in simple Ac-Hel$_1$ derivatives, and then examine the helicity of longer peptides containing multiple lysines. Chapter 5 will determine the helical propensity of the simplest amino acid, glycine. Due to its lack of a side chain, glycine is the least conformationally restricted $\alpha$-amino acid. In the context of a peptide, glycine diamides show a wide range of $\phi$ and $\psi$ angles and yields most easily to neighboring conformational preferences. Using glycine to probe various lysine-containing alanine-rich peptide conjugates will then expose the scope of the helix-stabilizing ability of lysine. Lastly, a templated octapeptide that has been used in the Kemp laboratories to obtain an s-value scale will be studied for its suitability as a host.

# Chapter 3

# Simple Ac-Hel$_1$ Derivatives

## Introduction

In the preceding chapter the properties of the helix nucleating template Ac-$Hel_1$ were summarized. This chapter presents results of three brief studies of very simple derivatives of Ac-$Hel_1$ that can form only one intramolecular hydrogen bond. Characterization of derivatives of this type are a necessary first step toward understanding the mechanism by which this reporting template induces helicity in linked peptides, and detailed analyses of this issue have appeared in the literature.[84,86] The properties of these derivatives can also shed light on the properties of single intramolecular hydrogen bonds in water, and the studies in this chapter were carried out as parts of collective research efforts in the Kemp group aimed at using the unique reporter features of the Ac-$Hel_1$ system to study aqueous hydrogen bonding.

Hydrogen bonds were proposed by Pauling as a dominant factor in the stabilization of polypeptide α-helices and β-sheets,[61] but their role in stabilizing these structures either in isolation or as parts of native conformations of proteins remains controversial nearly fifty years after Pauling's proposals. Although an NH - OC hydrogen bond between a pair of secondary amides is strongly stabilizing in vacuum and in nonpolar solvents, the stability must be much lower in water or other solvents that form strong donor and acceptor hydrogen bonds to the amide NH and OC functions. Thus early experiments with simple models imply that $\Delta G^\circ$ for Eq. 3.1 must be very close to zero,[87] and the biophysics community has henceforth largely held the opinion that intramolecular amide-amide hydrogen bonding contributes little or nothing to the folding energy of a protein in water. Relying on new models workers have recently challenged this view, but large experimental errors and significant assumptions underlie their analyses. A brief review of the experimental methods for detecting intramolecular hydrogen bonds is appropriate.

---

[86] a) Kemp, D. S.; Curran, T. P.; Davis, W. M.; Boyd, J. G.; Muendel, C. *J. Org.Chem.* **1991**, *56*, 6672. b) Kemp, D. S.; Boyd, J. G.; Muendel, C. C. *Nature* **1991**, *352*, 451.

[87] Klotz, I. M.; Franzen, J. S. *J. Am. Chem. Soc.* **1962**, *84*, 3461.

Eq. 3.1 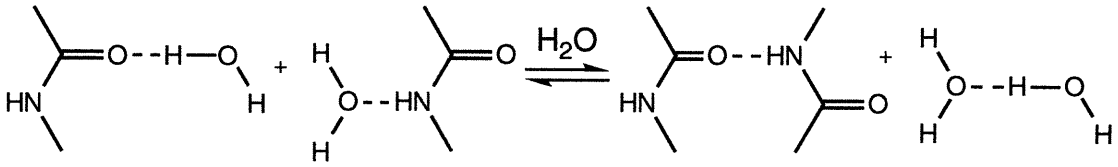

Distinctions between hydrogen and non-hydrogen bonded forms in biological structures are made most commonly with the use of IR and NMR. For simple molecules capable of intramolecular hydrogen bonding, the IR stretch of a non-hydrogen bonded amide N-H is *ca.* 3450 to 3460 $cm^{-1}$ and for the hydrogen bonded form, a broader less intense band at *ca.* 3300 to 3350 $cm^{-1}$.[88] NMR spectroscopy offers several avenues of examination. Proton chemical shifts generally move downfield upon hydrogen bonding. In organic solvents, Gellman has observed amide proton chemical shifts as low as 4.8 ppm for non-hydrogen bonded protons and as high as 8.4 ppm for hydrogen bonded protons.[88] NMR studies of cyclopeptide metal complexes, such as ferrichromes and alumichromes,[89] and short peptide fragments[90] have shown that solvent shielded or intramolecularly hydrogen-bonded amide hydrogens display a lower temperature dependence, with a temperature coefficient ($\Delta\delta/\Delta K$) in the range of -0.001 to -0.004 ppm/K in 9:1 $D_2O/H_2O$, whereas solvent exposed amide hydrogens exhibit a higher temperature coefficient in the range of -0.006 to -0.008 ppm/K. Trifluoroethanol (TFE) has often been used to extend the range of secondary structure observable by NMR. Although other simple alcohols show a helical stabilizing effect in peptides, TFE does so to a greater extent, with a maximal effect in the range of 5-15 mol %.[90] Recent experimental evidence from the Kemp group implies that in dilute aqueous solution TFE acts by reducing the capacity of water to hydrogen bond to amides, selectively destabilizing solvent exposed amides.[84b]

---

[88] Gellman, S. H.; Dado, G. P.; Liang, G.-B.; Adams, B. R. *J. Am. Chem. Soc.* **1991**, *113*, 1164.
[89] a) Constantine, K. L.; De Marco, A.; Madrid, M.; Brooks III, C. L.; Llinás, M. *Biopolymers* **1990**, *30*, 239. b) Llinás, M.; Klein, M. P.; Neilands, J. B. *J. Mol. Biol.* **1970**, *52*, 399.
[90] Dyson, H. J.; Rance, M.; Houghton, R. A.; Lerner, R. A.; Wright, P. E. *J. Mol. Biol.* **1988**, *201*, 161.

**Ac-Hel$_1$-NHMe**

One of the simplest template derivatives capable of intramolecular hydrogen bonding is Ac-Hel$_1$-NHMe. The IR shows a broad band at 3359 cm$^{-1}$ in $CDCl_3$, independent of concentration, which is consistent with a hydrogen bonded state. The chemical shift of the amide proton in $CDCl_3$ is 7.23 ppm for the t state and 6.06 ppm for the c state at 25 °C (Fig. 3.1). In 9:1 $D_2O/H_2O$ the temperature coefficient is -0.0084 ppm/K for the c state and -0.0040 ppm/K for the t state (Fig. 3.2). From the nearly temperature independent t/c ratio of 2.0 in water and using Eq. 2.3 and 2.4, one can compute the relative amounts of the ts and te states ($\chi_{ts}$ = 0.26, $\chi_{te}$ = 0.41); and assuming that $\Delta\delta/\Delta K_{cs}$ approximates $\Delta\delta/\Delta K_{ts}$, the temperature coefficient $\Delta\delta/\Delta K_{te}$ is -0.0012 ppm/K indicating substantial solvent shielding. Applying Eq. 2.5 to the amide chemical shifts (Fig. 3.3) and t/c ratios found in varying TFE concentrations,[91] the limiting chemical shift for the te state is calculated to be 7.30 ppm, comparable to the chemical shift of the t state in $CDCl_3$, suggesting an insensitivity to solvent change. A NOESY experiment in $CDCl_3$ showed a crosspeak between the t state C8-H and the t state amide hydrogen, consistent with the model for the te state; no C8-H to NH crosspeak is observed for the c state. Thus all the experimental data indicate that intramolecular hydrogen bonding is present only in the te state, as expected.

---

[91] Oslick, S. O., Ph.D. Thesis, Massachusetts Institute of Technology, 1996.

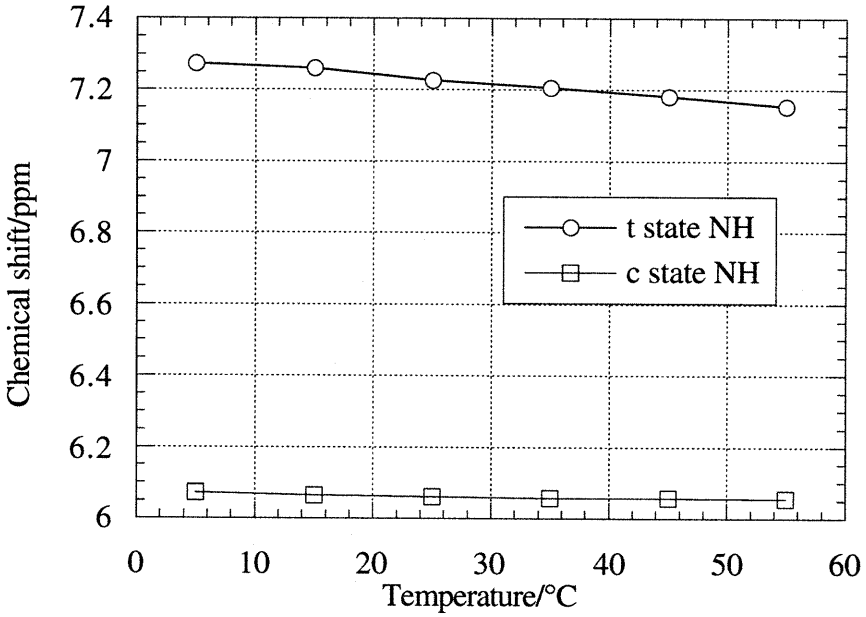


Fig 3.1 Temperature dependence of amide chemical shifts of AcHel$_1$-NHMe in $CDCl_3$.

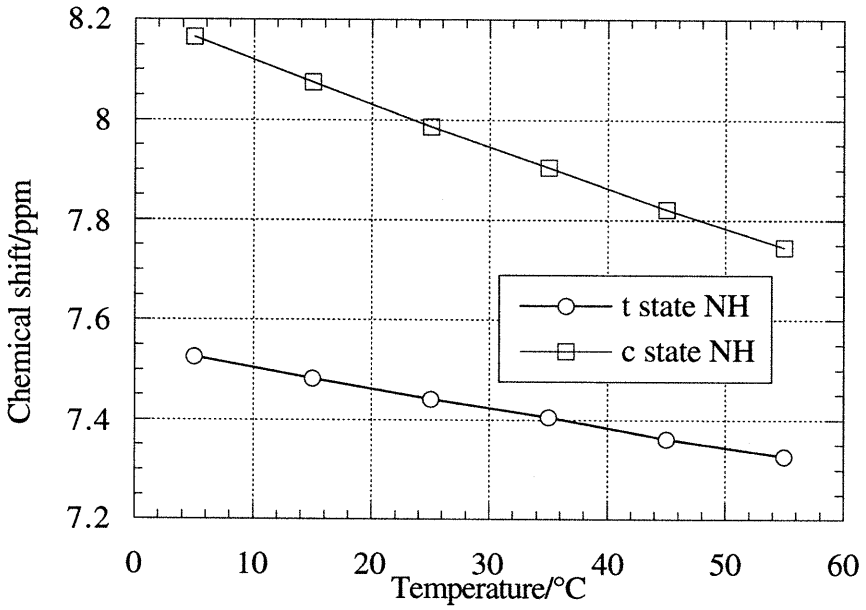


Fig. 3.2 Amide chemical shifts of Ac-Hel$_1$-NHMe in 9:1 $D_2O/H_2O$.

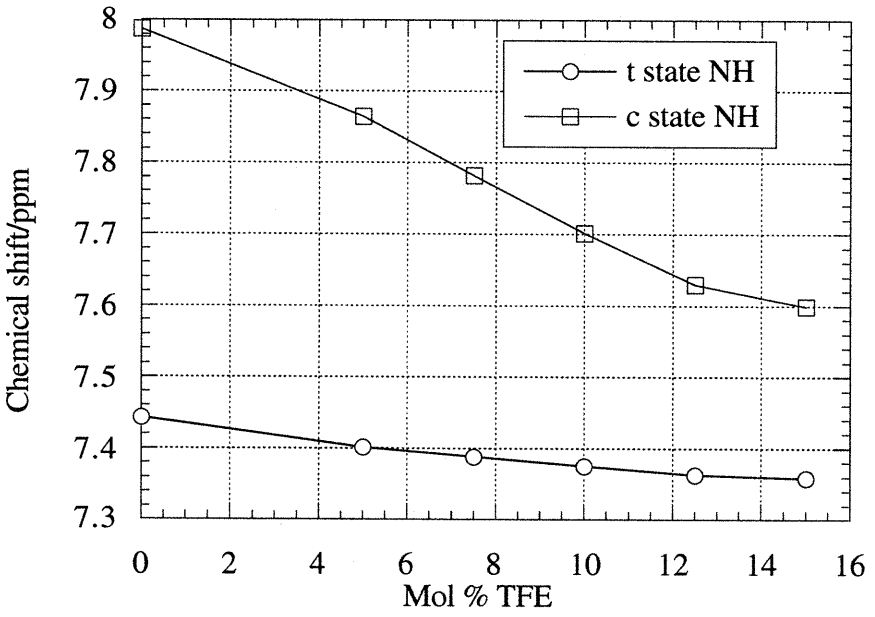


Fig. 3.3 Amide chemical shifts of Ac-Hel$_1$-NHMe in 9:1 $D_2O/H_2O$ with TFE at 25 °C.

## Ac-Hel$_1$-Val-OH

In previous work that characterized the properties of Ac-Hel$_1$-NH-R monoamides, it was noted that the alanine derivative Ac-Hel$_1$-Ala-OH exhibited an unusually small t/c value in water of 0.65, which may be compared with values of 1.3, 1.8 and 2.1 for R= $CH_2CO_2H$ (Gly), $NH_2$, and NHMe, respectively. To test whether this small value is unique to alanine, the corresponding valine derivative was prepared and studied. Valine was selected because it bears a relatively hydrophobic β-branched side chain that is positioned close to the hydrogen bonding site.

Ac-Hel$_1$-Val-OH was synthesized from Ac-Hel$_1$-OH and HCl.$H_2$N-Val-O*t*Bu, followed by cleavage of the *t*-butyl group. The amide proton in $CDCl_3$ for the t state appears downfield of that

for the c state (Fig. 3.4). The t/c ratio shows a general insensitivity to temperature in $CDCl_3$ and in $D_2O$ (Fig. 3.5). With the addition of TFE, the t/c ratio rises from 0.75 at 0 mol % TFE to 2.27 at 20 mol % TFE. In comparison, Ac-$Hel_1$-Ala-OH shows a t/c ratio of 0.65 at 0 mol % TFE and *ca.* 2.2 at 20 mol % TFE. The greater steric bulk of the valine side chain does not seem to significantly favor the hydrogen bonding conformer. Although only one derivative was studied, these data suggest that the anomalous t/c value is that of glycine, not alanine.

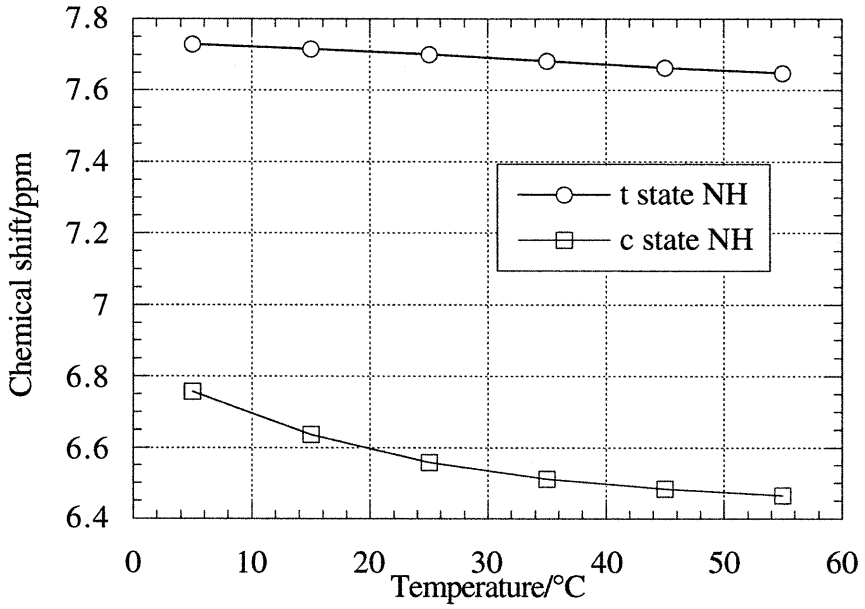


Fig 3.4 Amide chemical shifts for Ac-$Hel_1$-Val-OH in $CDCl_3$.

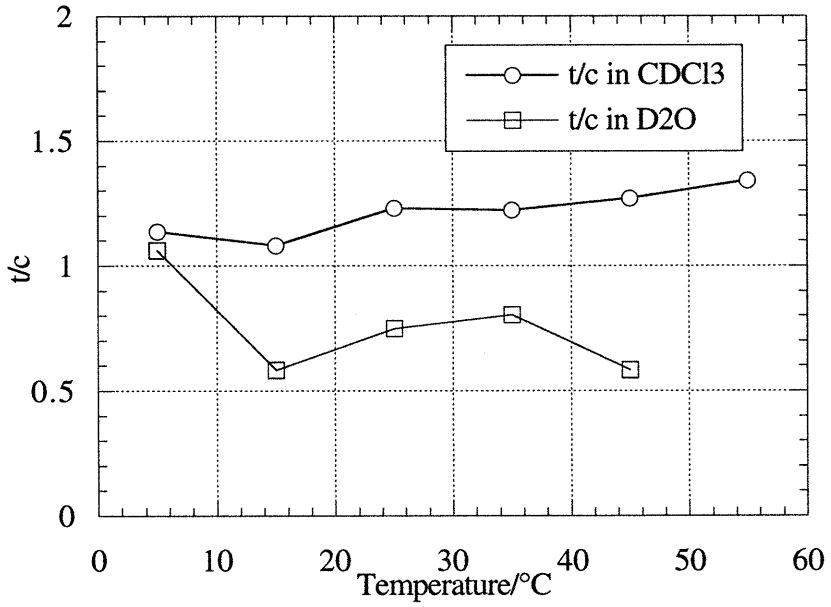


Fig 3.5 Temperature dependence of Ac-Hel$_1$-Val-OH in $CDCl_3$ and in $D_2O$.

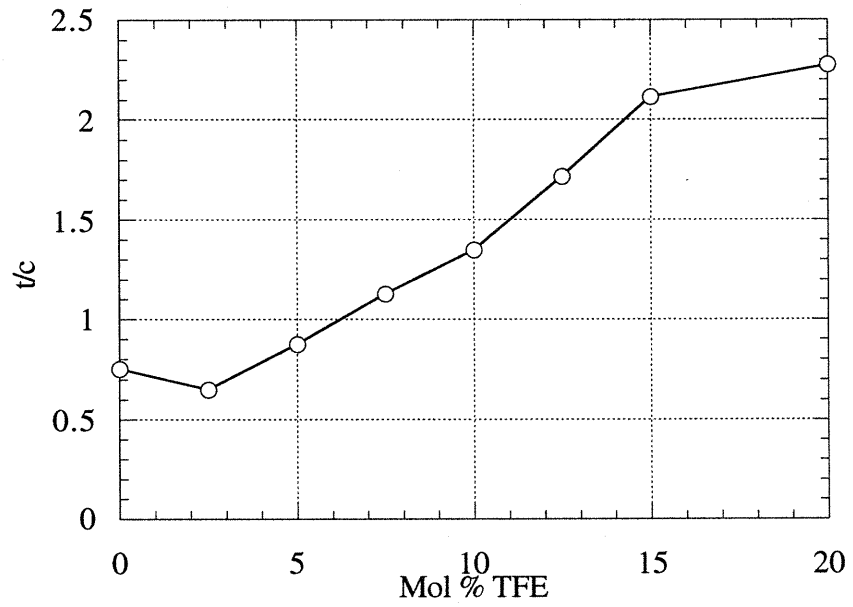


Fig 3.6 Dependence of Ac-Hel$_1$-Val-OH in $D_2O$ on mol % TFE at 25 °C.

**Reduced template thiol**

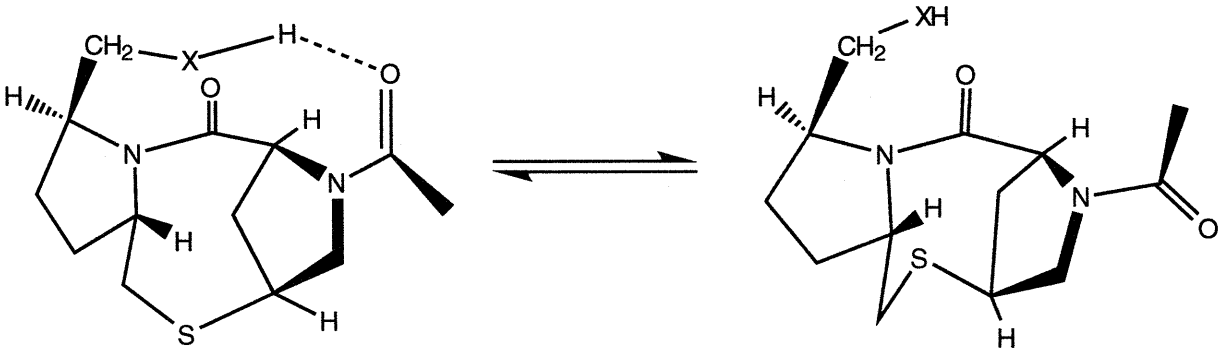


**7a** **7b**

Dr. McClure and Mr. Powers in the Kemp group have prepared a series of analogs of the Ac-Hel$_1$ amides in which the 5-carboxamido function has been replaced by $CH_2$-X where X = OH, $NH_2$, $NH_3^+$, and $NHCOCH_3$. The t/c ratios of these derivatives have been measured in water and in water-TFE mixtures to define a new scale of experimentally derived hydrogen bonding affinities between the donor group X and the acceptor proline acetamido function. Although the hydrogen bond between an amide carbonyl and a thiol is expected to be very weak, it was important to include the thiol function on the list of hydrogen bond donors subjected to this analysis.

The relatively high acidity of a thiol ($pK_a$ *ca.* 9-10) and the greater length of a S-H bond relative to an amide N-H bond (1.33 Å vs. 1.02 Å) suggests the possibility of both inter and intramolecular hydrogen bonding. An analysis of the protein database by Gregoret *et al.*[92] shows that the frequency of cysteine SH - carbonyl oxygen distances peaked at 3.5 Å, but with no preferred geometry. Although weaker than hydrogen bonding between hydroxyl and carbonyl groups, thiol to carbonyl oxygen hydrogen bonding has been observed.[93]

---

92 Gregoret, L. M.; Rader, S. D.; Fletterick, R. J.; Cohen, F. E. *Prot. Struct. Funct. Genetics* **1991**, *9*, 99.
93 Spur, R. A.; Byers, H. F. *J. Phys. Chem.* **1958**, *62*, 425. b) Mori, N.; Kaido, S.; Suzuki, K.; Nakamura, M.; Tsuzuki, Y. *Bull. Chem. Soc. Jpn.* **1971**, *44*, 1858. c) Giseler, G.; Stache, F. *Chem. Ber.* **1961**, *94*, 337.

The reduced template thiol **7**, X = SH, was synthesized from Ac-Hel$_1$-OMe by reduction to the primary alcohol, a Mitsunobu conversion to the thioacetate, and cleavage of the thioacetate to the free thiol. The thioacetate, incapable of hydrogen bonding, showed a t/c ratio of 0.23 in $CDCl_3$. The temperature dependence of the free thiol in $CDCl_3$ is negligible, but in $D_2O$ is modest (Fig. 3.7). No t/c increase is obtained with addition of TFE (Fig. 3.8). The t/c value of the reduced thiol in $D_2O$ is slightly higher than the corresponding reduced alcohol, (1.97 *vs.* 1.79). The t/c data obtained in water and in TFE-water mixtures are consistent with a negligible hydrogen bonding affinity between thiol and tertiary amide in this system.

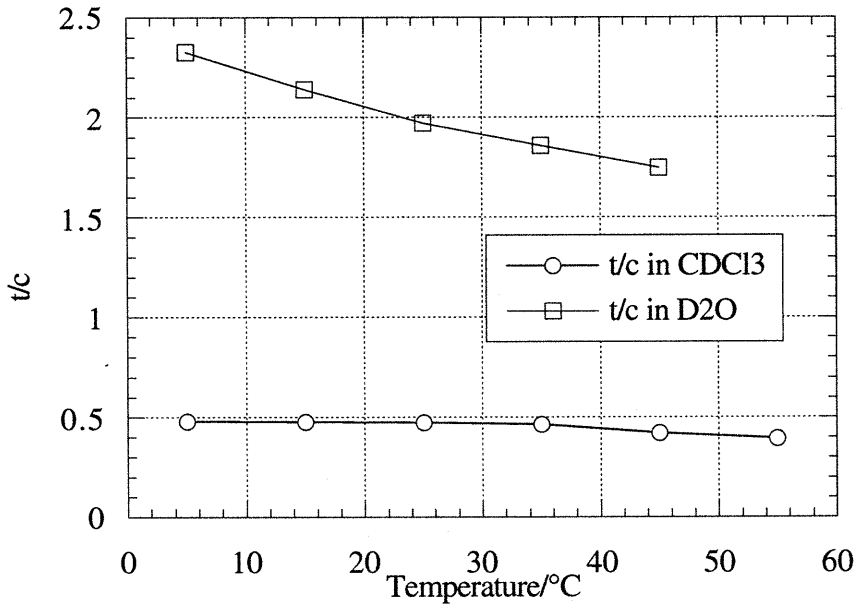


Fig. 3.7 Temperature dependence of t/c of reduced template thiol **7** in $CDCl_3$ and in $D_2O$.

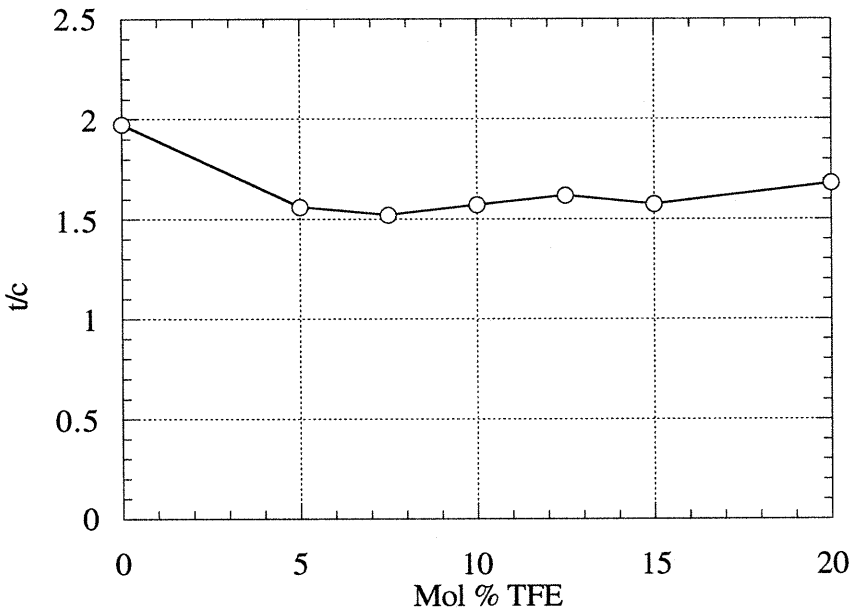


Fig. 3.8 Reduced template thiol **7** in $D_2O$ with varying concentrations of TFE at 25 °C.

# Chapter 4

## Templated Oligopeptides Containing Multiple Lysines

## Introduction

Effects which must be considered when charged residues are present in a helical sequence are salt bridges to nearby positively charged residues, electrostatics, and charge-dipole interactions. In the case of lysine, hydrophobic interactions must be considered as well. For a heteropeptide containing multiple charged residues, these effects are interdependent and the position and spacing of these residues determine whether they stabilize or destabilize a helix. The relevance of their combined interactions lies in the unavoidable use of charged residues to confer water-solubility. In 1989 Baldwin and coworkers found certain 16-mers with a fewer number of lysines to be significantly more helical: Ac-AK(AAAAK)$_2$AAAA-NH$_2$ > Ac-AK(AAKAA)$_2$-AAKA-NH$_2$ > Ac-AK(AAKAK)$_2$-AAKA-NH$_2$.[59] These observations were presumed by Baldwin to be due to a helix destabilizing effect by lysine; hence the helical stability of these peptides was attributed to an unusually high helical propensity for alanine. Recently, this conclusion has been challenged by Kemp and coworkers, reporting a sequence dependent destabilizing effect of KA$_2$K sequences.[84f]

Further evidence credits lysine for the stability of alanine-lysine peptides, with alanine a neutral participant.[84e] Structurally this may be due to a conformation of the lysine in which its side chain packs against the helix barrel, providing hydrophobic contact with the *i*-3 alanine side chain and hydrogen bonding of the lysine ε-NH$_3^+$ and the *i*-4 alanine carbonyl. Indeed this model had been proposed by Scheraga in 1992 in conjunction with computational calculations that suggested the high helix content of Baldwin's reference peptides is due not to any noteworthy helical propensity of alanine, but to that of the charged lysine residues.[94]

---

[94] Vila, J.; Williams, R.L.; Grant, J.A.; Wojcik, J.; Scheraga, H.A. *Proc. Natl. Acad. Sci. USA* **1992**, *89*, 7821.

Nevertheless, the $(A_4K)_n$ peptides of Baldwin has been used extensively in helicity studies, of which circular dichroism (CD) has been one of the main tools. Using currently accepted CD calibration scales for helicity, many researchers have accredited certain peptides in solution at low temperature or high TFE concentration with the status of 100% helicity. Since both ends of short peptides in solution are most likely frayed to some extent, limiting CD spectra of α-helical peptides only crudely approximates 100% helicity, *i.e.* canonical α-helical φ and ψ angles at every residue. The Ac-$Hel_1$ system is unique among peptide systems because CD spectra can be independently calibrated by t/c ratios obtained by NMR. As stated in Chapter 2, recent results of Drs. Shimizu and Wallimann of the Kemp laboratory suggest that the current scales overestimate helicity for certain peptides.[85] One of the two objectives in this chapter is to determine the quantitative criteria of helicity for templated peptides containing the $A_4K$ motif. Notwithstanding the conclusions of Baldwin, a single lysine in a neutral matrix appears to stabilize a helix for templated peptide helices. Two or more contiguous lysine residues in a helical sequence, however, cause some degree of destabilization due to electrostatic repulsion of their positively charged side chains. Noting that a positively charged residue at the C-terminus stabilizes the negatively charged end of a helix dipole, placement of such charges at the C-terminus may offset the unfavorable side chain - side chain interactions. The second objective of this chapter is to determine the net balance between the stabilization effect of terminal lysines and the destabilization effect of contiguous lysines. Since the helicity studies presented in this chapter rely on CD, we must first introduce the basis of CD and the features that make it a valuable tool in helicity studies. The CD signals associated with Ac-$Hel_1$ will then be discussed and finally the CD signals of the peptides attached to the template will be analyzed.

## Circular Dichroism

Circular dichroism utilizes right and left circularly polarized light, which are two orthogonal components of plane polarized light. The two are absorbed by chiral molecules to different extents and the difference (Eq. 4.1) is governed by the Beer-Lambert Law (Eq. 4.2), where A is the absorbance; $\varepsilon$ is the molar absorption coefficient; c is the concentration in M; l is the path length in cm; and the subscripts L and R refer to left and right circularly polarized light, respectively.

Eq. 4.1 $$\Delta A = A_L - A_R = (\varepsilon_L - \varepsilon_R)\, c\, l = \Delta\varepsilon\, c\, l$$

Eq. 4.2 $$A = \varepsilon\, c\, l$$

The standard quantity used in CD is molar ellipticity, $[\theta]$, which are in units of deg•cm$^2$/dmol and which can be shown to be proportional to the molar circular dichroism, $\Delta\varepsilon$ (Eq. 4.3).[95]

Eq. 4.3 $$[\theta] = 3298.2\, \Delta\varepsilon$$

The label itself reflects the elliptically polarized nature of the transmitted light (Fig. 4.1). The ellipticity is directly related to the ratio of the minor to major amplitudes of the electric field component of the transmitted light. Although CD spectra can be derived from optical rotary dispersion (ORD) spectra, the extended tails of the dispersive curves of ORD spectra complicate the transformation for all but the simplest spectra.[96]

---

[95] a) Moscowitz, A. In *Optical Rotary Dispersion*; Djerassi, C., Ed.; McGraw-Hill Book Co., Inc.: New York, 1960. b) Li, Z. Q., Ph. D. Thesis, Massachusetts Institute of Technology, 1996, p. 243.

[96] Woody, R. W. In *The Peptides*, vol. 7; Hruby, V. J., Ed.; Academic Press, Inc.: New York, 1985; p.15.

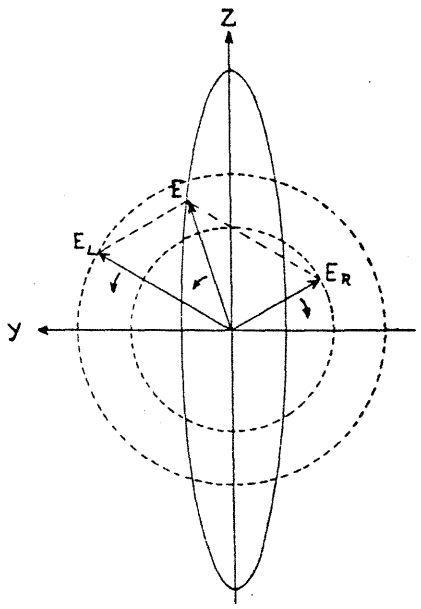


Fig. 4.1 Ellipse traced out by the tip of vector E, the electric field component of the resultant elliptically polarized light, when the magnitude of $E_L$ is not equal to $E_R$ Note that the angles which $E_L$ and $E_R$ make with the z-axis are equal. [97]

CD is also a sensitive technique, as the ratio of $\Delta\varepsilon$ to the average of $\varepsilon_L$ and $\varepsilon_R$ is typically on the order of $10^{-4}$. The typical CD spectra for the $\alpha$-helix, $\beta$-sheet and random coil conformations are shown in Fig. 4.2. The CD features for an $\alpha$-helical peptide are a maximum at *ca.* 190 nm and minima at *ca.* 222 and 208 nm, with a ratio of the molar ellipticities of these minima close to 1. The signal at 222 nm arises from the n-$\pi^*$ transitions of the amide chromophores; the signals at 190 and 208 nm are due to exciton splitting of the $\pi$-$\pi^*$ transitions of the amide chromophores.[98] Unlike NMR, CD does not afford fine structural information, but does offer information on the relative abundances of a multitude of conformations after data analysis. Temperature, TFE, and other additives have often been variables in studies of the helix-coil transition, with the presence of a single isodichroic point at or near 203 nm a validation of the two state model. The other limiting CD in these studies is the random coil, which has a large negative signal at 200 nm and for certain

---

[97] Wong, K.-P. *J. Chem. Ed.* **1974**, *51*, A573.

[98] Woody, R. W., In *Circular Dichroism: Principles and Applications*; Nakanishi, K., Berova, N., Woody, R. W. Eds.; VCH Publishers, Inc.: New York, 1994; p. 473.

systems, a small positive signal near 220 to 230 nm (Fig. 4.2). The random coil state is not a collection of residues with truly random $\phi$ and $\psi$ angles, but rather precludes sterically inaccessible $\phi$ and $\psi$ angles. Furthermore, many researchers have taken the large negative CD at 200 nm as an indication that the random coil state contains substates with restricted conformations.[99] Theoretical predictions of CD signals based on $\phi$ and $\psi$ angles show some dependence on the distortions of the $\phi$ and $\psi$ angles, and on length.[100]

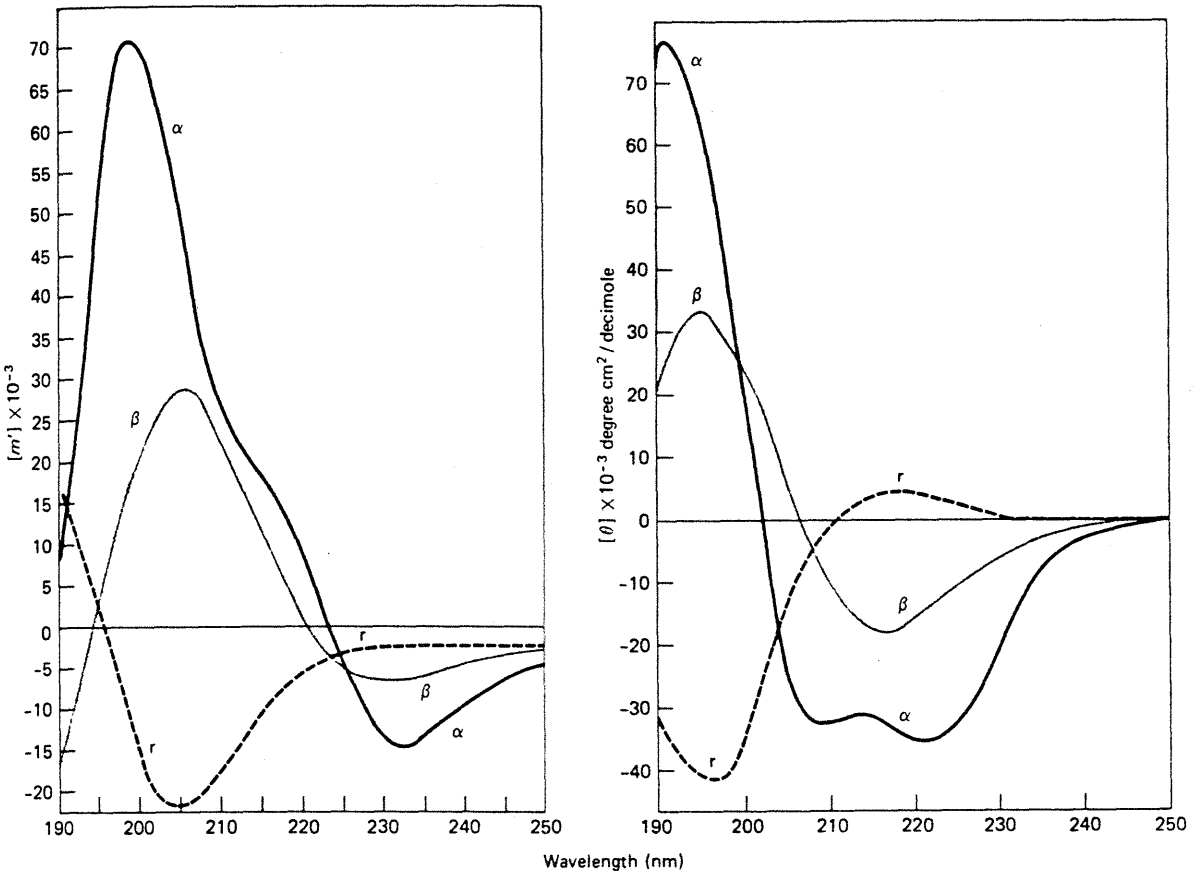


Fig. 4.2 ORD (left) and CD (right) spectra of α-helical (α), anti-parallel β-sheet (β), and random coil (r) conformations for poly-L-lysine .[101]

---

[99] Towell III, J. F.; Manning, M. C. In *Analytical Applications of Circular Dichroism*; Purdie, N. and Brittain, H. G., Eds.; Elsevier Science B. V.: Amsterdam, 1994; p. 175.

[100] a) Vournakis, J. N.; Yan, J. F.; Scheraga, H. A. Biopolymers 1968, 6, 1531. b) Tinoco, J. I.; Woody, R. W.; Bradley, D. F. J. Chem. Phys. 1963, 38, 1317.

[101] a) Greenfield, N.; Davidson, B.; Fasman, G. D. *Biochemistry* **1967**, *6*, 1630. b) Greenfield, N. J.; Fasman, G. D. *Biochemistry* **1969**, *8*, 4108.

## Circular Dichroism of the Ac-$Hel_1$ Chromophore

One assumption of CD analysis is that the total ellipticity is a weighted sum of the ellipticities of independent chromophores among different conformations and also within any given substate. CD signals of the template chromophore Ac-$Hel_1$ arise from the two carbonyls and the thioether bridge. Since in solution the template may exist in three different states their contribution to the overall spectrum of a templated peptide must all be corrected for; the cs+ts states can be grouped together. The limiting CD spectra for the cs+ts and the te state of the template were determined by Dr. Oslick from a study of Ac-$Hel_1$-$NH_2$.[91] Of the two convenient ways to perturb the mole fraction of the te state, temperature and TFE, the latter was used. Using t/c ratios obtained by NMR and Eq. 2.4, Dr. Oslick obtained a set of seven $\chi_{te}$'s. A linear regression using seven equations in the form of Eq. 4.4 to solve for two unknowns then gives the limiting CD spectra of the template in the cs+ts and the te states, $[\theta_{AcHel,cs+ts}]$ and $[\theta_{AcHel,te}]$ (Fig. 4.3).

Eq. 4.4 $$[\theta_{obs}]=(1-\chi_{te})[\theta_{AcHel,cs+ts}]+\chi_{te}[\theta_{AcHel,te}]$$

For peptide conjugates of Ac-$Hel_1$, correction for the template (Eq. 4.5) gives CD spectra for the peptidyl portion, but a further correction can be made. Peptides attached to the cs+ts state of the template are random coil in nature and can also be subtracted from the observed ellipticities, leaving only partially helical peptides attached to the te nucleating state. To obtain the limiting spectrum of a short peptide in a random coil state, $[\theta_{pept,cs+ts}]$, Dr. Oslick performed a TFE study on the series Ac-$Hel_1$-$Ala_n$-$NH_2$ and Ac-$Hel_1$-$Ala_n$-OH, n=1 to 6. With t/c ratios obtained by NMR and corresponding CD spectra, Eq. 4.6, rewritten as Eq. 4.7, allows the intercept $[\theta_{pept,cs+ts}]$ to be calculated. This is possible since the conformational properties of peptides attached to the cs+ts state of the template are not affected by TFE, in contrast to the partially helical

peptides attached to the te state of the template. The limiting spectrum of a short peptide attached to the cs+ts state resembles typical CD spectra of peptides in the random coil conformation (Fig. 4.3).

Eq. 4.5 $$[\theta_{obs}]=[\theta_{AcHel}]+[\theta_{pept}]$$

Eq. 4.6 $$[\theta_{pept}]=(1-\chi_{te})[\theta_{pept,cs+ts}]+\chi_{te}[\theta_{pept,te}]$$

Eq. 4.7 $$[\theta_{pept}]=[\theta_{pept,cs+ts}]+\chi_{te}([\theta_{pept,te}]-[\theta_{pept,cs+ts}])$$

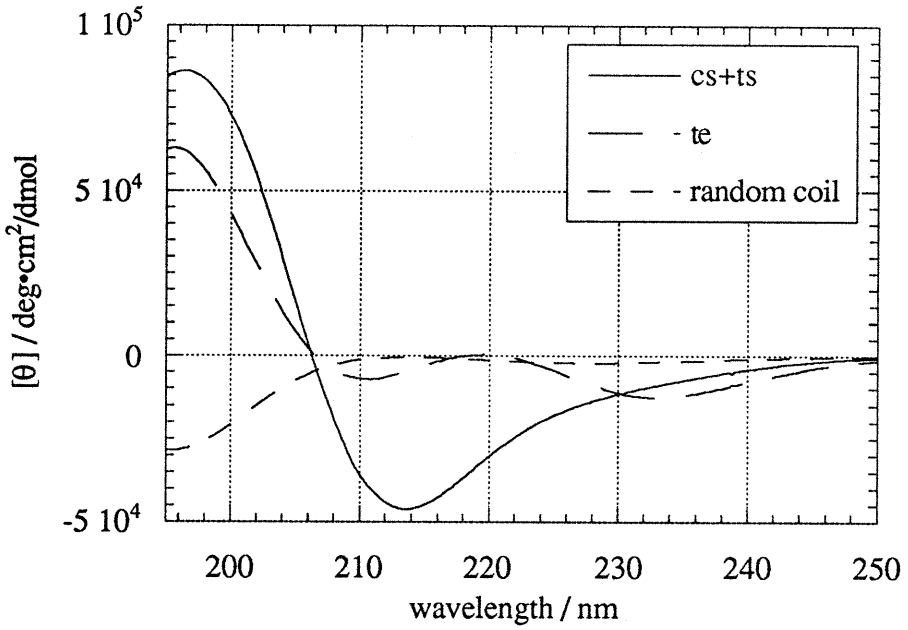


Fig 4.3 CD spectra of cs+ts and te states of $AcHel_1$; and random coil of peptide.

### $Ac\text{-}Hel_1\text{-}Ala_4LysAla_4LysAla_n\text{-}NH_2$, n = 3, 4

With the above limiting spectra for the cs+ts and te states of the template chromophore and the cs+ts state of the random coil conformation, the t/c ratios can be used to analyze the CD spectra of templated $A_4K$ peptides. The peptides $Ac\text{-}Hel_1\text{-}Ala_4LysAla_4LysAla_n\text{-}NH_2$, n = 3, 4 were synthesized and their t/c ratios and CD spectra are shown in Table 4.1 and Figures 4.4 and 4.5.

| Compound | 2 °C | 4 °C | 25 °C | 60 °C |
|---|---|---|---|---|
| Ac-$Hel_1$-$A_4KA_4KA_3$-$NH_2$ | 13.5 | 12.5 | 5.29 | 4.22 |
| Ac-$Hel_1$-$A_4KA_4KA_4$-$NH_2$ | 13.8 | 12.8 | 5.80 | 4.02 |

Table 4.1 t/c ratios for Ac-$Hel_1$-$A_4KA_4KA_3$-$NH_2$, n = 3, 4 at 2, 4, 25, anc 60 °C.

Based on a study by Dr. Tsang of templated dilysine derivatives it can be calculated that the s-value of the first and second lysines of templated peptides with a $(A_4K)_n$ motif are 2.7 and 1.8 respectively.[102] Using Eq. 4.8 and similar ones for the corresponding homologs and substituting values of A = 0.832, B = 0.156, s = 1.02, $s_{K1}$ = 2.7, $s_{K2}$ = 1.8, one calculates t/c ratios for Ac-$Hel_1$-$Ala_4LysAla_4LysAla_n$-$NH_2$ at 25 °C in $D_2O$ for n = 0, 2, 3, 4 of 5.0, 6.8, 7.8 and 8.8, respectively. Experimental t/c data for n = 0 and n = 2 are 5.07 and 6.21, provided by Drs. Tsang and Renold, respectively. The calculated t/c ratios for n = 3, 4 are significantly larger than the experimental values obtained in this study, and it should be noted that the t/c value for n = 2 of 6.21 obtained by Dr. Renold significantly exceeds that for the n = 3, 4 cases; the origin of this discrepancy is unclear and requires further study.

Eq. 4.8
$$\frac{t}{c}_{A4KA4KA3} = A + B(1 + s + \ldots + s^4 + s^4 s_{K1} + s^5 s_{K1} + \ldots + s^8 s_{K1} s_{K2} + s^9 s_{K1} s_{K2} + \ldots + s^{11} s_{K1} s_{K2})$$

Correcting the CD spectra of Ac-$Hel_1$-$Ala_4LysAla_4LysAla_n$-$NH_2$, n = 3, 4 for the template using the t/c ratios shown in Table 4.1 results in the spectra shown in Figures 4.6 and 4.7. The curves at 2 and 4 °C are fairly close.

[102] Tsang, K. Y.; Kemp, D. S. unpublished results.

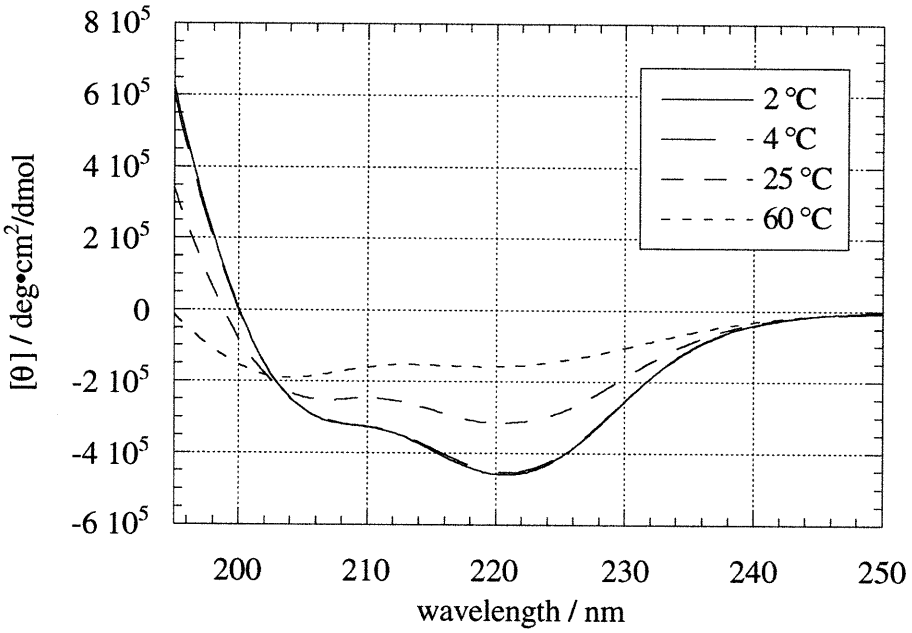


Fig 4.4 CD spectra of Ac-$Hel_1$-$Ala_4LysAla_4LysAla_3$-$NH_2$ at 2, 4, 25, and 60 °C.

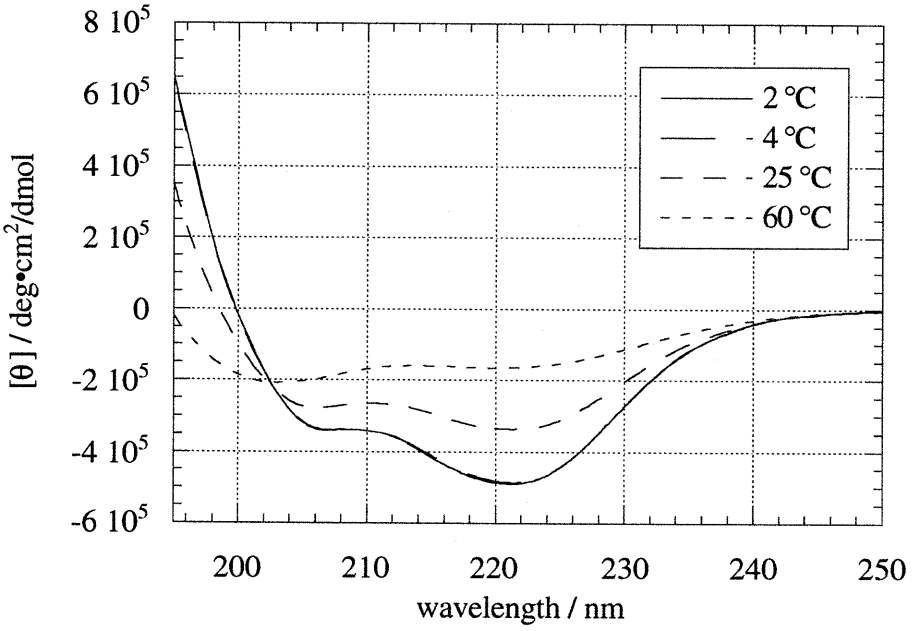


Fig 4.5 CD spectra of Ac-$Hel_1$-$Ala_4LysAla_4LysAla_4$-$NH_2$ at 2, 4, 25 and 60 °C.

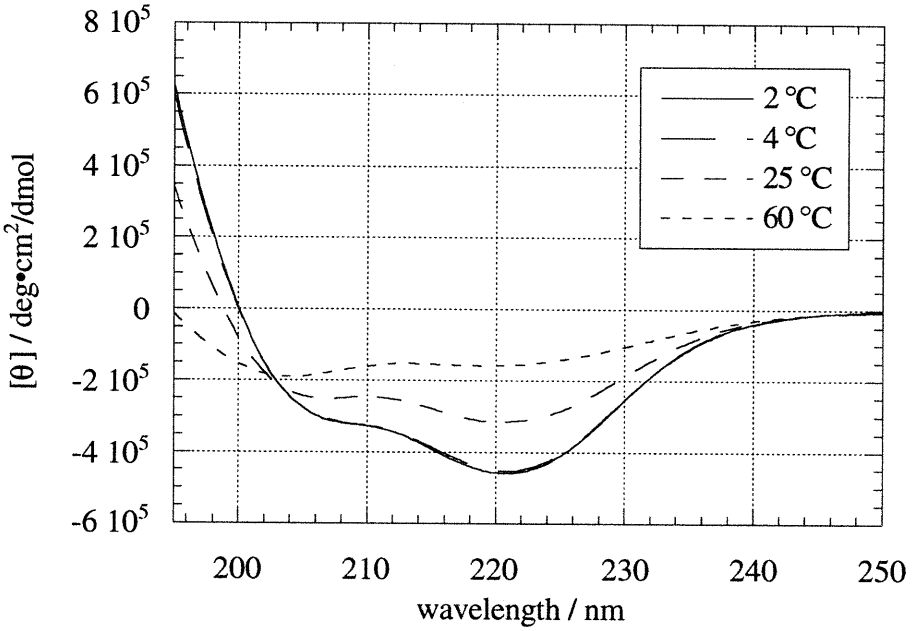


Fig. 4.6 Spectra for Ac-Hel$_1$-$A_4KA_4KA_3$-$NH_2$, at 2, 4, 25, 60 °C corrected for template contributions.

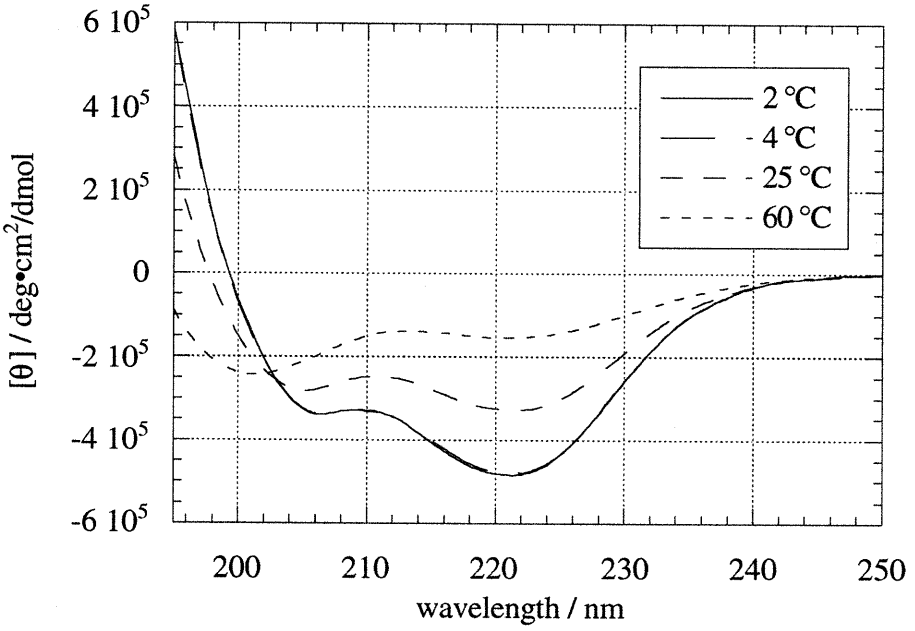


Fig. 4.7 Spectra for Ac-Hel$_1$-$A_4KA_4KA_4$-$NH_2$ at 2, 4, 25, and 60 °C corrected for template contributions.

Further correction for the random coil peptide of the cs+ts states yields the spectra in Fig. 4.8 and 4.9.

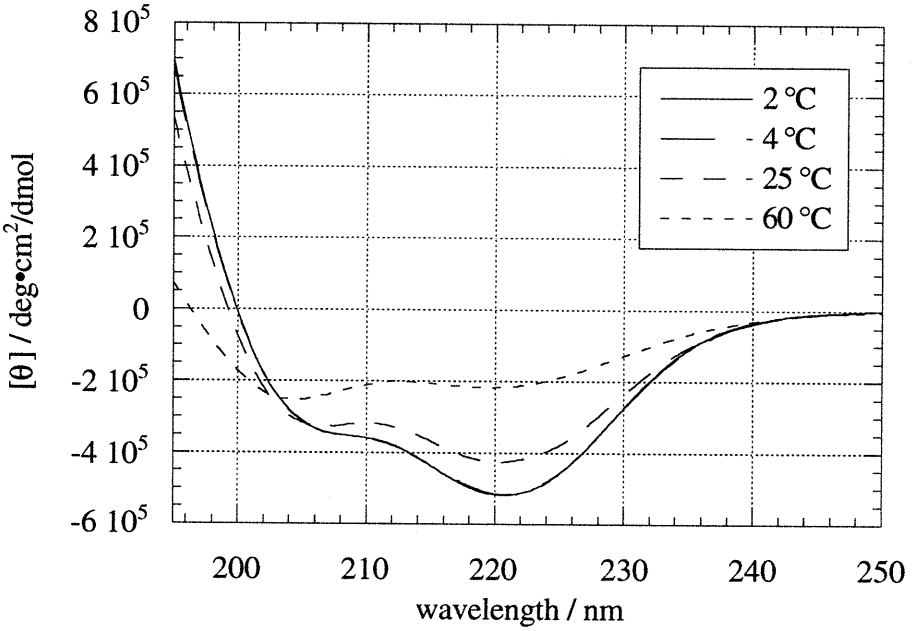


Fig. 4.8 CD spectra of Ac-Hel$_1$-$A_4KA_4KA_3$-$NH_2$ at 2, 4, 25, and 60 °C corrected for template and random coil residues of the cs and ts states.

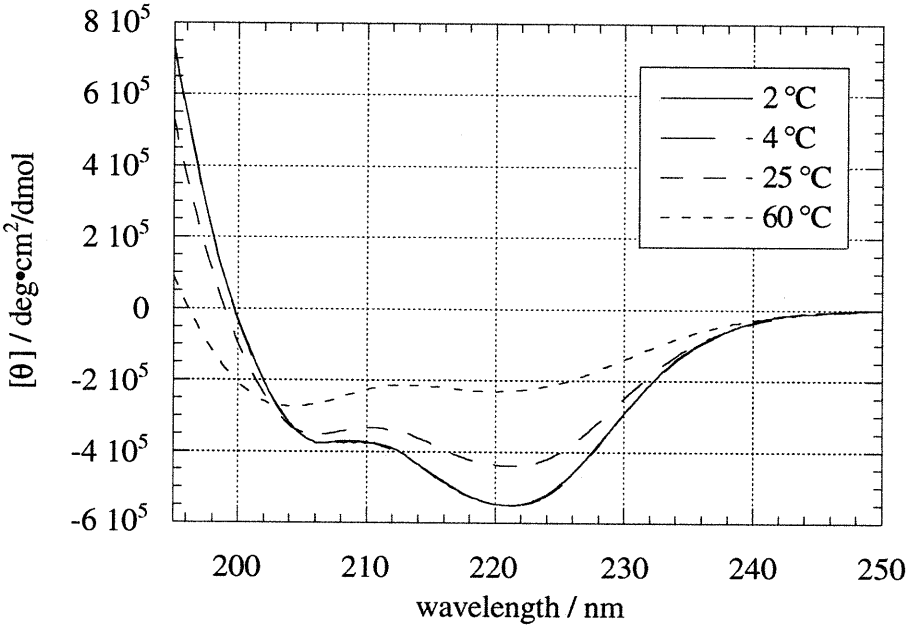


Fig. 4.9 CD spectra of Ac-Hel$_1$-$A_4KA_4KA_4$-$NH_2$ at 2, 4, 25, and 60 °C corrected for template and random coil residues of the cs and ts states.

| | $[\theta]_{222}$ / deg•cm$^2$/dmol | | | |
|---|---|---|---|---|
| Compound | 2 °C | 4 °C | 25 °C | 60 °C |
| Ac-Hel$_1$-A$_4$KA$_4$KA$_3$-NH$_2$ | -512,665 | -511,368 | -419,211 | -211,330 |
| Ac-Hel$_1$-A$_4$KA$_4$KA$_4$-NH$_2$ | -549,323 | -549,969 | -440,586 | -228,896 |

Table 4.2 Molar ellipticities at 222 nm of Ac-Hel$_1$-A$_4$KA$_4$KA$_n$-NH$_2$, n = 3,4 at 2, 4, 25, and 60 °C corrected for template and cs+ts state of peptide.

Using the data from Table 4.2, the per residue ellipticities at 222 nm of the helical peptidyl manifold of Ac-Hel$_1$-A$_4$KA$_4$KA$_n$-NH$_2$, n = 3, 4, are -32,247 and -31,470 deg•cm$^2$/dmol at 25 °C, respectively, similar to the expected values of -31,700 and -32,200 deg•cm$^2$/dmol calculated from the literature formula shown in Eq. 4.9.[103]

Eq. 4.9 $$[\theta]_{\text{per residue, 222 nm}} = -39{,}500 \text{ deg•cm}^2/\text{dmol} \left(1 - \frac{2.57}{N}\right), \text{ where N = peptide length}$$

At 2 °C, the experimental per residue ellipticities at 222 nm are -39,436 and -39,237 deg•cm$^2$/dmol. These values are at the lower, more intense end of the range reported in the literature. However, these peptides have not been corrected for random coil residues within the te state helical manifold and are expected to be slightly more intense upon further correction. Dr. Shimizu has determined the per residue ellipticity at 222 nm to be larger than accepted literature values, up to *ca.* -63,000 deg•cm$^2$/dmol using data from the series Ac-Hel$_1$-Ala$_5$LysAla$_n$-NH$_2$, n = 0 to 7.[85] These large values have been corroborated by Dr. Wallimann with uncorrected values of *ca.* -53,000 deg•cm$^2$/dmol for Ac-Hel$_1$-(Ala$_4$Lys)$_3$Ala$_2$-NH$_2$ at 2 °C.

---

[103] a) Chen, Y. H.; Yang, J. T.; Chau, K. H. *Biochemistry* **1974**, *13*, 3350. b) Gans, P. J.; Lyu, P. C.; Manning, M. C.; Woody, R. W.; Kallenbach, N. R. *Biopolymers* **1991**, *31*, 1605.

**Ac-Hel$_1$-Ala$_5$LysAla$_4$Lys$_n$-NH$_2$, n = 2, 3, 4**

Charged residues at the C-terminus of templated peptides exhibit large t/c ratios, a finding that will be discussed in greater detail in Chapter 5. Presumably this is due to a stabilization by the charged residue of the helix dipole. A study of dilysine derivatives by Dr. Tsang showed that the stability of polyalanine-dilysine isomers is dependent on the number of alanine residues between the two lysine residues. From inspection of the rank order of stability, $KA_4K > KAK > KA_3K \approx KK > KA_2K$, it is apparent that two lysines within one helical turn of the matrix destabilizes the helix. This destabilization could theoretically be neutralized by placing the charged residues at the C-terminus of a peptide. To test this, three peptides that contained multiple adjacent lysines, Ac-Hel$_1$-Ala$_5$LysAla$_4$Lys$_n$-NH$_2$, n = 2, 3, 4, were synthesized. Their t/c ratios and CD spectra are shown in Table 4.3 and Figures 4.7 through 4.9.

| Compound | 2 °C | 4 °C | 25 °C | 60 °C |
|---|---|---|---|---|
| Ac-Hel$_1$-A$_5$KA$_4$K$_2$-NH$_2$ | 12.5 | 11.3 | 5.57 | 4.65 |
| Ac-Hel$_1$-A$_5$KA$_4$K$_3$-NH$_2$ | 14.9 | 14.2 | 5.91 | 4.45 |
| Ac-Hel$_1$-A$_5$KA$_4$K$_4$-NH$_2$ | 16.9 | 16.5 | 5.94 | 4.34 |

Table 4.3 t/c ratios for Ac-Hel$_1$-A$_5$KA$_4$K$_n$-NH$_2$ n = 2, 3, 4 at 2, 4, 25, and 60 °C.

Comparison of the data in Table 4.3 with a t/c ratio of 6.76 for Ac-Hel$_1$-A$_5$KA$_4$KA-NH$_2$ at 25 °C obtained by Dr. Tsang shows that the single substitution of Ala -> Lys at the C-terminus yielding a KK sequence decreases the t/c ratio significantly. The calculated t/c ratio for Ac-Hel$_1$-Ala$_5$LysAla$_4$Lys$_2$-NH$_2$ is given by Eq. 4.10; the corresponding equations for the homologs include additional terms and the additional variables $s_{K4}$ and $s_{K5}$. Using s = 1.0, $s_{K1}$ = 2.7 and the gross approximations $s_{K2}$ = 3.0 and $s_{K3} = s_{K4} = s_{K5}$ = 1.0, the calculated t/c ratios for the series Ac-Hel$_1$-Ala$_5$LysAla$_4$Lys$_n$-NH$_2$ at 25 °C in $D_2O$ for n = 2, 3, and 4 are 6.4, 7.6, and 8.9, respectively. A more reasonable approximation is that $s_{K3} > s_{K4} > s_{K5}$. Using the experimental t/c

ratios for Ac-Hel$_1$-$A_5KA_4KA$-$NH_2$ and Ac-Hel$_1$-$A_5KA_4K_n$-$NH_2$, n = 2, 3, 4 above, one can obtain $s_{K2} = 3.35$ and $s_{K3} = 0.21$. If one assumes that $s_{K3} \approx s_{K4} \approx s_{K5}$, values in the range of 0.2 to 0.4 can be used to fit the experimental data.

Eq. 4.10 $$\frac{t}{c}_{A5KA4K2} = A + B(1 + s + \ldots + s^5 + s^5 s_{K1} + s^6 s_{K1} + \ldots + s^9 s_{K1} s_{K2} + s^9 s_{K1} s_{K2} s_{K3})$$

The CD spectra for Ac-Hel$_1$-$A_5KA_4K_n$-$NH_2$, n = 2, 3, 4 show slightly more intense signals as peptide length increases, with the spectra for n = 3 being very similar to those for n = 4. In addition, a large temperature dependence can be seen, while the curves at 2 and 4 °C are nearly identical.

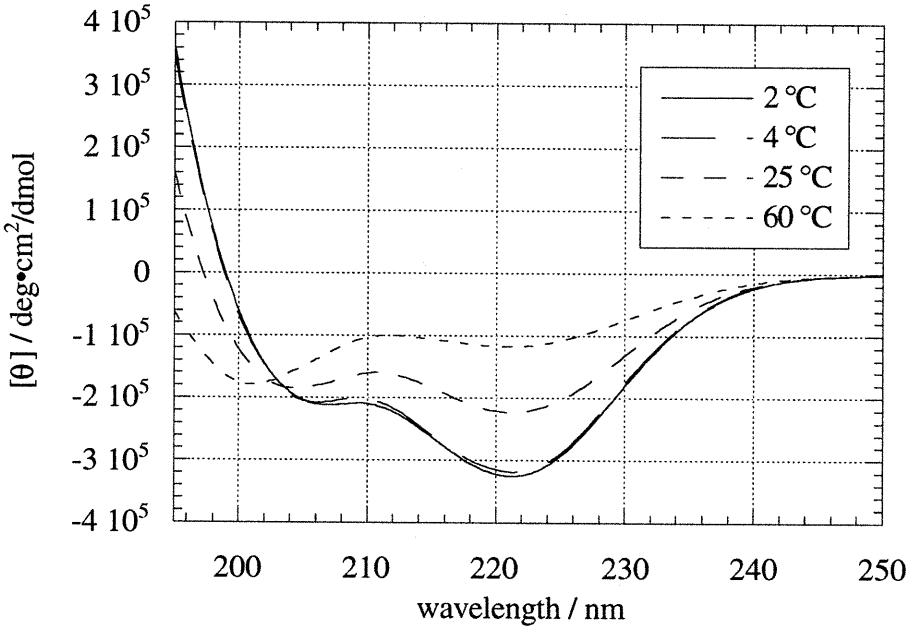


Fig 4.10 CD spectra of Ac-Hel$_1$-$Ala_5LysAla_4Lys_2$-$NH_2$ at 2, 4, 25 and 60 °C.

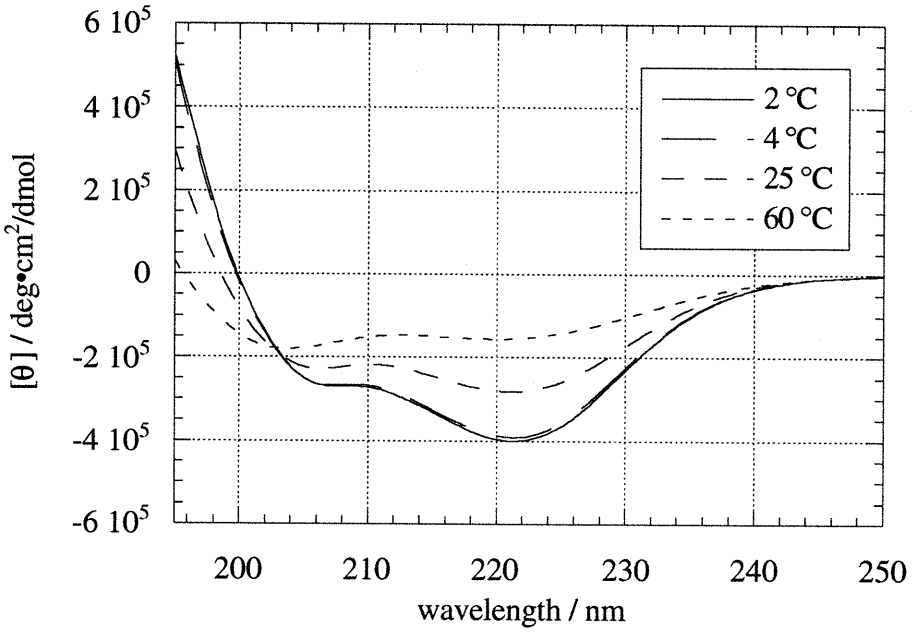


Fig 4.11 CD spectra of Ac-$Hel_1$-$Ala_5LysAla_4Lys_3$-$NH_2$ at 2, 4, 25 and °60 C.

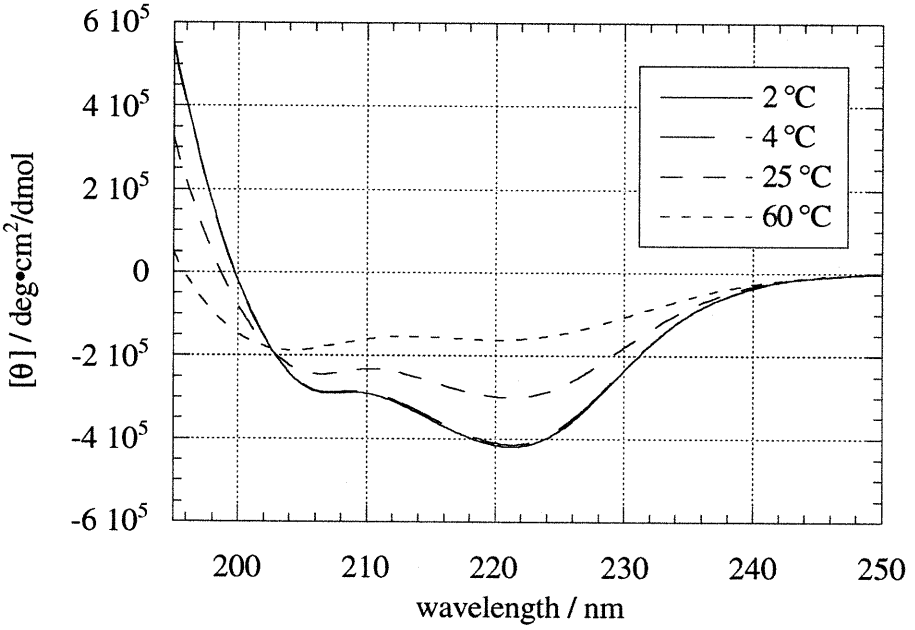


Fig 4.12 CD spectra of Ac-$Hel_1$-$Ala_5LysAla_4Lys_4$-$NH_2$ at 2, 4, 25 and 60 °C.

Correction for the template yields Figures 4.13 through 4.15 using the t/c ratios shown in Table 4.3. As shown before, the template corrected spectra are not too different from the uncorrected spectra.

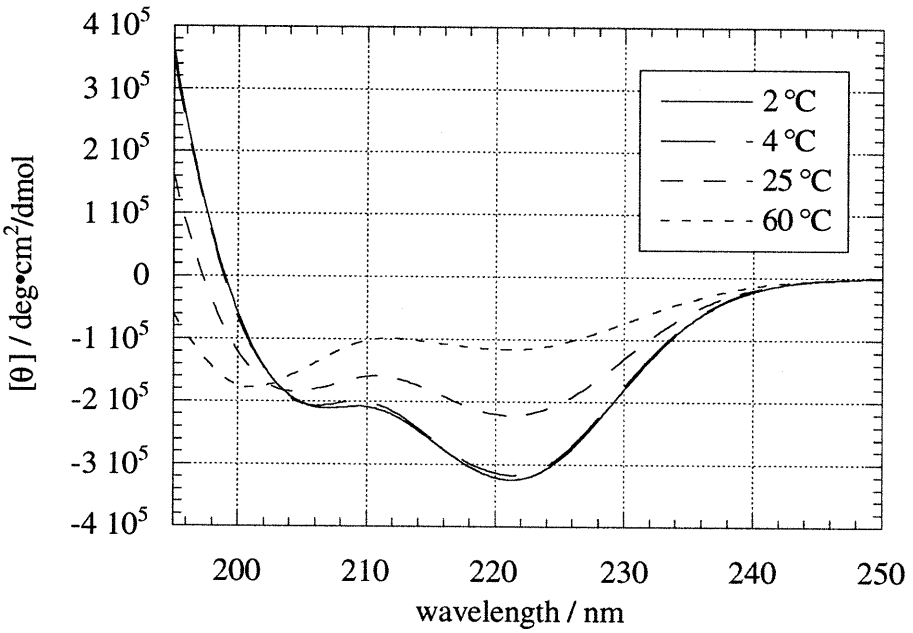


Fig. 4.13 CD spectra of Ac-$Hel_1$-$Ala_5LysAla_4Lys_2$-$NH_2$ at 2, 4, 25 and °60 C corrected for template contributions.

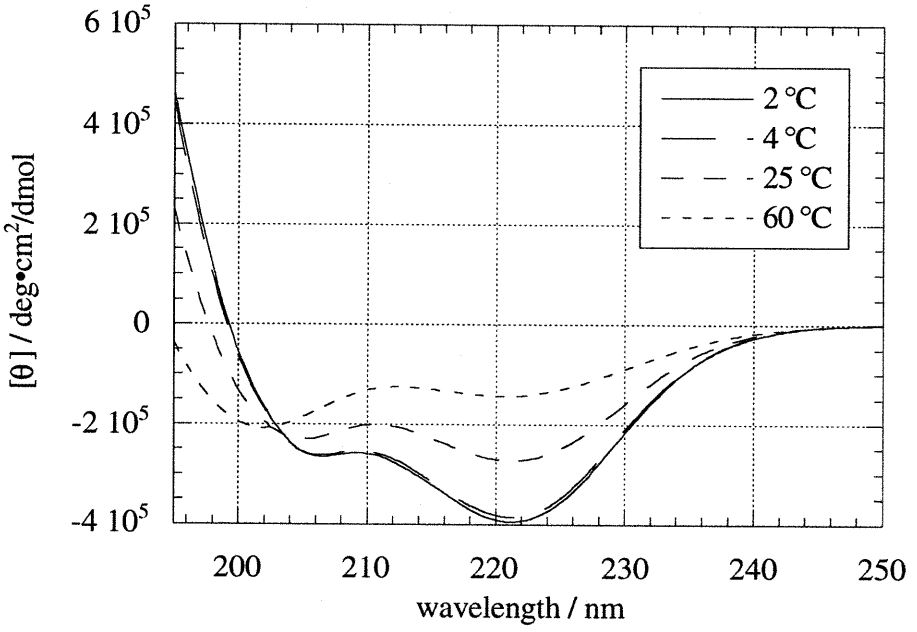


Fig. 4.14 CD spectra of Ac-$Hel_1$-$Ala_5LysAla_4Lys_3$-$NH_2$ at 2, 4, 25 and 60 °C corrected for template contributions.

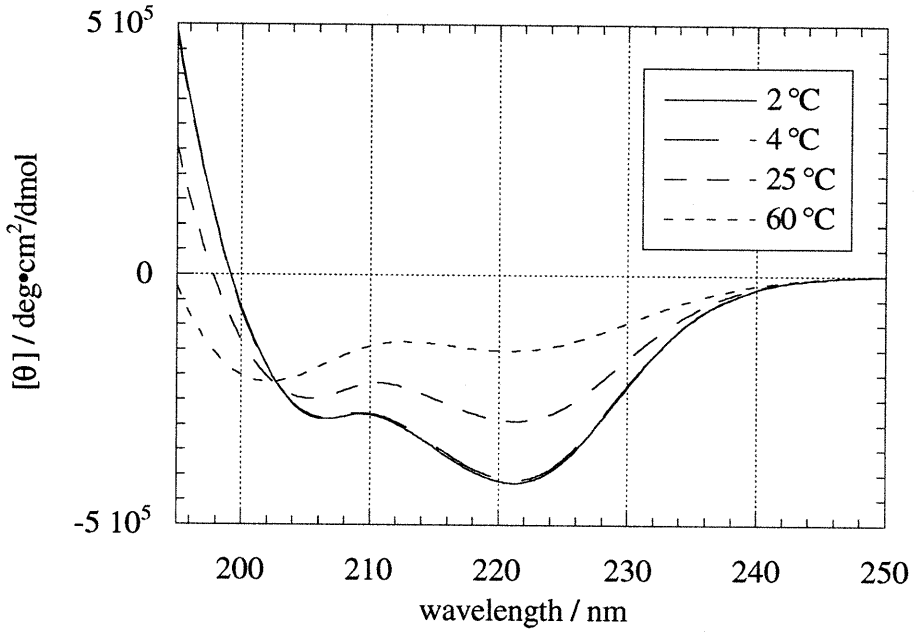


Fig. 4.15 CD spectra of Ac-$Hel_1$-$Ala_5LysAla_4Lys_4$-$NH_2$ at 2, 4, 25 and 60 °C corrected for template contributions.

Correction for the peptide attached to the cs+ts state of the template gives the CD spectra shown in Fig. 4.16 - 4.18.

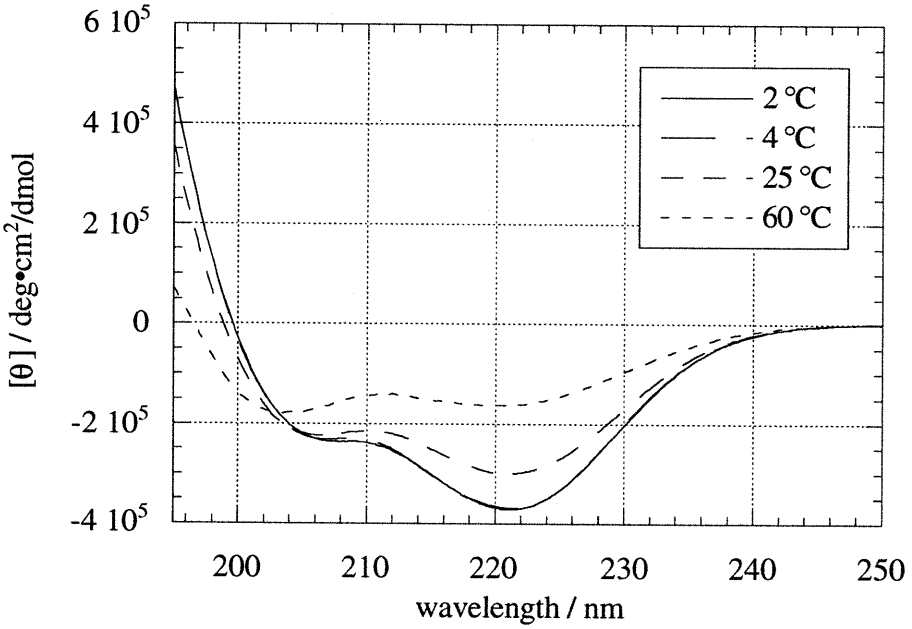


Fig. 4.16 CD spectra of Ac-$Hel_1$-$Ala_5LysAla_4Lys_2$-$NH_2$ at 2, 4, 25 and 60 °C corrected for template and random coil peptide of cs+ts states.

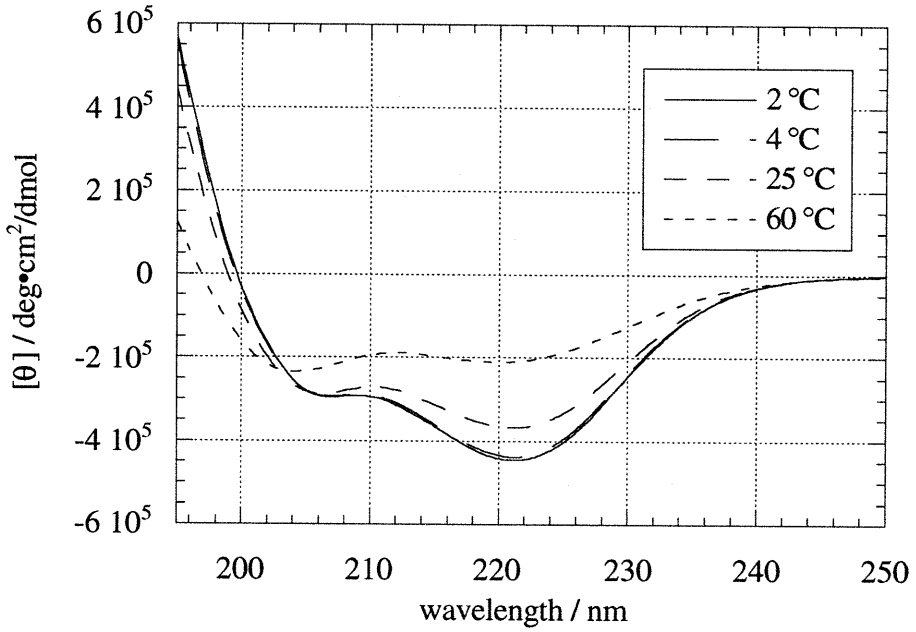


Fig. 4.17 CD spectra of Ac-$Hel_1$-$Ala_5LysAla_4Lys_3$-$NH_2$ at 2, 4, 25 and 60 °C corrected for template and random coil peptide of cs+ts states.

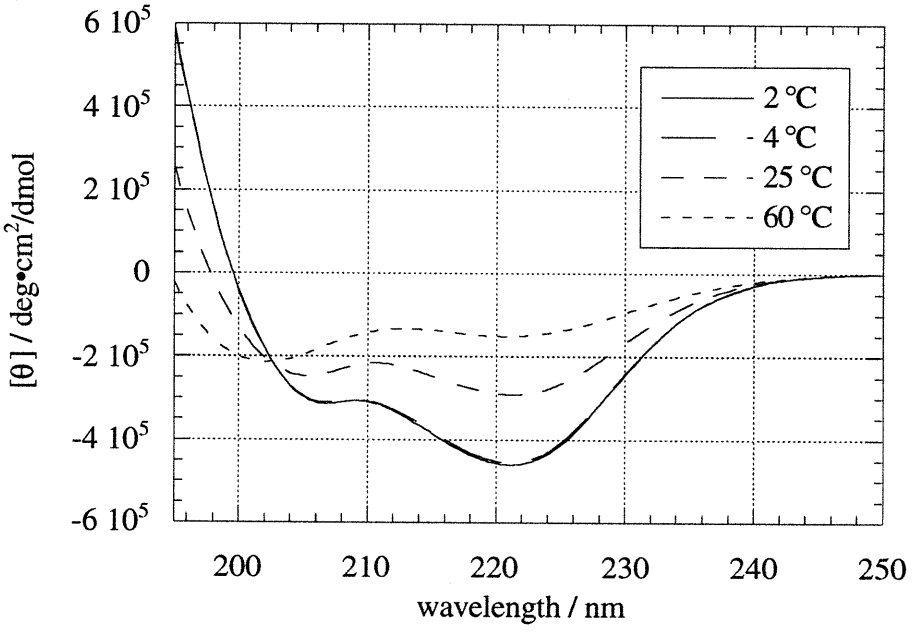


Fig. 4.18 CD spectra of Ac-$Hel_1$-$Ala_5LysAla_4Lys_4$-$NH_2$ at 2, 4,25, and 60 °C corrected for template and random coil peptide of cs+ts states.

| | $[\theta]_{222}$ / deg•cm$^2$/dmol | | | |
|---|---|---|---|---|
| Compound | 2 °C | 4 °C | 25 °C | 60 °C |
| Ac-Hel$_1$-$A_5KA_4K_2$-$NH_2$ | -371,334 | -369,252 | -299,322 | -163,337 |
| Ac-Hel$_1$-$A_5KA_4K_3$-$NH_2$ | -443,378 | -436,800 | -365,249 | -207,080 |
| Ac-Hel$_1$-$A_5KA_4K_4$-$NH_2$ | -459,102 | -454,923 | -388,569 | -217,661 |

Table 4.4 Molar ellipticities at 222 nm of peptides attached to te state of template for Ac-Hel$_1$-$A_5KA_4K_n$-$NH_2$, n = 2, 3, 4.

As can be calculated from the data in Table 4.4 the per residue ellipticities at 222 nm are -24,944, -28,096, and -27,755 deg•cm$^2$/dmol at 25 °C, respectively for n = 2, 3, and 4. At 2 ℃ the values are -30,945, -34,106, and -32,793 deg•cm$^2$/dmol, respectively. The NMR and CD evidence concur that placement of multiple charges at the C-terminus of a peptide chain does not compensate for the electrostatic repulsion of their adjacent side chains that most likely results in greater fraying.

This chapter has shown that templated peptides with the $A_4K$ motif exhibit per residue molar ellipticities within the range reported in the literature and that $s_K$ is position dependent. CD may be sensitive to even slight distortions of a helix and this will be further discussed in the Appendix. In Chapter 5, we examine a context in which lysine is highly stabilizing.

# Chapter 5

## Utilization of Glycine as a Probe of Structure in Ac-$Hel_1$-$Ala_7$-Lys-$NH_2$

## Introduction

Among the natural amino acids, only proline has a higher helix breaking propensity than glycine. In natural proteins glycine is often found at the ends of α helices, particularly at the C-terminus.[104] As noted in Chapter 2, diamides of glycine have exceptionally unconstrained torsional angles ϕ and ψ. Constraining these angles to a helical region requires a higher entropic price, and as a result glycine is expected to be a helix breaker. Unlike proline, glycine can be incorporated within the core of a helix without interrupting the hydrogen bonding pattern or introducing unusual intraloop van der Waals interactions, and for this reason site replacements of particular amino acids by glycine residues has been used to probe local helical structure within a peptide sequence. If a glycine substitution at a site results in a small decrease in overall helicity as measured by a global technique like circular dichroism, then the fractional helical structure at that site prior to the replacement must be low. If by contrast glycine substitution markedly decreases CD-monitored helicity, the fractional helical structure at that site must be high. This test can only be applied with confidence if the helical propensity (s value) of glycine is known reasonably precisely for a variety of peptide sites. Unfortunately, the reported s-values for glycine show a much larger range than for any other amino acid residue. This chapter presents results of a glycine scanning protocol for Ac-$Hel_1$ peptides that allow definition of the ratio $s_{Gly}/s_{Ala}$ and $s_{Gly}$ itself at a series of peptide sites and these values obtained by this protocol are then used to determine the helical propensities of alanine and lysine in particular contexts.

A brief review of the literature of the $s_{Gly}$ problem is appropriate. The oldest experimental value for $s_{Gly}$ was measured by Scheraga and coworkers using random copolymers of glycine and hydroxybutylglutamine; the s-value of glycine was found to be 0.6, with only a slight temperature dependence.[105] These workers noted that although a single glycine residue is not a helix breaker, a

[104] Richardson, J. S.; Richardson, D. C. *Science* **1988**, *240*, 1648.
[105] Ananthanarayanan, V. S.; Andreatta, R. H.; Poland, D.; Scheraga, H. A. *Macromolecules* **1971**, *4*, 417.

block of two or three glycine residues terminates a helix in a polyhydroxybutylglutamine host, as expected from the products $(s_{Gly})^2 = 0.36$ and $(s_{Gly})^3 = 0.22$.[106] A very different value of $s_{Gly} = 0.05$ was reported by Baldwin and coworkers from CD analysis of a $A_2GAK$ context [107c] when compared with an Ac-$YGGKA_4KA_4KA_4K$-$NH_2$ reference peptide.[107ab] These workers also used a glycine scan to probe the dependence of local helicity on amino acid site for this peptide.[107a] It should be noted that the assignment of guest amino acid propensities in this host site are dependent upon the selection of values for the helical propensities for host alanine and lysine, and these values are dramatically inconsistent with corresponding values reported recently with Ac-$Hel_1$ derivatives in the Kemp group.[84ef]

The Scheraga and Baldwin $s_{Gly}$ values are measured in model peptide host contexts. Based on their measurements of the destabilizing effects of Ala -> Gly substitutions within helical contexts of the protein barnase, Fersht and coworkers have noted that stabilization is observed at particular sites, while destabilization is observed at certain other sites.[108] They concluded that contextual factors such as local hydrophobicity within small neighborhoods of the protein override the intrinsic helical propensities of glycine and alanine. If they are correct, s values are nearly irrelevant to helix formation within a protein. A likely alternative hypothesis is that the s value of glycine is exceptionally sensitive to local distortions in helical geometry, such as may arise in particular local protein contexts. If correct, this hypothesis suggests that a large $s_{Gly}$ at a site may reflect the greater tolerance of glycine for deviations in $\phi$ and $\psi$ angles. A first step toward

---

106 Kotelchuck, D.; Scheraga, H. A. *Proc. Natl. Acad. Sci. USA* **1969**, *62*, 14.

107 a) Chakrabartty, A.; Schellman, J. A.; Baldwin, R. L. *Nature* **1991**, *351*, 586. b) Chakrabartty, A.; Kortemme, T.; Padmanabhan, S.; Baldwin, R. L. *Biochemistry* **1993**, *32*, 5560.c) Chakrabartty, A.; Kortemme, T.; Baldwin, R. L. *Prot. Sci.* **1994**, *3*, 843.

108 Serrano, L.; Neira, J.-L.; Sancho, J.; Fersht, A. *Nature* **1992**, *356*, 453.

clarifying this issue is measurement of $s_{Gly}$ in a wide variety of helix contexts using Ac-$Hel_1$ peptide conjugates.

**Ac-$Hel_1$-$Ala_{n-1}GlyAla_{5-n}$-$NH_2$ , n = 2 - 5**

Preliminary studies that provide bounds for $s_{Gly}$ have been carried out by Drs. Boyd[109] and Allen [110] in the Kemp group. The series Ac-$Hel_1$-$G_n$-OH, n = 2, 4, 6 (Boyd) and n = 1, 3, 5, 6 (Allen) can only give results of low precision in the range of 0.2 to 0.6 in water; since helical structure in templated polyglycine diminishes rapidly from the N-terminus, a greater degree of error is associated with the longer peptides. Dr. Allen also prepared Ac-$Hel_1$-$Ala_2GlyAla_3$-OH and Ac-$Hel_1$-$Ala_2GlyAla_4Lys$-$NH_2$, and comparisons with the t/c ratios for the G -> A mutants allowed placement of $s_{Gly}$ in the range of 0.2 to 0.3 for these derivatives. Dr. Boyd also carried out a residue scan in which the alanine residues of Ac-$Hel_1$-$Ala_6$-OH were sequentially replaced with a single glycine. With the exception of site 1 at the template junction, which gave a much higher s-value for glycine, t/c values consistent with $0.2 < s_{Gly} < 0.4$ were observed.

In the remainder of this section a series of glycine substitutions in an alanine host will be used to determine $s_{Gly}$ with greater precision and provide site-dependent values for $s_{Gly}$. It will utilize two analyses of the t/c data for templated heteropeptides Ac-$Hel_1$-$Ala_{n-1}GlyAla_{5-n}$-$NH_2$, n = 2 - 5, to determine the s-value of glycine. The first analysis requires knowledge of the t/c value for the parent pentaalanine Ac-$Hel_1$-$Ala_5$-$NH_2$, as well as the s-value for alanine and the template constant B. It yields an average of $s_{Gly}$ over the n = 2 to 5 series. This analysis depends upon a fundamental relationship among the difference ($s_{Gly}$-s), as well as t/c values for the parent Ac-

[109] Boyd, J. G., Ph.D. Thesis, Massachusetts Institute of Technology, 1989.
[110] Allen, T. J., Ph.D. Thesis, Massachusetts Institute of Technology, 1993.

$Hel_1$-$Ala_5$-$NH_2$ and a corresponding glycyl heteropeptide, shown in Eq. 5.1.

Eq. 5.1 $$\left(\frac{t}{c}\right)_{A(n-1)GA(5-n)} = \left(\frac{t}{c}\right)_{A5} + B\left(s_G - s\right)s^{n-1}\frac{s^{6-n}-1}{s-1}$$

A derivation of Eq. 5.1 for the case of n = 2 begins with the mass action expression for the homoalanine parent (Eq. 5.2) and that for the heteropeptide (Eq. 5.3) which can be rewritten as shown.

Eq. 5.2 $$\left(\frac{t}{c}\right)_{A5} = A + B\left(\frac{s^6-1}{s-1}\right) = A + B\left(1+s+s^2+s^3+s^4+s^5\right)$$

Eq. 5.3 $$\left(\frac{t}{c}\right)_{AGA3} = A + B(1+s+ss_G+s^2s_G+s^3s_G+s^4s_G)$$

$$= A + B(1+s) + Bss_G(1+s+s^2+s^3)$$

$$= A + B(1+s) + \left[B\left(s^2+s^3+s^4+s^5\right)\right.$$

$$\left. - Bs^2\left(1+s+s^2+s^3\right)\right]$$

$$+ Bss_G\left(1+s+s^2+s^3\right)$$

$$= A + B(1+s+s^2+s^3+s^4+s^5)$$

$$+ Bs(s_G-s)(1+s+s^2+s^3)$$

$$\left(\frac{t}{c}\right)_{AGA3} = \left(\frac{t}{c}\right)_{A5} + Bs(s_G-s)\frac{s^4-1}{s-1}$$

Eq. 5.1 shows that the measured t/c values for the series Ac-$Hel_1$-$Ala_{n-1}$GlyAla$_{5-n}$-$NH_2$ must be a linear function of $s^{n-1}(s^{6-n}-1)/(s-1)$ with a zero intercept of $(t/c)_{A5}$ and a slope of $B(s_G-s)$. Tests of the assumption that $s_{Gly}$ is nearly constant over the series are provided by the accuracy of the linear correlation and a correspondence between the calculated and experimental values of $(t/c)_{A5}$. Table 5.1 shows experimental values for $(t/c)_{A(n-1)GA(5-n)}$ at 25 °C in $D_2O$, pH 7, with a likely error of ± 0.1. The data show unambiguously that replacement of an alanine residue by a structure-breaking glycine results in the largest t/c reduction at the site closest to the template-

peptide junction and the smallest at the C-terminus. This result is consistent with the helix fraying pattern expected for helix nucleation from the N-terminus. Figure 5.1 shows their dependence on $s^{n-1}(s^{6-n}-1)/(s-1) = s^{n-1}(1+s+s^2+...+s^{5-n})$ for s = 1.0, the value obtained by Dr. Tsang from a least squares analysis of the t/c values for more than thirty templated peptides Ac-$Hel_1$-$Ala_n$LysAla$_m$-$NH_2$, n = 2 to 6, m = 1 to 6.[112b] The correlation is clearly linear within the error limits of the data, and the zero intercept of 1.82 is consistent with the experimental values of 1.78 and 1.93 for the t/c ratio of Ac-$Hel_1$-$Ala_5$-$NH_2$. The calculated slope is -0.122, equal to $B(s_G-s)$. Values of s = 1.0 and B = 0.156 obtained from the large lysine data set yield an average value of $s_{Gly}$ for the series of 0.22, in the range previously determined for other templated peptides by Drs. Allen and Boyd.

| Compound | t/c at 25 °C |
|---|---|
| Ac-$Hel_1$-AAAAA-$NH_2$ | 1.78 ± 0.09, 1.93 ± 0.10 |
| Ac-$Hel_1$-AGAAA-$NH_2$ | 1.29 ± 0.06 |
| Ac-$Hel_1$-AAGAA-$NH_2$ | 1.51 ± 0.08 |
| Ac-$Hel_1$-AAAGA-$NH_2$ | 1.56 ± 0.08 |
| Ac-$Hel_1$-AAAAG-$NH_2$ | 1.68 ± 0.08 |

Table 5.1 Experimental t/c ratios for Ac-$Hel_1$-$Ala_{n-1}$GlyAla$_{5-n}$-$NH_2$, n = 2, 3, 4, and 5 at 25 °C in $D_2O$, pH 7. Data for Ac-$Hel_1$-$A_5$-$NH_2$ from Drs. McClure and Tsang, respectively.

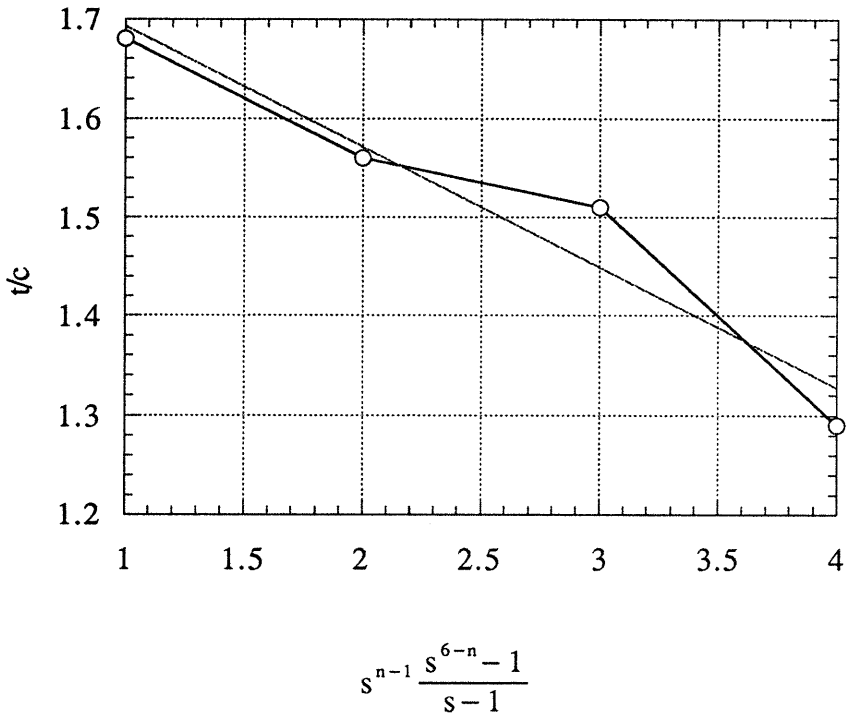


Fig. 5.1 t/c *vs.* $s^{n-1}(s^{6-n}-1)/(s-1)$ for Ac-$Hel_1$-$Ala_{n-1}GlyAla_{5-n}$-$NH_2$, n = 2 to 5, using s = 1.0.

The second analysis uses experimental t/c ratios for templated mono- to tetraalanine peptides and gives site-specific s-values for glycine. The general form for the t/c ratios of the series Ac-$Hel_1$-$Ala_{n-1}GlyAla_{5-n}$-$NH_2$, although shown in one form in Eq. 5.3, can also be written as Eq. 5.4.

Eq. 5.4 $$\left(\frac{t}{c}\right)_{A(n-1)GA(5-n)} = A + B\left(\frac{s^n-1}{s-1} + s^{n-1}s_G\frac{s^{6-n}-1}{s-1}\right)$$

Eq. 5.5 $$\alpha_{n-1} = \left(\frac{t}{c}\right)_{A(n-1)} = A + B\left(\frac{s^n-1}{s-1}\right)$$

Let $\alpha_{n-1}$ correspond to the t/c ratios for Ac-Hel$_1$-Ala$_{n-1}$-NH$_2$ (Eq. 5.5) for which experimental values are known. Then subtracting Eq. 5.5 from Eq. 5.4 and from Eq. 5.2 gives Eq. 5.6 and Eq. 5.7, respectively.

Eq. 5.6 $$\left(\frac{t}{c}\right)_{A(n-1)GA(5-n)} - \alpha_{n-1} = B\left(s^{n-1}s_G\frac{s^{6-n}-1}{s-1}\right)$$

Eq. 5.7 $$\left(\frac{t}{c}\right)_{A5} - \alpha_{n-1} = B\left(\frac{s^6-1}{s-1} - \frac{s^n-1}{s-1}\right) = B\left(\frac{s^6-s^n}{s-1}\right)$$

Dividing Eq. 5.6 by Eq. 5.7 gives Eq. 5.8, which is equal to the ratio of $s_{Gly}/s_{Ala}$:

Eq. 5.8 $$\frac{\left(\frac{t}{c}\right)_{A(n-1)GA(5-n)} - \alpha_{n-1}}{\left(\frac{t}{c}\right)_{A5} - \alpha_{n-1}} = \frac{s^{n-1}s_G(s^{6-n}-1)}{s^6-s^n} = \frac{s_G(s^5-s^{n-1})}{s^6-s^n}\cdot\frac{s}{s}$$

$$= \frac{s_G(s^6-s^n)}{(s^6-s^n)s} = \frac{s_G}{s}$$

Eq. 5.8 implies that $s_{Gly}/s_{Ala}$ at a given site equals the ratio of a pair of differences of t/c values. Since the error of a difference is the sum of the errors in the components, the ratio is poorly determined when the magnitude of the difference in the numerator is small relative to the components, as is the case for the glycine substitutions close to the C-terminus. The best results for this analysis are obtained by using values for $\alpha_{n-1}$ that are calculated from a linear regression, as shown in Table 5.2. Values calculated for $s_{Gly}/s_{Ala}$ are shown in Table 5.3; within the error limits of the analysis (*ca.* 0.14 to 0.61) they show no position dependence.

| Compound | t/c at 25 °C |
|---|---|
| Ac-$Hel_1$-$NH_2$ | 1.86 ± 0.09 |
| Ac-$Hel_1$-A-$NH_2$ | 1.16 ± 0.06 |
| Ac-$Hel_1$-AA-$NH_2$ | 1.31 ± 0.07 |
| Ac-$Hel_1$-AAA-$NH_2$ | 1.46 ± 0.07 |
| Ac-$Hel_1$-AAAA-$NH_2$ | 1.62 ± 0.08 |
| Ac-$Hel_1$-AAAAA-$NH_2$ | 1.77 ± 0.09 |
| Ac-$Hel_1$-AAAAAA-$NH_2$ | 1.92 ± 0.10 |

Table 5.2 t/c ratios for Ac-$Hel_1$-$Ala_{n-1}$-$NH_2$, n = 1 to 7 at 25 °C derived from least squares fit of experimental values except for n = 1. Data from Dr. McClure.

| Compound | $s_{Gly}/s_{Ala}$ at 25 °C |
|---|---|
| Ac-$Hel_1$-AGAAA-$NH_2$ | 0.20 ± 0.14 |
| Ac-$Hel_1$-AAGAA-$NH_2$ | 0.39 ± 0.21 |
| Ac-$Hel_1$-AAAGA-$NH_2$ | 0.28 ± 0.31 |
| Ac-$Hel_1$-AAAAG-$NH_2$ | 0.30 ± 0.61 |

Table 5.3 $s_{Gly}/s_{Ala}$ for Ac-$Hel_1$-$Ala_{n-1}$ $GlyAla_{5-n}$-$NH_2$, n = 2 to 5 at 25 °C.

The temperature dependence of s values is an important parameter. Previous work in this group by Drs. Shimizu, Tsang, and Renold[112b] has shown that the temperature dependence of $s_{Ala}$ in templated peptides in the range of 0 to 60 °C is small and within the error limits of the analysis. The data of Fig. 5.2 show that the temperature dependence of t/c ratios for templated glycine derivatives in this series is also small, implying that $s_{Gly}$ in this case must be nearly temperature independent. The limited temperature data for $Ala_n$ homologs do not permit accurate determination of the temperature dependence of $s_{Gly}/s_{Ala}$.

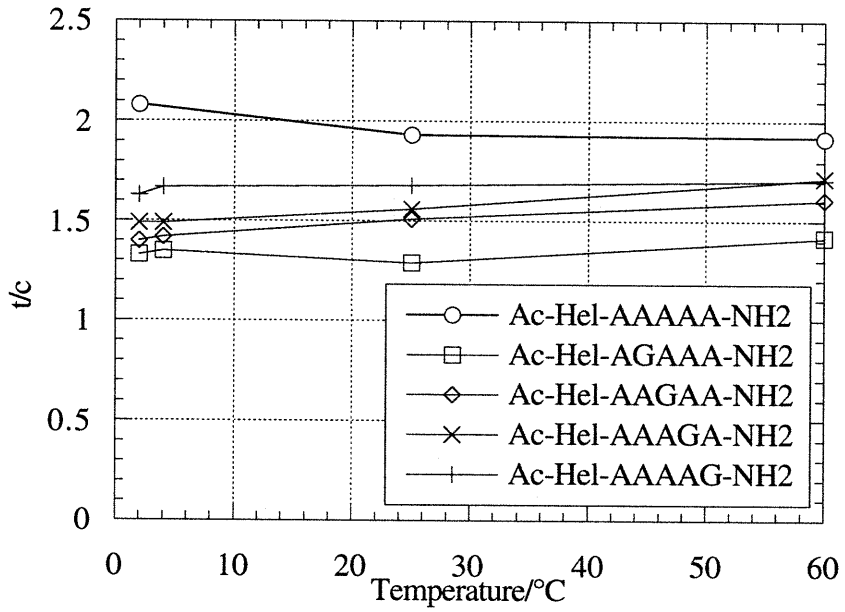


Fig 5.2 t/c ratio vs. temperature for Ac-$Hel_1$-$A_5$-$NH_2$ and Ac-$Hel_1$-$A_{n-1}GA_{5-n}$-$NH_2$, n = 2 to 5. Data for Ac-Hel-$Ala_5$-$NH_2$ from Dr. Tsang.

In this section, the s-value of glycine has been determined to be in the range of 0.2 to 0.3 using two different analyses. Consistent with the results, Dr. Tsang has shown $s_{Gly}$ to be *ca.* 0.3 for a series of alanine-rich peptides. The values obtained in the Kemp laboratories are smaller than the value of 0.6 reported by Scheraga and significantly larger than the $s_{Gly} = 0.05$ value reported by Baldwin. A source of this substantial discrepancy probably stems from Baldwin's assignment of a very high s value for alanine. For any given fractional helicity of an alanine rich peptide, an unusually high s-value for alanine results in an unusually low s-value for glycine. This returns us to the issue of the s-value for alanine. The remainder of this chapter will also employ a glycine scan to investigate the s-values of alanine and lysine in the alanine-rich templated peptide Ac-$Hel_1$-$Ala_7$-Lys-$NH_2$. A side result of this will be that $s_{Gly}/s_{Ala}$ falls in the range of 0.20 to 0.35, providing additional support for the results presented heretofore in this chapter.

## $Ac\text{-}Hel_1\text{-}Ala_7Lys\text{-}NH_2$ and $Ac\text{-}Hel_1\text{-}A_{n-1}GlyAla_{7-n}Lys\text{-}NH_2$, n = 1 - 7

Positively charged residues such as Lys and His at the C-terminus of a helical segment confer stability due to an electrostatic interaction between the charged side chain and the helix dipole. Lysine also has a long and flexible side chain that may wrap around the helix barrel, raising the issue of hydrophobic effects.[84e,111] The majority of the peptide matrices used in helicity studies include lysine to solubilize alanine rich peptides, with the assumption that lysine does not introduce too great a helical bias. Baldwin's comparison of alanine based peptide isomers shows that a greater number of lysine residues results in a decrease in helicity, and the unusual stability of the $(A_4K)_n$ host must therefore be due to a high helical propensity for alanine. Inspection of these sequences show that each isomer of decreasing helicity introduces a $KA_2K$ segment, which has been shown by work of Dr. Tsang in these laboratories to destabilize the helix.[84f] In fact this is the worst placement that two lysines can have relative to one another in terms of helicity. The remainder of this chapter will show by an independent analysis that alanine is not responsible for the large helix-stabilizing effect in an $Ala_7Lys$ context, but rather lysine.

The most suitable residue for use as a matrix in helicity studies is one in which the side chain interferes least. Although glycine would be just such a residue, an untemplated homoglycine sequence would have no significant helical population. Homoalanine has thus been the matrix of choice. Since aggregation is observed with sequences containing over seven contiguous alanines, lysine or glutamic acid residues are often included for solubility.

A charged residue at the termini of helices, however, has a special effect. When placed at the terminus of the helix dipole of opposite charge, stabilization is expected. This charge-dipole effect has been investigated by many researchers in protein and in peptide systems. Baldwin and coworkers have studied the effect of a histidine residue at the C-terminus of a $(A_4K)_n$ host; a

---

[111] Padmanabhan, S.; York, E. J.; Stewart, J. M.; Baldwin, R. L. *J. Mol. Biol.* **1996**, *257*, 726.

charged histidine at the C-terminus of the host gives a more intense CD signal compared to neutral histidine.[112] The remainder of this section will determine whether lysine stabilizes a helix in an $A_7K$ sequence and what role alanine plays, if any. This work is built upon studies in this group by Dr. Tsang, who measured the temperature dependence of t/c ratios for the series Ac-$Hel_1$-$Ala_7$-X-$NH_2$, X = Arg, Orn, His, and noted the exceptional helicity increase for all members as the temperature approached 0 °C.

A glycine scan of the alanine region of Ac-$Hel_1$-$Ala_7$-Lys-$NH_2$ is first used to determine the amount of helical structure up to each site. The t/c ratios for the series Ac-$Hel_1$-$A_{n-1}GlyAla_{7-n}$Lys-$NH_2$, n=1-7 and for the parent compound are shown in Table 5.4. With one notable exception, the data of the table at all temperatures show the expected monotonic decrease in t/c-measured helicity as the glycine site approaches the template junction. Substitution at that junction results in a much less dramatic decrease, implying that glycine at that site is only moderately destabilizing. Boyd has also noted this effect in other series, which has been attributed to the anomalous $3_{10}$-α hybrid geometry at this site; at the peptide junction the glycyl NH, for which there is no formal hydrogen bond acceptor, may interact favorably with a water molecule.[109]

---

[112] Armstrong, K. M.; Baldwin, R. L. *Proc. Natl. Acad. Sci. USA* **1993**, *90*, 11337.

| Compound | t/c at 2 °C | t/c at 25 °C | t/c at 60 °C | $s_{Gly}/s_{Ala}$ at 25 °C |
|---|---|---|---|---|
| Ac-$Hel_1$-AAAAAAAK-$NH_2$ | 5.16 ± 0.26 | 3.45 ± 0.17 | 2.52 ± 0.13 | n/a |
| Ac-$Hel_1$-GAAAAAAK-$NH_2$ | 3.55 ± 0.18 | 2.94 ± 0.15 | 2.41 ± 0.12 | 0.68 ± 0.14 |
| Ac-$Hel_1$-AGAAAAAK-$NH_2$ | 1.75 ± 0.09 | 1.66 ± 0.08 | 1.72 ± 0.09 | 0.22 ± 0.05 |
| Ac-$Hel_1$-AAGAAAAK-$NH_2$ | 1.79 ± 0.09 | 1.74 ± 0.09 | 1.99 ± 0.10 | 0.20 ± 0.05 |
| Ac-$Hel_1$-AAAGAAAK-$NH_2$ | 2.10 ± 0.11 | 1.98 ± 0.10 | 2.11 ± 0.11 | 0.26 ± 0.07 |
| Ac-$Hel_1$-AAAAGAAK-$NH_2$ | 2.27 ± 0.11 | 2.10 ± 0.11 | 2.18 ± 0.11 | 0.26 ± 0.08 |
| Ac-$Hel_1$-AAAAAGAK-$NH_2$ | 2.68 ± 0.13 | 2.35 ± 0.12 | 2.27 ± 0.11 | 0.35 ± 0.10 |
| Ac-$Hel_1$-AAAAAAGK-$NH_2$ | 3.48 ± 0.17 | 2.75 ± 0.14 | 2.48 ± 0.12 | 0.54 ± 0.13 |

Table 5.4 t/c ratios at 2, 25, and 60 °C in $D_2O$ at pH 7; and $s_{Gly}/s_{Ala}$ at 25 °C for the series T-$A_{n-1}GA_{7-m}K$-$NH_2$, n = 1 to 7.

The mass action equations relating the t/c ratio and the s-values for Ac-$Hel_1$-$A_7K$-$NH_2$ in its simplest form is shown in Eq. 5.9. This can be rewritten as Eq. 5.10 for use with the corresponding equations for the glycine isomers, where n will be the site of substitution.

Eq. 5.9 $$\left(\frac{t}{c}\right)_{A7K} = A + B\left(\frac{s^8 - 1}{s - 1} + s^7 s_K\right)$$

Eq. 5.10 $$\left(\frac{t}{c}\right)_{A7K} = A + B\left[\frac{s^n - 1}{s - 1} + s^{n-1} s\left(\frac{s^{8-n} - 1}{s - 1} + s^{7-n} s_K\right)\right]$$

Let $\alpha_{n-1}$ again be the t/c ratio for the longest templated homoalanine compound contained in the glycine isomer (Eq. 5.5).

Eq. 5.11 $$\left(\frac{t}{c}\right)_{A(n-1)GA(7-n)K} = A + B\left[\frac{s^n - 1}{s - 1} + s^{n-1} s_G\left(\frac{s^{8-n} - 1}{s - 1} + s^{7-n} s_K\right)\right]$$

Subtraction of $\alpha_{n-1}$ from Eq. 5.10 and from Eq. 5.11, and algebraic manipulation analogous to Eq. 5.6 to 5.8 allows $s_{Gly}/s_{Ala}$ to be related to experimental t/c ratios (Eq. 5.12). Unlike the data for the Ac-$Hel_1$-$Ala_5$-$NH_2$ series described previously, the two terms in the numerator of Eq. 5.12 are significantly different, and the error in $s_{Gly}/s_{Ala}$ values obtained by this analysis is

correspondingly lower, *ca.* 0.05 to 0.14.

Eq. 5.12 $$\frac{\left(\frac{t}{c}\right)_{A(n-1)GA(7-n)K} - \alpha_{n-1}}{\left(\frac{t}{c}\right)_{A7K} - \alpha_{n-1}} = \left(\frac{s_G}{s}\right)_n$$

Using Eq. 5.12 and the t/c ratios from Tables 5.4 and 5.2, one can obtain the calculated ratios of $s_{Gly}/s_{Ala}$ shown in Table 5.4. Excepting the two sites adjacent to the template and to the lysine, the range of $s_{Gly}$ (assuming $s_{Ala}$ *ca.* 1) is consistent with the results of the previous section. There appears to be a general trend of higher $s_{Gly}$ approaching either terminus, suggesting that in Ac-$Hel_1$-$Ala_7$-Lys-$NH_2$ there are helix-distorting effects at either end. As discussed in the previous section, the template induces structure at the template-peptide junction. In the remainder of this chapter we will confirm the helix-stabilizing ability of lysine and the passive nature of alanine.

Using Eq. 5.9, the t/c ratio for Ac-$Hel_1$-$Ala_7$-Lys-$NH_2$, and the values of A = 0.832 and B = 0.156 reported by Dr. Tsang, one can obtain a list of possible solutions in the form of s-value pairs ($s_{Ala}$,$s_{Lys}$). Examples of such pairs are shown in Fig. 5.3. As can be seen, a small value of $s_{Ala}$ correlates with a large $s_{Lys}$. We now use these correlated pairs, the $s_G/s_A$ ratios and the experimental t/c ratios of Table 5.4 to determine the most valid ($s_{Ala}$,$s_{Lys}$) pair.

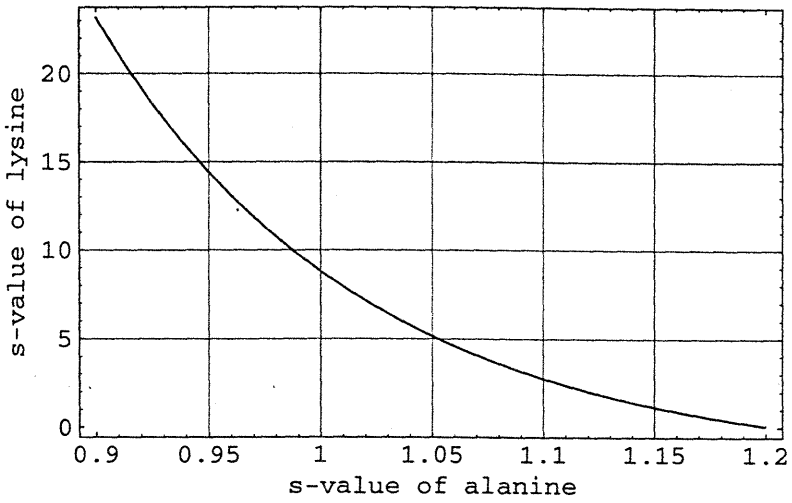


Fig. 5.3 $s_{Lys}$ vs. $s_{Ala}$ using Eq. 5.9 and t/c for Ac-$Hel_1$-$Ala_7$-Lys-$NH_2$ at 25 °C.

The iterative calculation starts by selection of an ($s_{Ala}$, $s_{Lys}$) pair from Fig. 5.3. Substitution of the $s_{Ala}$ value into the $s_{Gly}/s_{Ala}$ ratios from Table 5.4 yields an $s_{Gly}$ for each member of the series. Substituting A, B, $s_{Ala}$, $s_{Lys}$, and $s_{Gly}$ into Eq. 5.11 yields a calculated t/c ratio for each member of the substitution series, as shown in Table 5.5. Finally, substitution of $(t/c)_{calc}$ and $(t/c)_{exptl}$ pairs into Eq. 5.13 yields an overall estimate of fit for the seven-member substitution series. The results of this calculation for a series of choices of ($s_{Ala}$, $s_{Lys}$) are shown in Fig. 5.4.

| s(Ala) | s(Lys) | n=1 | n=2 | n=3 | n=4 | n=5 | n=6 | n=7 |
|---|---|---|---|---|---|---|---|---|
| 0.96 | 13.1 | 2.66 | 1.64 | 1.72 | 1.95 | 2.05 | 2.29 | 2.69 |
| 0.97 | 11.8 | 2.66 | 1.64 | 1.72 | 1.96 | 2.06 | 2.71 | 2.71 |
| 0.98 | 10.7 | 2.66 | 1.64 | 1.72 | 1.96 | 2.07 | 2.72 | 2.72 |
| 0.99 | 9.7 | 2.66 | 1.65 | 1.73 | 1.97 | 2.08 | 2.74 | 2.74 |
| 1.00 | 8.8 | 2.66 | 1.65 | 1.73 | 1.98 | 2.09 | 2.75 | 2.75 |
| 1.01 | 7.9 | 2.66 | 1.65 | 1.74 | 1.98 | 2.11 | 2.77 | 2.77 |
| 1.02 | 7.1 | 2.66 | 1.65 | 1.74 | 1.99 | 2.12 | 2.78 | 2.78 |

Table 5.5 Calculated t/c ratios of Ac-$Hel_1$-$Ala_{n-1}GlyAla_{7-n}$Lys-$NH_2$ at 25 °C for selected $s_{Ala}$,$s_{Lys}$ pairs.

Eq. 5.13 $$\text{error} = \sqrt{\sum_{i=1}^{7}\left[\left(\frac{t}{c}\right)_{exptl} - \left(\frac{t}{c}\right)_{calc}\right]^2}$$

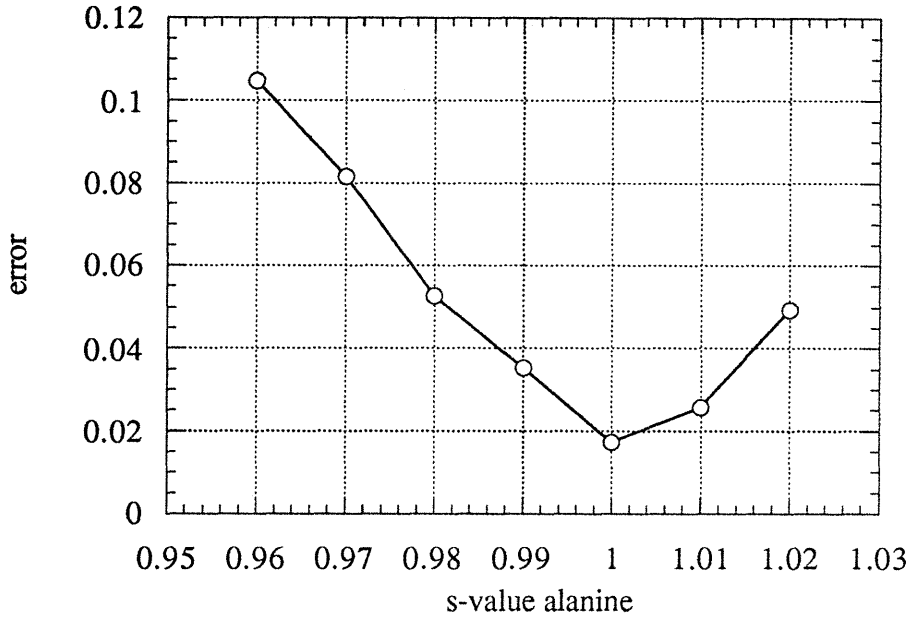


Fig. 5.4 Error *vs.* $s_{Ala}$ for the series Ac-$Hel_1$-$Ala_{n-1}GlyAla_{7-n}Lys$-$NH_2$, n = 1 to 7 at 25 °C.

As shown in Fig. 5.4, the ($s_{Ala}$, $s_{Lys}$) pair that minimizes the error is $s_{Ala}$ = 1.00 and $s_{Lys}$ = 8.78, indicating a lack of helical bias on the part of alanine and a particularly high helical propensity for the terminal lysine. The error associated with measured t/c ratios is ± 5%, which translates to $s_{Ala}$ = 1.00 ± 0.01. The significant role of positively charged residues at the C-terminus is manifested as well in the high t/c ratios for Ac-$Hel_1$-$Ala_7$-X-$NH_2$, X = Arg, His, Orn measured by Dr. Tsang (Table 5.6 and Fig. 5.5). Since histidine does not have a long hydrophobic side chain, electrostatic effects due to a C-terminal positive charge may be sufficient for the degree of helicity seen in the peptides shown in Table 5.6.

| Compound | t/c at 2 °C | t/c at 25 °C | t/c at 60 °C |
|---|---|---|---|
| Ac-$Hel_1$-$Ala_7$-Arg-$NH_2$ | 5.35 | 3.51 | 2.55 |
| Ac-$Hel_1$-$Ala_7$-Lys-$NH_2$ | 5.16 | 3.45 | 2.52 |
| Ac-$Hel_1$-$Ala_7$-Orn-$NH_2$ | 4.40 | 3.41 | 2.49 |
| Ac-$Hel_1$-$Ala_7$-His-$NH_2$ | 4.36 | 3.43 | 2.47 |

Table 5.6 t/c ratios of Ac-$Hel_1$-$Ala_7$X-$NH_2$, X = Arg, Lys, Orn, His. Data for X = Arg, Orn, and His analogs from Dr. Tsang.

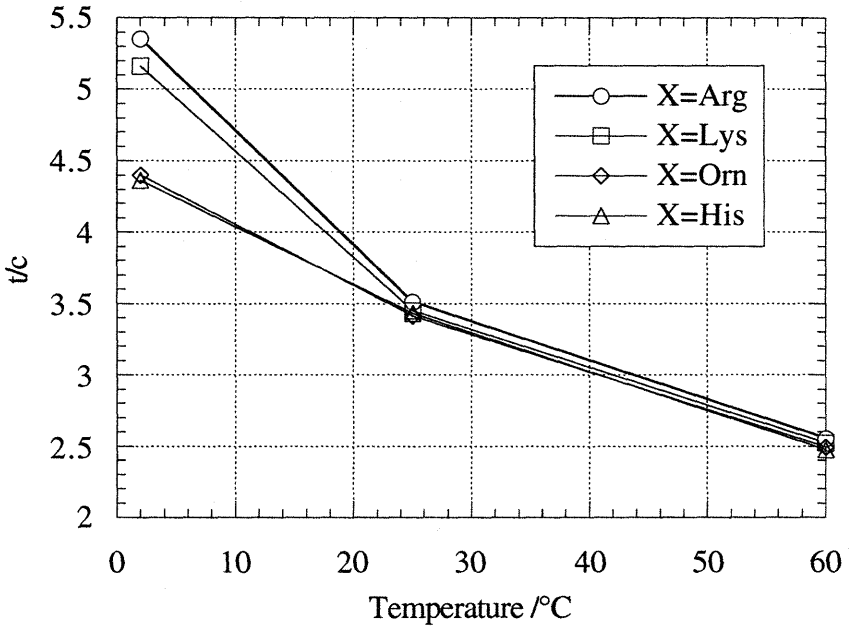


Fig 5.5 t/c ratios of Ac-$Hel_1$-$Ala_7$X-$NH_2$, X = Arg, Lys, Orn, His. Data for X = Arg, Orn, and His analogs from Dr. Tsang.

The results in this chapter independently support previous helicity studies performed in the Kemp laboratories. Many interesting inquiries on helicity have been reported in the literature, with the dual assumptions that alanine stabilizes a helix exceptionally well and that lysine destabilizes a helix. This chapter provides evidence to the contrary in one alanine rich context. The utility of Ac-$Hel_1$ should further improve our understanding of helicity.

# Appendix

## CD spectra of Ac-Hel$_1$-Ala$_7$-Lys-NH$_2$ and Ac-Hel$_1$-Ala$_{n-1}$GlyAla$_{7-n}$-Lys-NH$_2$, n = 1 to 7

In his Ph.D. thesis, Dr. Allen of the Kemp laboratories reported an s-value scale for 23 natural and unnatural residues (Table A.1).[110] This scale was derived by comparing the t/c values in $D_2O$ at 25 °C for a series of Ac-$Hel_1$-$Ala_2$-X-$Ala_4$-Lys-$NH_2$ derivatives with the value for the standard host system Ac-$Hel_1$-$Ala_7$-Lys-$NH_2$. An alternative standard is the dilysine peptide Ac-$Hel_1$-$Ala_2$-Lys-$Ala_4$-Lys-$NH_2$ prepared and studied by Dr. Tsang as part of his 60+ member database of Ac-$Hel_1$ alanine rich mono and dilysine containing peptides. As seen in Table A.1 the two standards result in significantly different s value assignments, although one data set is a simple linear function of the other. It is clear that the two standards do not give consistent results. This inconsistency is noticeably reflected in the anomalously high s value that the second analysis assigns to alanine, which is inconsistent with the findings of Drs. Tsang, Renold, and Shimizu[84f] in this group as well as the analyses given in Chapter 5 of this thesis. Using Ac-$Hel_1$-$Ala_2$-Lys-$Ala_4$-Lys-$NH_2$ as a standard, Ac-$Hel_1$-$Ala_7$-Lys-$NH_2$ exhibits anomalously high helicity, and as noted in Chapter 5, this is best attributed to an exceptional helical propensity of a lysine residue at the C-terminus of a sequence of seven alanine residues.

Dr. Tsang has observed that the $A_7X$ motif exhibits similarly high helicity when X is any positively charged amino acid residue and that at or below 25 °C, $s_K = s_R = s_H$, in strong contrast to the more typical $s_R > s_K > s_H$ illustrated by the t/c values of Table A.1. Interpretation of the t/c data of Table A.1 is contingent upon an understanding of this unusual helical stabilization and its effects on the structure of this helix. A circular dichroism study of Ac-$Hel_1$-$Ala_7$-Lys-$NH_2$ and Ac-$Hel_1$-$Ala_{n-1}GlyAla_{7-n}$Lys-$NH_2$, n = 1 to 7 was undertaken as a first step toward clarifying these issues.

As noted in Chapter 2, CD spectroscopy is very useful for determining that a particular previously characterized CD-active chiral chromophore dominates the conformational ensemble of

a series of related peptides. It is very much less useful for assigning structures to new chiral chromophores that lack literature precedents. A conformational issue for which precedent exists is the presence within a helical manifold of both $3_{10}$ and α-helical conformations. As noted in Chapter 2, Millhauser and associates have argued from ESR spectra of double spin-labelled short Baldwin-Marqusee peptides that $3_{10}$ helices can dominate the helical manifold. The assignment of the familiar CD spectrum of Fig. 4.1(a) to an α-helix has been confirmed many times by independent NOE studies. Instances of CD spectra for characterized $3_{10}$ helices are much rarer, although Jung[113] has reported examples, and recently Toniolo has reported a CD spectrum of a $3_{10}$ helix using the octapeptide Ac-[L-(α-Me)Val]$_8$-O$^t$Bu in TFE solution (Fig A.1).[114] This spectrum displays minima at 184 and 207 nm, a maximum at 195 nm, and a shoulder at 222 nm. The ratio of $\theta_{222}/\theta_{207}$ was observed to be 0.4, much smaller then the *ca.* 1 : 1 ratio expected for an α-helix. If this assignment is typical, a marked drop in intensity of the 222 nm mean residue molar ellipticity is expected for an α to $3_{10}$ change.

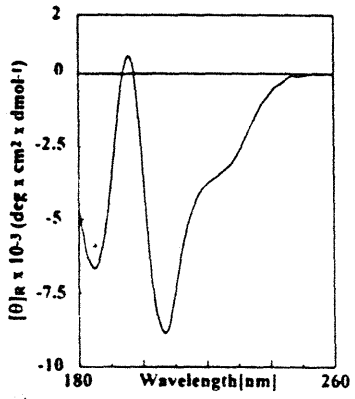


Fig A.1 CD spectrum of Ac-[L-(α-Me)Val]$_8$-O$^t$Bu

113 a) Jung, G.; Dubischar, N.; Leibfritz, D. *Eur. J. Biochem.* **1975**, *54*, 395. b) Mayr, W; Oekonomopulos, R.; Jung, G. Biopolymers 1979, 18, 425. c) Oekonomopulos, R.; Jung, G.*Biopolymers* **1980**, *19*, 203. d) Jung, G.; Bosch, R.; Katz, E.; Schmitt, H.; Voges, K.-P.; Winter, W. *Biopolymers* **1983**, *22*, 241.

114 Toniolo, C.; Polese, A.; Formaggio, F.; Crisma, M.; Kamphnis, J.; *J. Am. Chem. Soc.* **1996**, *118*, 2744.

| Derivative X | t/c of Ac-Hel$_1$-A$_2$XA$_4$K-NH$_2$ | $s_{x3}$ using Ac-Hel$_1$-A$_7$K-NH$_2$ as standard | $s_{x3}$ using Ac-Hel$_1$-A$_2$KA$_4$K-NH$_2$ as standard |
|---|---|---|---|
| Aib | 3.93 | 1.35 | 2.30 |
| Ala | 3.34 | 1.07 | 1.80 |
| Glu$^0$ | 3.27 | 1.04 | 1.70 |
| Met | 3.18 | 1.00 | 1.65 |
| Arg$^{+1}$ | 3.15 | 0.99 | 1.60 |
| Leu | 3.06 | 0.94 | 1.50 |
| Nle | 3.00 | 0.92 | 1.45 |
| Gln | 2.91 | 0.88 | 1.40 |
| Lys$^{+1}$ | 2.87 | 0.86 | 1.37 |
| Nve | 2.83 | 0.84 | 1.35 |
| Abu | 2.73 | 0.79 | 1.25 |
| Ile | 2.66 | 0.76 | 1.23 |
| Tyr | 2.66 | 0.76 | 1.15 |
| His$^{+1}$ | 2.64 | 0.75 | 1.15 |
| Phe | 2.49 | 0.68 | 1.05 |
| Val | 2.22 | 0.56 | 0.80 |
| Asp$^0$ | 2.14 | 0.52 | 0.75 |
| Asn | 2.14 | 0.52 | 0.75 |
| Ser | 2.09 | 0.50 | 0.69 |
| Thr | 2.08 | 0.49 | 0.67 |
| (D)-Ala | 1.84 | 0.38 | 0.45 |
| Gly | 1.74 | 0.33 | 0.38 |
| Tle | 1.65 | 0.29 | 0.30 |

Table A.1 t/c, $s_{x3}$ for AcHel$_1$-A$_2$XA$_4$K-NH$_2$. Aib = alpha-aminoisobutyric acid, Nle = norleucine, Nve = norvaline, Abu = aminobutyric acid, Tle = *t*-butylleucine.

## Ac-Hel$_1$-Ala$_7$-Lys-NH$_2$ and Ac-Hel$_1$-Ala$_{n-1}$GlyAla$_{7-n}$Lys-NH$_2$, n = 1 to 7

The CD spectra for Ac-Hel$_1$-Ala$_7$-Lys-NH$_2$ and Ac-Hel$_1$-Ala$_{n-1}$GlyAla$_{7-n}$-Lys-NH$_2$, n = 1 to 7 will be presented, followed by corrections for the Ac-Hel$_1$ chromophore and for random coil residues. The deconvoluted spectra at 25 °C will then be analyzed.

The CD spectra of Ac-Hel$_1$-Ala$_7$-Lys-NH$_2$ at 2, 25, and 60 °C are shown in Figure A.2. The CD spectra of Ac-Hel$_1$-Ala$_{n-1}$GlyAla$_{7-n}$-Lys-NH$_2$, n = 1 to 7 at 2, 25, and 60 °C are shown in Figures A.3 through A.9. These spectra show a moderate to strong temperature dependence, and those for the glycine mutants show a strong glycine positional dependence. The CD spectrum of Ac-Hel$_1$-Gly-Ala$_6$-Lys-NH$_2$ is similar to the parent compound, though diminished in intensity. Spectra corresponding to glycine substitution at sites 2, 3, and 4 show drastic changes in the shape of the curves relative to the parent compound. As the site of glycine substitution is moved away from the template, the spectra more closely resembles that of the parent compound both in shape and intensity.

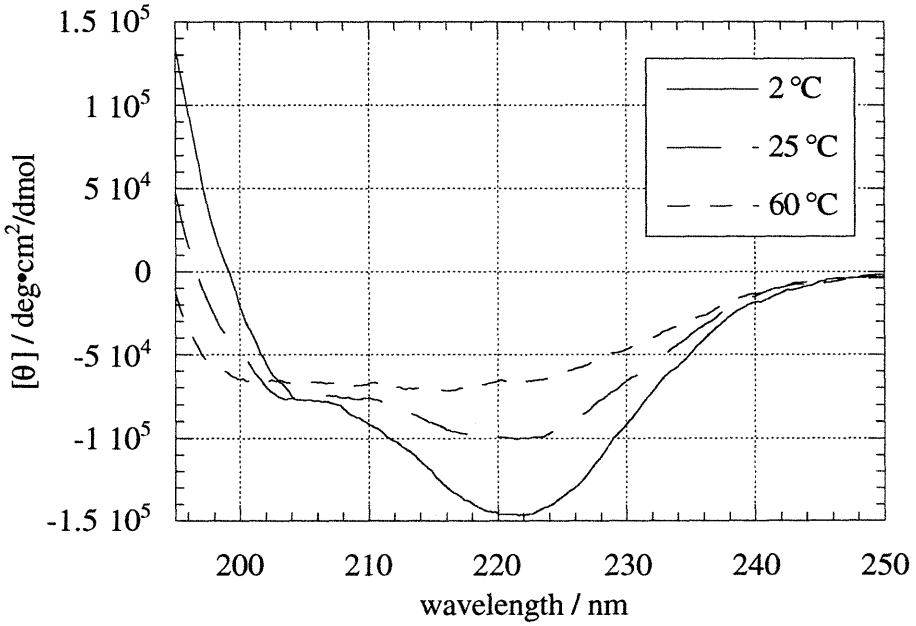


Fig. A.2 CD spectra of Ac-Hel$_1$-Ala$_7$-Lys-NH$_2$ at 2, 25, and 60 °C.

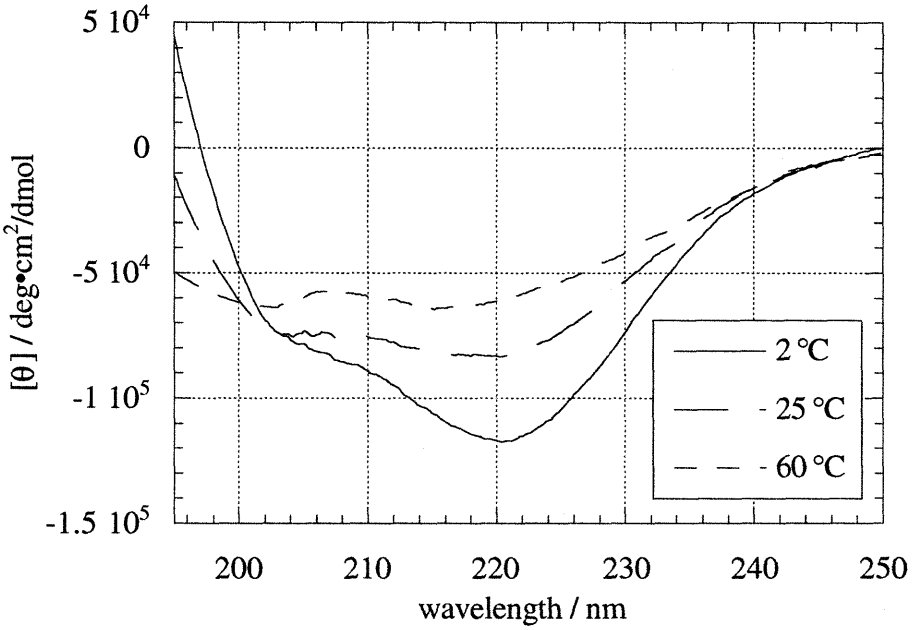


Fig. A.3 CD spectra of Ac-$Hel_1$-Gly-$Ala_6$-Lys-$NH_2$ at 2, 25, and 60 °C.

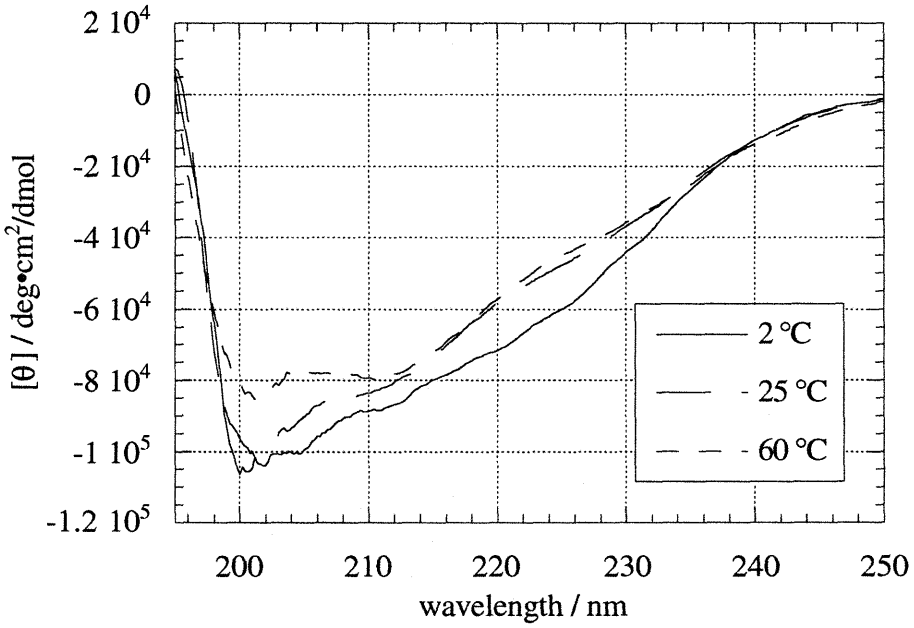


Fig. A.4 CD spectra of Ac-$Hel_1$-Ala-Gly-$Ala_5$-Lys-$NH_2$ at 2, 25, and 60 °C.

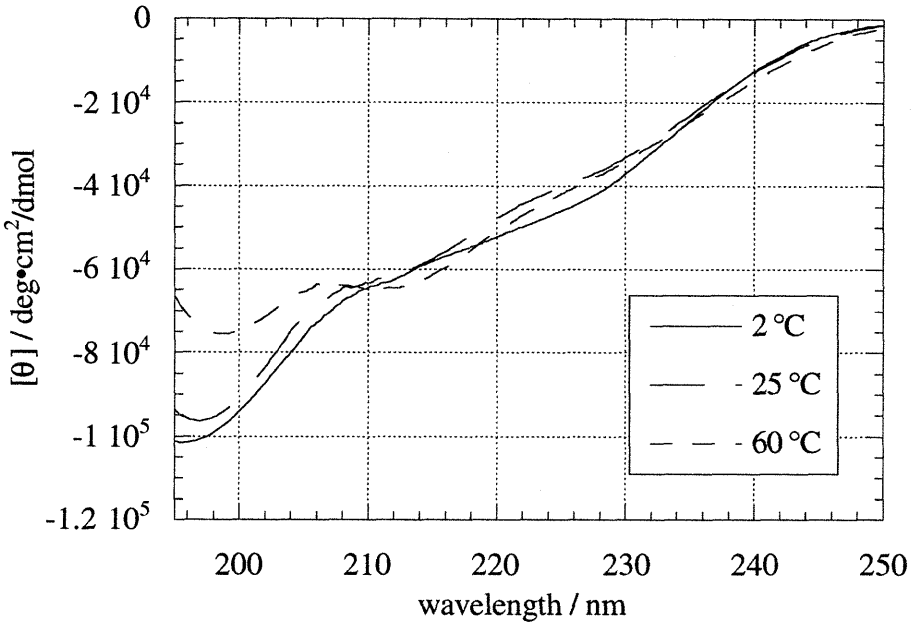


Fig. A.5 CD spectra of Ac-$Hel_1$-$Ala_2$-Gly-$Ala_4$-Lys-$NH_2$ at 2, 25, and 60 °C.

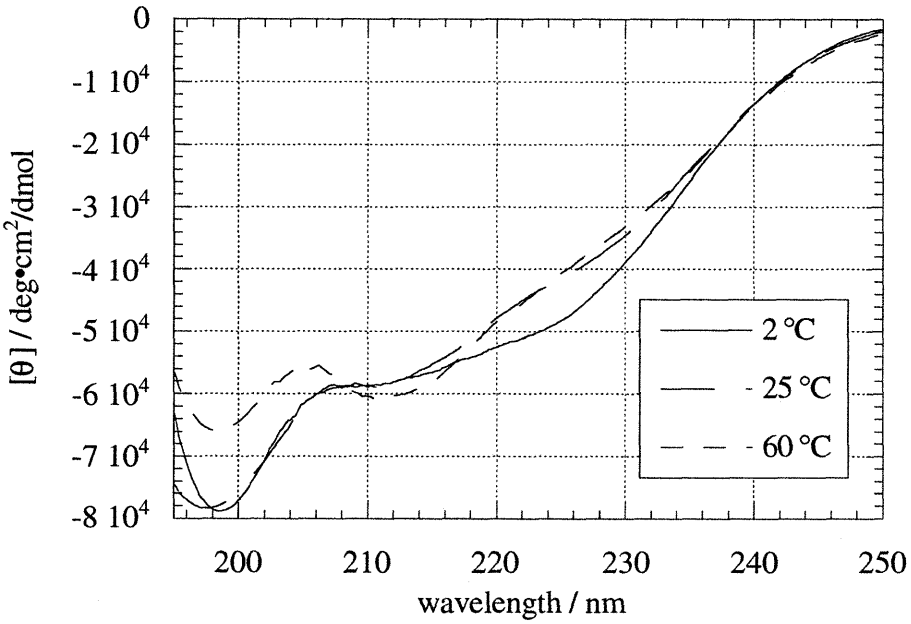


Fig. A.6 CD spectra of Ac-$Hel_1$-$Ala_3$-Gly-$Ala_3$-Lys-$NH_2$ at 2, 25, and 60 °C.

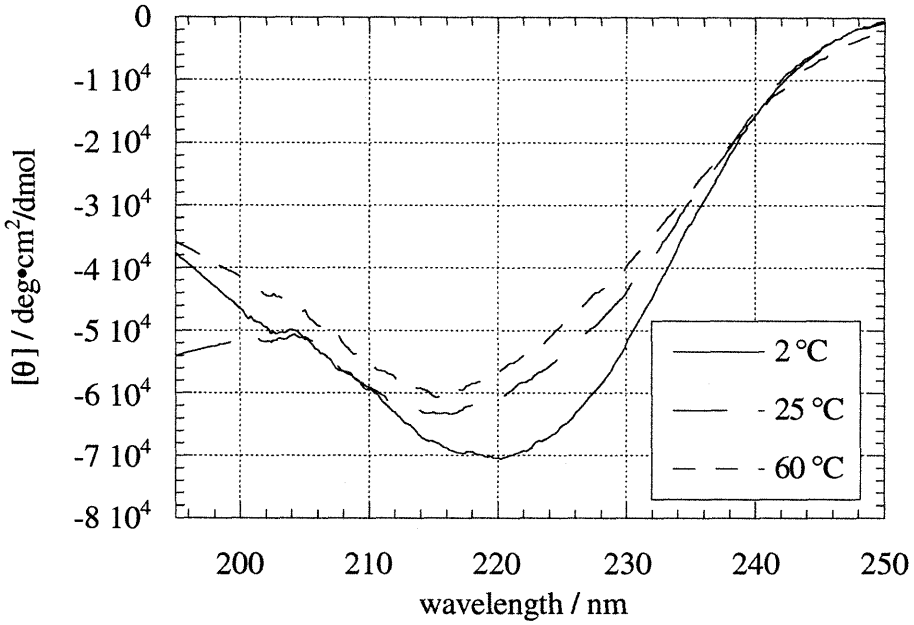


Fig. A.7 CD spectra of Ac-$Hel_1$-$Ala_4$-Gly-$Ala_2$-Lys-$NH_2$ at 2, 25, and 60 °C.

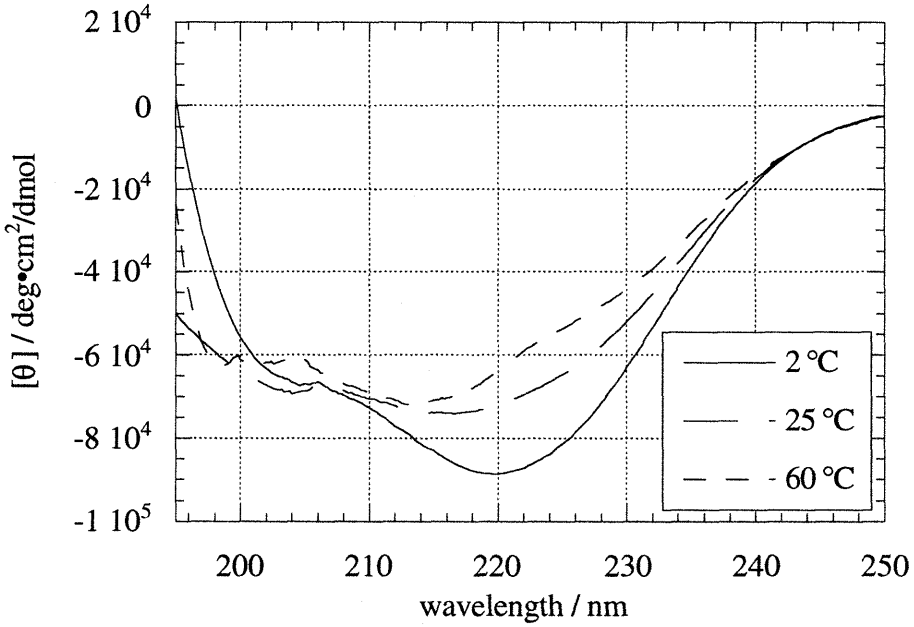


Fig. A.8 CD spectra of Ac-$Hel_1$-$Ala_5$-Gly-$Ala_1$-Lys-$NH_2$ at 2, 25, and 60 °C.

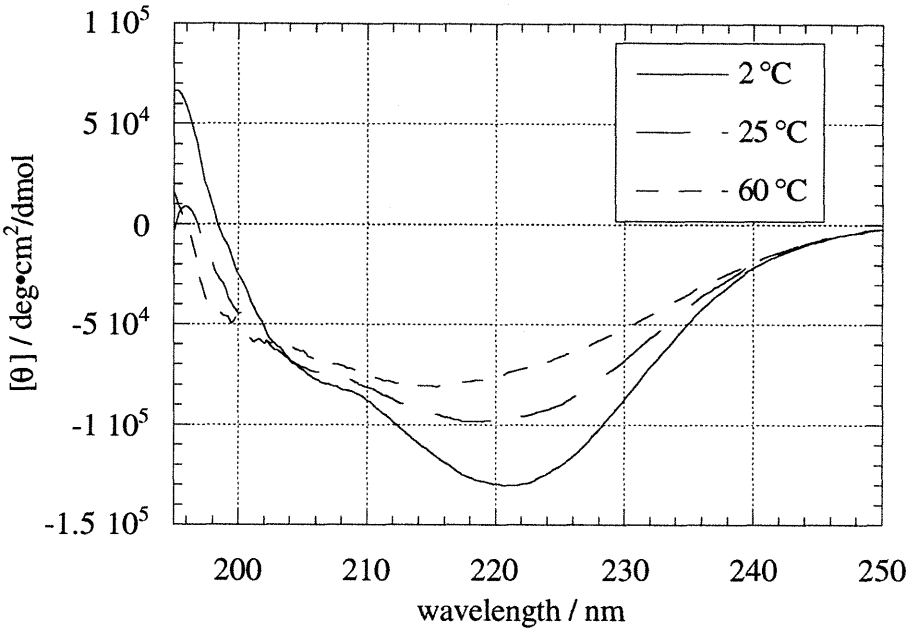


Fig. A.9 CD spectra of Ac-$Hel_1$-$Ala_6$-Gly-Lys-$NH_2$ at 2, 25, and 60 °C.

Removal of template contributions and cs+ts peptide contributions, anaologous to the procedure used in Chapter 4, gives the spectra shown in Figures A.10 through A.17, which are more intense and have more helical character, as expected. Upon correction, the CD spectra corresponding to glycine substitutions at sites 3, 4, and 5 show more discernable bands. Comparison of Figures A.14 and A.15, corresponding to glycine substitutions at sites 4 and 5, show a noticeable difference in the $\theta_{222}/\theta_{203}$ ratios.

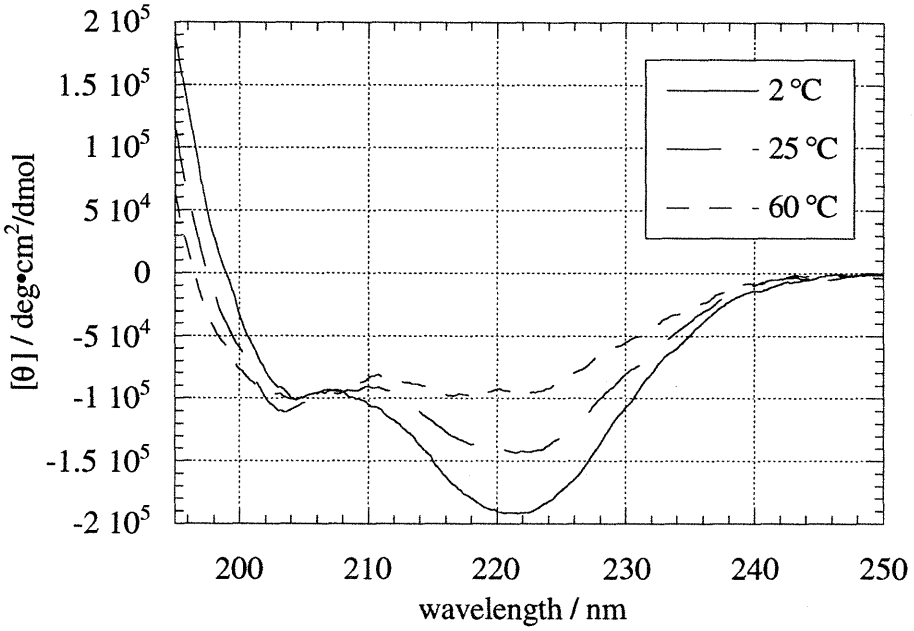


Fig. A.10 CD spectra of Ac-$Hel_1$-$Ala_7$-Lys-$NH_2$ at 2, 25, and 60 °C corrected for template and cs+ts peptide contributions.

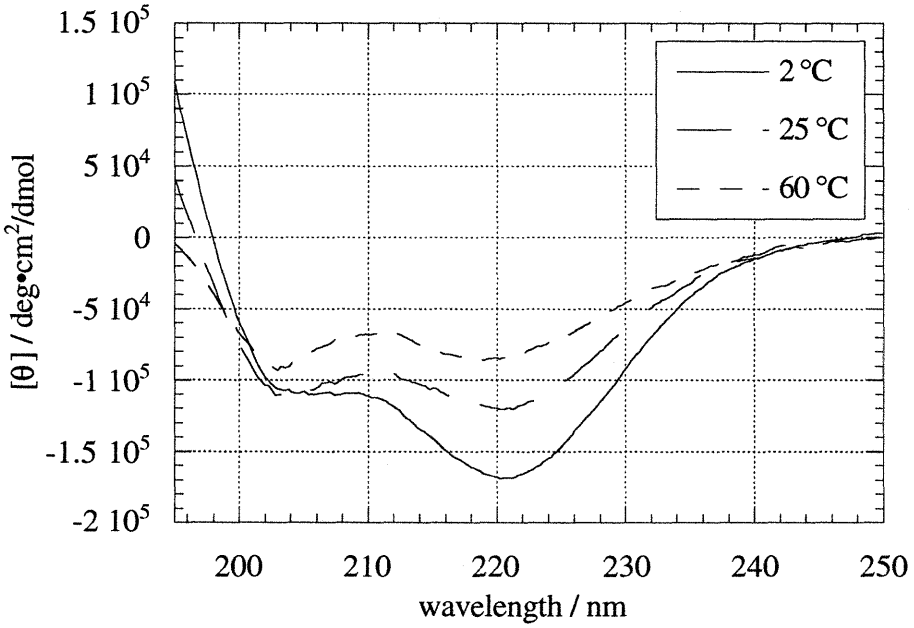


Fig. A.11 CD spectra of Ac-$Hel_1$-Gly-$Ala_6$-Lys-$NH_2$ at 2, 25, and 60 °C corrected for template and cs+ts peptide contributions.

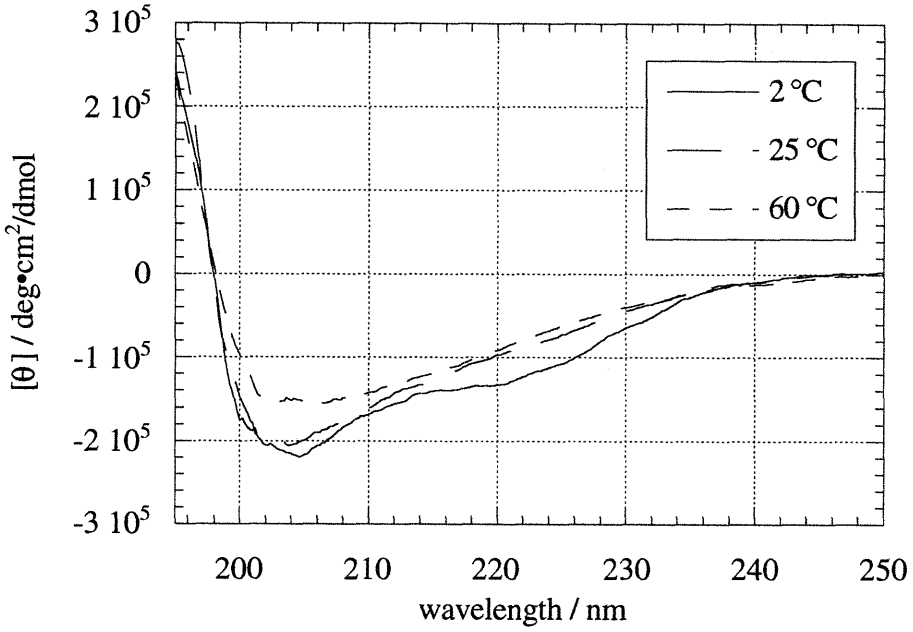


Fig. A.12 CD spectra of Ac-Hel$_1$-Ala-Gly-Ala$_5$-Lys-NH$_2$ at 2, 25, and 60 °C corrected for template and cs+ts peptide contributions.

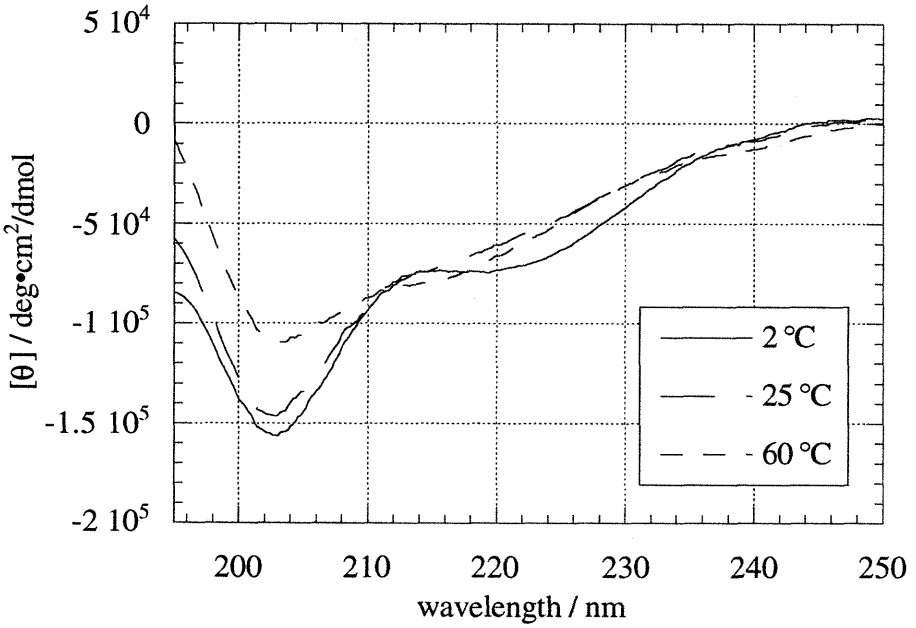


Fig. A.13 CD spectra of Ac-Hel$_1$-Ala$_2$-Gly-Ala$_4$-Lys-NH$_2$ at 2, 25, and 60 °C corrected for template and cs+ts peptide contributions.

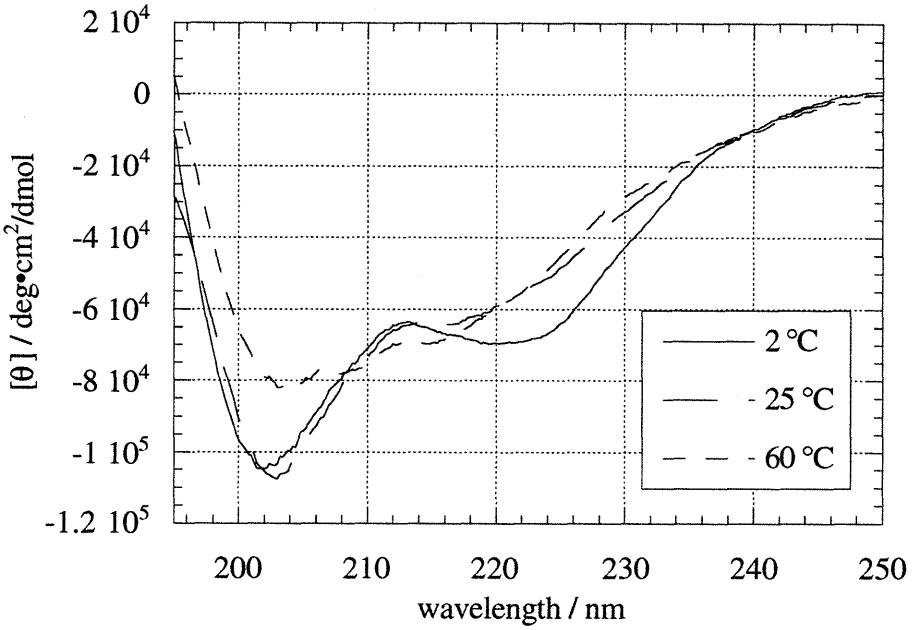


Fig. A.14 CD spectra of Ac-Hel$_1$-Ala$_3$-Gly-Ala$_3$-Lys-NH$_2$ at 2, 25, and 60 °C corrected for template and cs+ts peptide contributions.

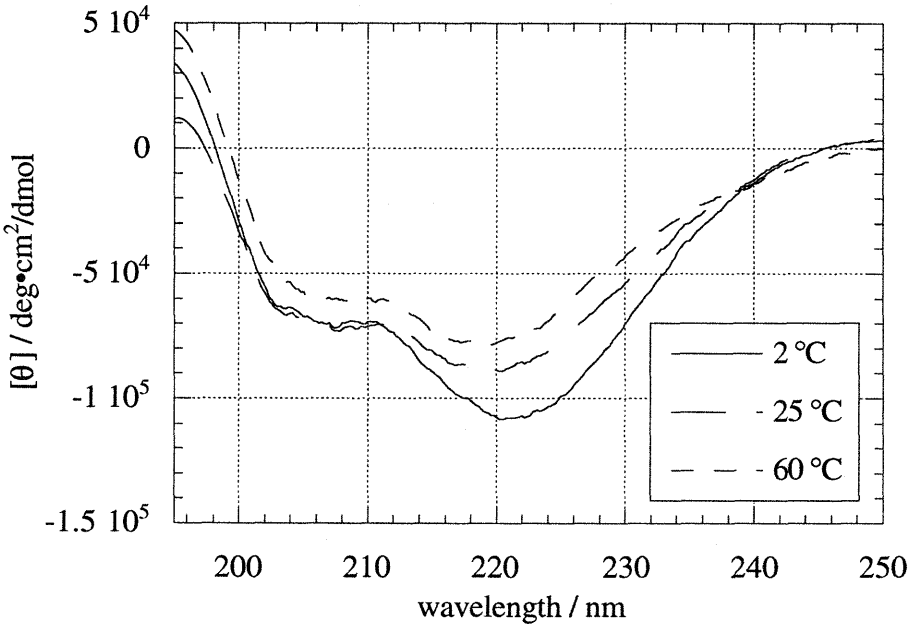


Fig. A.15 CD spectra of Ac-Hel$_1$-Ala$_4$-Gly-Ala$_2$-Lys-NH$_2$ at 2, 25, and 60 °C corrected for template and cs+ts peptide contributions.

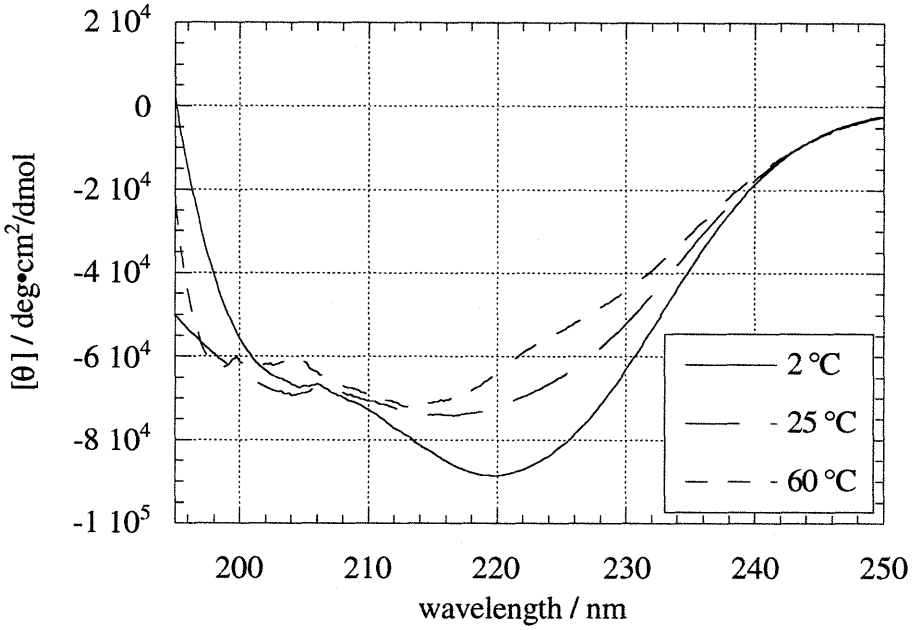


Fig. A.16 CD spectra of Ac-$Hel_1$-$Ala_5$-Gly-$Ala_1$-Lys-$NH_2$ at 2, 25, and 60 °C corrected for template and cs+ts peptide contributions.

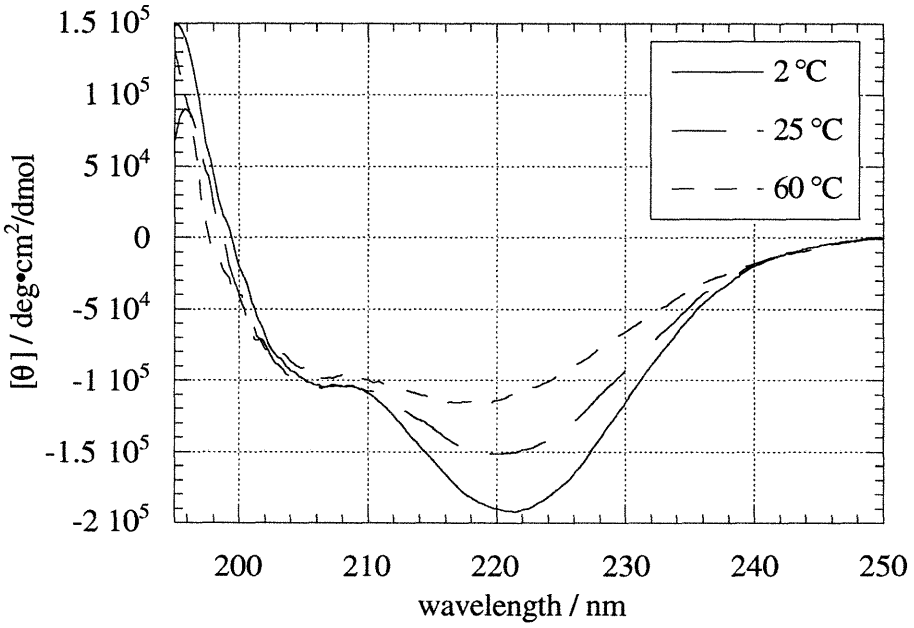


Fig. A.17 CD spectra of Ac-$Hel_1$-$Ala_6$-Gly-Lys-$NH_2$ at 2, 25, and 60 °C corrected for template and cs+ts peptide contributions.

Using the s-values of alanine, glycine, and lysine obtained in Chapter 5 ($s_{Ala}$ = 1.00, $s_{Lys}$ = 8.78, $s_{Gly}$ calculated from Table 5.4), one can calculate the state sum and fractional helicity for each compound of the series and the parent compound at 25 °C, as shown in Table A.2 for the example of Ac-$Hel_1$-Gly-$Ala_6$-Lys-$NH_2$. The relative weight is the product of the s-values of each helical residue; the state sum is the sum of the relative weights for each helical substate; the mole fraction for each helical substate is its relative weight divided by the state sum. These quantities will allow us to subtract contributions from the random coil residues within the te state helical peptide manifold.

| helical substate | no. helical residues | no. coil residues | relative weight | mol fraction |
|---|---|---|---|---|
| hlccccccccc | 0 | 8 | 1 | 0.09 |
| hlhccccccc | 1 | 7 | $s_G$ = 0.679 | 0.06 |
| hlhhcccccc | 2 | 6 | $s_G s$ = 0.679 | 0.06 |
| hlhhhccccc | 3 | 5 | $s_G s^2$ = 0.679 | 0.06 |
| hlhhhhcccc | 4 | 4 | $s_G s^3$ = 0.679 | 0.06 |
| hlhhhhhccc | 5 | 3 | $s_G s^4$ = 0.679 | 0.06 |
| hlhhhhhhcc | 6 | 2 | $s_G s^5$ = 0.679 | 0.06 |
| hlhhhhhhhc | 7 | 1 | $s_G s^6$ = 0.679 | 0.06 |
| hlhhhhhhhh | 8 | 0 | $s_G s^6 s_K$ = 5.962 | 0.51 |
| Total | - | - | SS = 11.71 | 1.00 |

Table A.2 Mole fractions of each helical substate of Ac-$Hel_1$-Gly-$Ala_6$-Lys-$NH_2$ at 25 °C; hl denotes Ac-$Hel_1$; helical state sum = SS = $1+s_G+s_G\, s+s_G\, s^2+s_G\, s^3+s_G\, s^4+s_G\, s^5+s_G\, s^6+s_G\, s^6 s_K$ = 11.71.

By this procedure, the mole fractions of each substate for each compound are calculated and shown in Table A.3.

| | Number of helical residues in substate | | | | | | | | |
|---|---|---|---|---|---|---|---|---|---|
| Compound | 0 | 1 | 2 | 3 | 4 | 5 | 6 | 7 | 8 |
| Ac-$Hel_1$-AAAAAAAK-$NH_2$ | 0.06 | 0.06 | 0.06 | 0.06 | 0.06 | 0.06 | 0.06 | 0.06 | 0.52 |
| Ac-$Hel_1$-GAAAAAAK-$NH_2$ | 0.09 | 0.06 | 0.06 | 0.06 | 0.06 | 0.06 | 0.06 | 0.06 | 0.51 |
| Ac-$Hel_1$-AGAAAAAK-$NH_2$ | 0.19 | 0.19 | 0.04 | 0.04 | 0.04 | 0.04 | 0.04 | 0.04 | 0.37 |
| Ac-$Hel_1$-AAGAAAAK-$NH_2$ | 0.17 | 0.17 | 0.17 | 0.03 | 0.03 | 0.03 | 0.03 | 0.03 | 0.31 |
| Ac-$Hel_1$-AAAGAAAK-$NH_2$ | 0.13 | 0.13 | 0.13 | 0.13 | 0.04 | 0.04 | 0.04 | 0.04 | 0.31 |
| Ac-$Hel_1$-AAAAGAAK-$NH_2$ | 0.12 | 0.12 | 0.12 | 0.12 | 0.12 | 0.03 | 0.03 | 0.03 | 0.28 |
| Ac-$Hel_1$-AAAAAGAK-$NH_2$ | 0.10 | 0.10 | 0.10 | 0.10 | 0.10 | 0.10 | 0.04 | 0.04 | 0.31 |
| Ac-$Hel_1$-AAAAAAGK-$NH_2$ | 0.08 | 0.08 | 0.08 | 0.08 | 0.08 | 0.08 | 0.08 | 0.04 | 0.39 |

Table A.3 Mole fractions of helical substates of Ac-$Hel_1$-$Ala_7$-Lys-$NH_2$ and Ac-$Hel_1Ala_{n-1}GlyAla_{7-n}Lys$-$NH_2$, n = 1 to 7 at 25 °C.

The average number of helical residues <h> for each compound is then calculated by the sum of the mole fractions each weighted by the number of helical residues in that substate. This is shown for each compound in Table A.4. The fractional helicity is the average number of helical residues divided by the total number of amino acid residues.

| Compound | <h> | <c> | Fractional helicity |
|---|---|---|---|
| Ac-$Hel_1$-AAAAAAAK-$NH_2$ | 5.9 | 2.1 | 0.73 |
| Ac-$Hel_1$-GAAAAAAK-$NH_2$ | 5.8 | 2.2 | 0.71 |
| Ac-$Hel_1$-AGAAAAAK-$NH_2$ | 4.2 | 3.8 | 0.53 |
| Ac-$Hel_1$-AAGAAAAK-$NH_2$ | 3.8 | 4.2 | 0.48 |
| Ac-$Hel_1$-AAAGAAAK-$NH_2$ | 4.1 | 3.9 | 0.51 |
| Ac-$Hel_1$-AAAAGAAK-$NH_2$ | 4.1 | 3.9 | 0.51 |
| Ac-$Hel_1$-AAAAAGAK-$NH_2$ | 4.5 | 3.5 | 0.56 |
| Ac-$Hel_1$-AAAAAAGK-$NH_2$ | 5.1 | 2.9 | 0.64 |

Table A.4 Average number of helical and random coil residues and fractional helicity at 25 °C.

Correction for the average number of coil residues <c> for each compound gives the CD spectra shown in Fig. A.18.

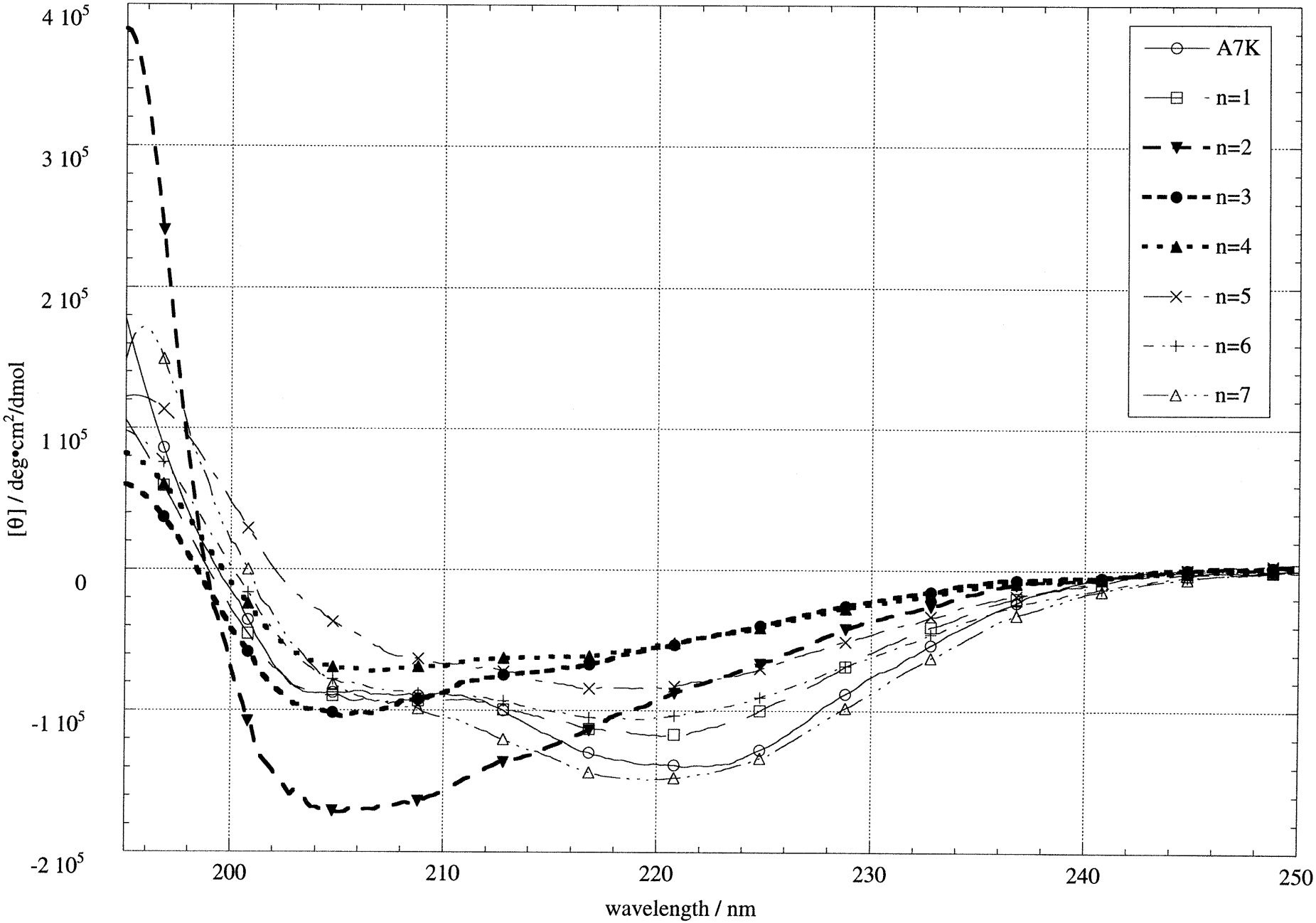


Fig. A.18 CD spectra corrected for template and cs+ts state peptide and te state random coil residues for Ac-$Hel_1$-$Ala_7$-Lys-$NH_2$ and Ac-$Hel_1$-$Ala_{n-1}$GlyAla$_{7-n}$-Lys-$NH_2$, n = 1 to 7.

Conspicuously, the curves corresponding to substitution at sites 2 and 3 do not show typical α-helical CD characteristics, but rather a minimum at 206 nm and an intense maximum at *ca.* 195 nm. These results show that for Ac-$Hel_1$-$Ala_7$Lys-$NH_2$, sites 2 and 3 may have anomalous characteristics, as studied by circular dichroism. The CD spectra corresponding to glycine substitution at each of these two sites bear some resemblance to the CD spectrum of the $3_{10}$-helix obtained by Toniolo and coworkers (Fig. A.1).[120] From Fig. A.18 and Table A.4, it can be seen that the ratio of $\theta_{222}/\theta_{205}$ is less than 1.0 for n = 2 to 5, the compounds with the lowest <h>. Ellipticity at 222 nm is often used as a measure of α-helical content. A plot of molar ellipticity at 222 nm *vs.* <h> is shown in Fig. A.19. The simplest model in which each helical residue contributes equally would result in a linear arrangement of the data points. Table A.4 shows that a length independent model gives per residue ellipticities between -13,455 and -29,313 deg•$cm^2$/dmol. In contrast, a length dependent model would result in a non-linear increase in negative ellipticity with increasing <h>. The wide scatter of the data shown in Fig. A.19 does not clearly indicate which model is appropriate. A length dependent model, however, is supported by the literature. Theory predicts a much different spectrum for helices less than five residues in length, due to changes in the contributions of π-π* bands.[115] Also, previous work in the Kemp group has suggested that peptides only 8 residues in length may not show a significant length dependency.[85]

---

115 Woody, R. W., in *Circular Dichroism: Principles and Applications*; Nakanishi, K., Berova, N., Woody, R. W. Eds.; VCH Publishers, Inc.: New York, 1994; p. 473.

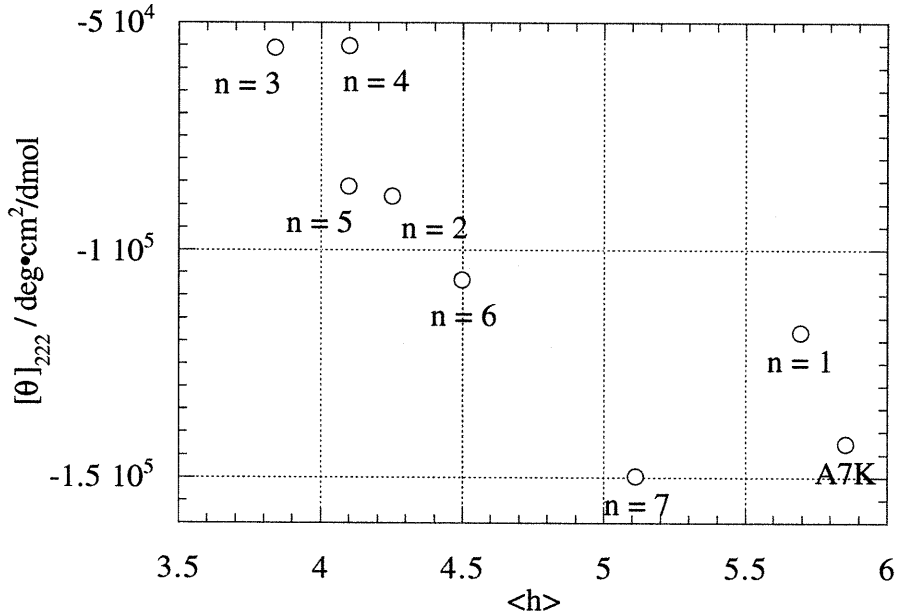


Fig. A.19 Molar ellipticity of Ac-Hel$_1$-Ala$_7$Lys-NH$_2$ and Ac-Hel$_1$-Ala$_{n-1}$GlyAla$_{7-n}$Lys-NH$_2$, n = 1 to 7 *vs.* <h> at 25 °C.

| Compound | corrected for template and cs+ts peptide $\theta_{222}$/deg•cm$^2$/dmol | corrected for random coil residues within te state $\theta_{222}$/deg•cm$^2$/dmol | length independent model $\theta_{222}$/deg•cm$^2$/dmol per helical residue |
|---|---|---|---|
| Ac-Hel$_1$-AAAAAAAK-NH$_2$ | -142589 | -142585 | -24354 |
| Ac-Hel$_1$-GAAAAAAK-NH$_2$ | -118135 | -118131 | -20746 |
| Ac-Hel$_1$-AGAAAAAK-NH$_2$ | -88166 | -88159 | -20739 |
| Ac-Hel$_1$-AAGAAAAK-NH$_2$ | -55603 | -55596 | -14486 |
| Ac-Hel$_1$-AAAGAAAK-NH$_2$ | -55171 | -55164 | -13455 |
| Ac-Hel$_1$-AAAAGAAK-NH$_2$ | -86015 | -86008 | -21000 |
| Ac-Hel$_1$-AAAAAGAK-NH$_2$ | -106627 | -106621 | -23703 |
| Ac-Hel$_1$-AAAAAAGK-NH$_2$ | -149811 | -149806 | -29313 |

Table A.4 Molar ellipticities at 222 nm for Ac-Hel$_1$-Ala$_7$Lys-NH$_2$ and Ac-Hel$_1$-Ala$_{n-1}$GlyAla$_{7-n}$Lys-NH$_2$, n = 1 to 7 at 25 °C after correction for template and cs+ts peptide, after correction for random coil residues within te state, and per helical residue after all corrections.

This appendix has analyzed the CD spectra of Ac-$Hel_1$-$Ala_7$-Lys-$NH_2$ and Ac-$Hel_1$-$Ala_{n-1}$-Gly-$Ala_{7-n}$-Lys-$NH_2$, n = 1 to 7 and shown that within the first turn of the helix, there exists the possibility of $3_{10}$ character. Indeed, $3_{10}$ helices are often found in short helices (*ca.* 3 - 4 residues) and at the ends of $\alpha$-helices in protein structures.[64] Pertinent to the Allen scale of s-values, the third position of Ac-$Hel_1$-$Ala_7$-Lys-$NH_2$ may accomodate hydrophilic and hydrophobic residues differently. Since hydrophobic residues are found less frequently at the ends of helices than hydrophilic ones, forcing a hydrophobic residue to occupy a position close to the end of a helix may give a reduced propensity than otherwise. Ongoing helicity studies in the Kemp group will determine a more reliable s-value scale than the one obtained using Ac-$Hel_1$-$Ala_7$-Lys-$NH_2$ as a host.

# Experimental Section

## Experimental Section for Part I

### Instrumentation.

Infrared spectra were obtained using a Perkin-Elmer 1320 grating spectrophotometer. $^{1}H$ NMR spectra were measured with Varian XL-300 (300 MHz), GE-300 (300 MHz), and VXR-500 (500 MHz) spectrometers. $^{13}C$ NMR spectra were determined on Varian XL-300 (75 MHz) and GE-300 (75 MHz) spectrometers. Chemical shifts are expressed in parts per million ($\delta$) downfield from tetramethylsilane. Elemental analyses were performed by Robertson Laboratory, Inc., of Madison, NJ. Melting points and boiling points are uncorrected.

### Materials

Commercial grade reagents and solvents were used without further purification except as indicated below. Diisopropylamine and pyridine were distilled from calcium hydride. Tetrahydrofuran was distilled from sodium benzophenone ketyl. 3-Methyl-2-butanone was distilled before use. S-Phenyl 3-phenylpropanethioate was recrystallized from pentane. S-Phenyl dodecanethioate and S-phenyl decanethioate were distilled before use. Merck or Baker silica gel (230-400 mesh) was used in the decarboxylation of $\beta$-lactones. *n*-Butyllithium was titrated with *sec*-butanol using 1,10-phenanthroline as indicator.[116]

### General Procedures

All reactions were performed in flame-dried or oven-dried glassware under a positive pressure of argon or nitrogen (except decarboxylations of ß-lactones, which do not require flame- or oven-dried glassware). Reactions were stirred magnetically unless otherwise indicated. Solutions of *n*-butyllithium reagents were transferred by syringe and were introduced into reaction vessels through rubber septa. Reaction product solutions were concentrated by using a Buchi rotary evaporator at 1-30 mm Hg. Column chromatography was performed on Merck or Baker silica gel (230-400 mesh).

---

116 Watson, S. C.; Eastham, J. F. *J. Organomet. Chem.* **1967**, *9*, 165.

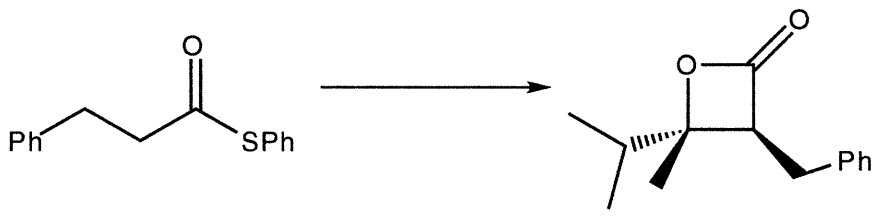


**1**

**4-Methyl-4-isopropyl-3-benzyl-oxetan-2-one (1).**

A 25-mL, 2-necked, round-bottomed flask equipped with an argon inlet adapter, rubber septum, and magnetic stirring bar was charged with 3 mL of THF and diisopropylamine (0.385 mL, 2.75 mmol), and then cooled in an ice-water bath. *n*-Butyllithium solution (1.58 M in hexanes, 1.66 mL, 2.63 mmol) was added dropwise via syringe. After 30 min, the ice-water bath was replaced with a dry ice-acetone bath (-78 °C), and a solution of S-phenyl hydrocinnamate (0.606 g, 2.50 mmol) in 2 mL of THF was added dropwise via syringe, rinsing with 1 mL THF. After 30 min, 3-methyl-2-butanone (0.267 mL, 2.50 mmol) was added dropwise via syringe. The reaction mixture was stirred at -78 °C for 30 min and then allowed to warm gradually to 0 °C over the course of 1.5 h. Half-saturated $NH_4Cl$ solution (5 mL) was then added, and the resulting mixture was partitioned between 10 mL of water and 10 mL of diethyl ether, The organic phase was washed with two 10-mL portions of 10% $K_2CO_3$ solution, 10 mL of saturated NaCl solution, dried over $MgSO_4$, filtered, and concentrated to give 0.542 g of a yellow oil, used in the next step without purification. A sample was purified by column chromatography on silica gel (gradient elution with ethyl acetate-hexanes), followed by kugelrohr distillation (oven temperature 110 °C, <0.001 mm Hg) to afford 0.285 g of clear colorless oil and crystals. The crystals were removed and washed with pentane to afford 0.104 g of **1** as clear colorless crystals, mp 37-40 °C.

$^1$H NMR (300 MHz, $CDCl_3$): 7.20-7.38 (m, 5 H), 3.49 (dd, J = 6.9, 9.0 Hz, 1 H), 3.20 (dd, J = 6.7, 15.1 Hz, 1 H), 2.87 (dd, J = 9.1, 14.6 Hz), 1.94 (sept, J = 6.9 Hz), 1.44 (s, 3 H), 0.92 (d, J = 6.7 Hz, 3 H), 0.67 (d, J = 6.9 Hz, 3 H).

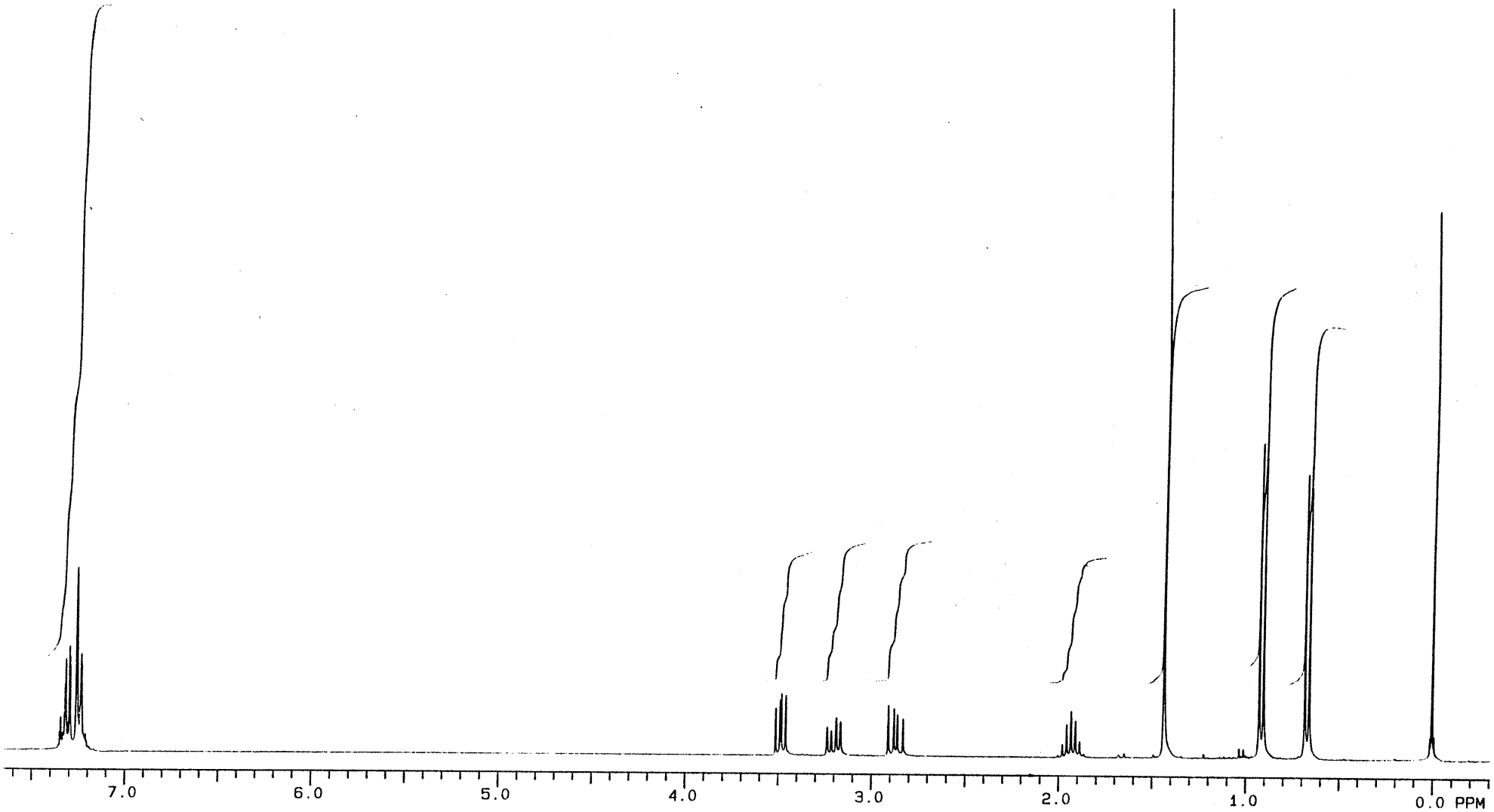


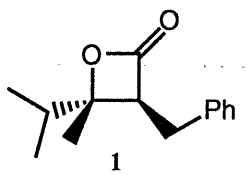


1

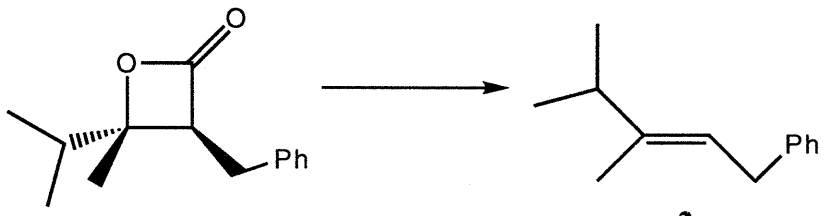


**2**

**(E)-3,4-Dimethyl-1-phenyl-2-pentene (2)**

A portion (0.301 g) of unpurified β-lactone prepared according to the preceding procedure was placed in a 50-mL, one-necked, round-bottomed flask equipped with a magnetic stirring bar and a reflux condenser, and silica gel (0.030 g) and 12 mL of cyclohexane were added. The reaction mixture was heated at reflux for 3 h and then allowed to cool to room temperature and filtered to give 0.265 g of a pale yellow oil. Column chromatography on silica gel (gradient elution with ethyl acetate-hexanes) afforded 0.123 g (44% from the thiol ester) of **2** as a colorless oil.

$^1$H NMR (300 MHz, $CDCl_3$): 7.20-7.42 (m, 5 H), 5.35 (appar t, J = 7.4 Hz, 1 H), 3.35 (d, J = 7.4 Hz, 3 H), 2.28 (sept, J = 7.0 Hz, 1 H), 1.67 (s, 1 H), 1.03 (s, 3 H), 1.01 (s, 3 H).

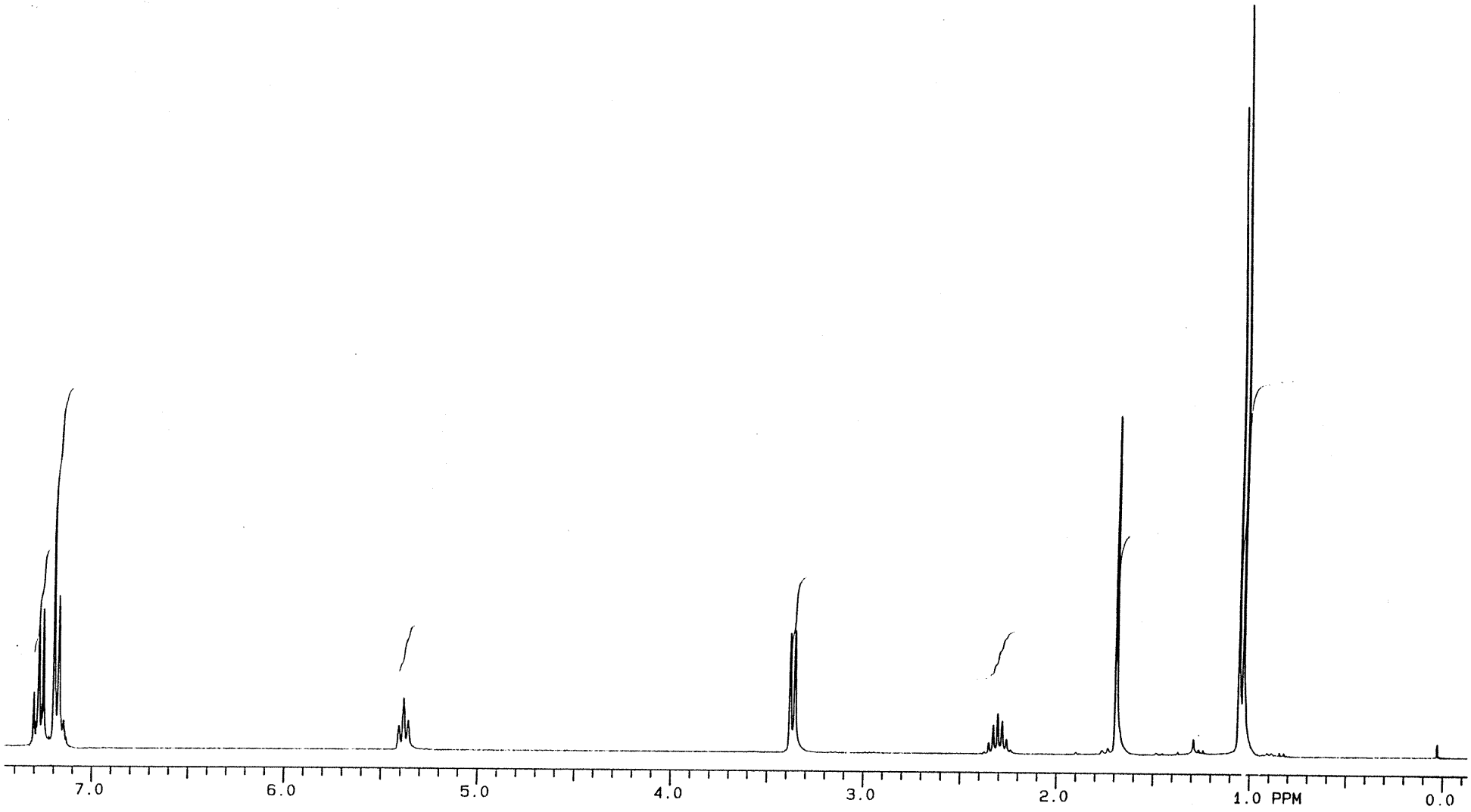


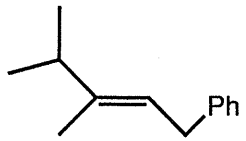


**2**

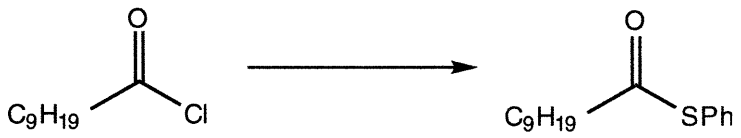


**3**

**S-Phenyl decanethioate (3)**[51,52]

A 500-mL, 3-necked, round-bottomed flask equipped with an argon inlet adapter, a 50-mL pressure-equalizing addition funnel fitted with a rubber septum, and a magnetic stirring bar was charged with 250 mL of methylene chloride, thiophenol (13.7 mL, 0.133 mol) and pyridine (10.8 mL, 0.133 mL) and then cooled in an ice-water bath. Decanoyl chloride (25.4 mL, 0.122 mol) was added dropwise via the addition funnel over the course of 15 min. The resulting suspension of white solid was stirred at 0 °C for 10 min and then at room temperature for 1 h. The reaction mixture was poured into 150 mL of water. The organic phase was separated and washed with 150 mL of 10% HCl and 150 mL of saturated NaCl solution, dried over $MgSO_4$, filtered, and concentrated to give 36.268 g of a liquid. Distillation through an 8-cm Vigreux column afforded 30.307 g (94%) of a clear, colorless, almost odorless oil, bp 142 °C *ca.* 0.1 mm Hg.

$^1$H NMR (300 MHz, $CDCl_3$): 7.39 (m, 5 H), 2.64 (t, J = 7.6 Hz, 2 H), 1.70 (m, 2 H), 1.27 (br s, 14 H), 0.88 (appar t, J = 6.9 Hz, 3 H).

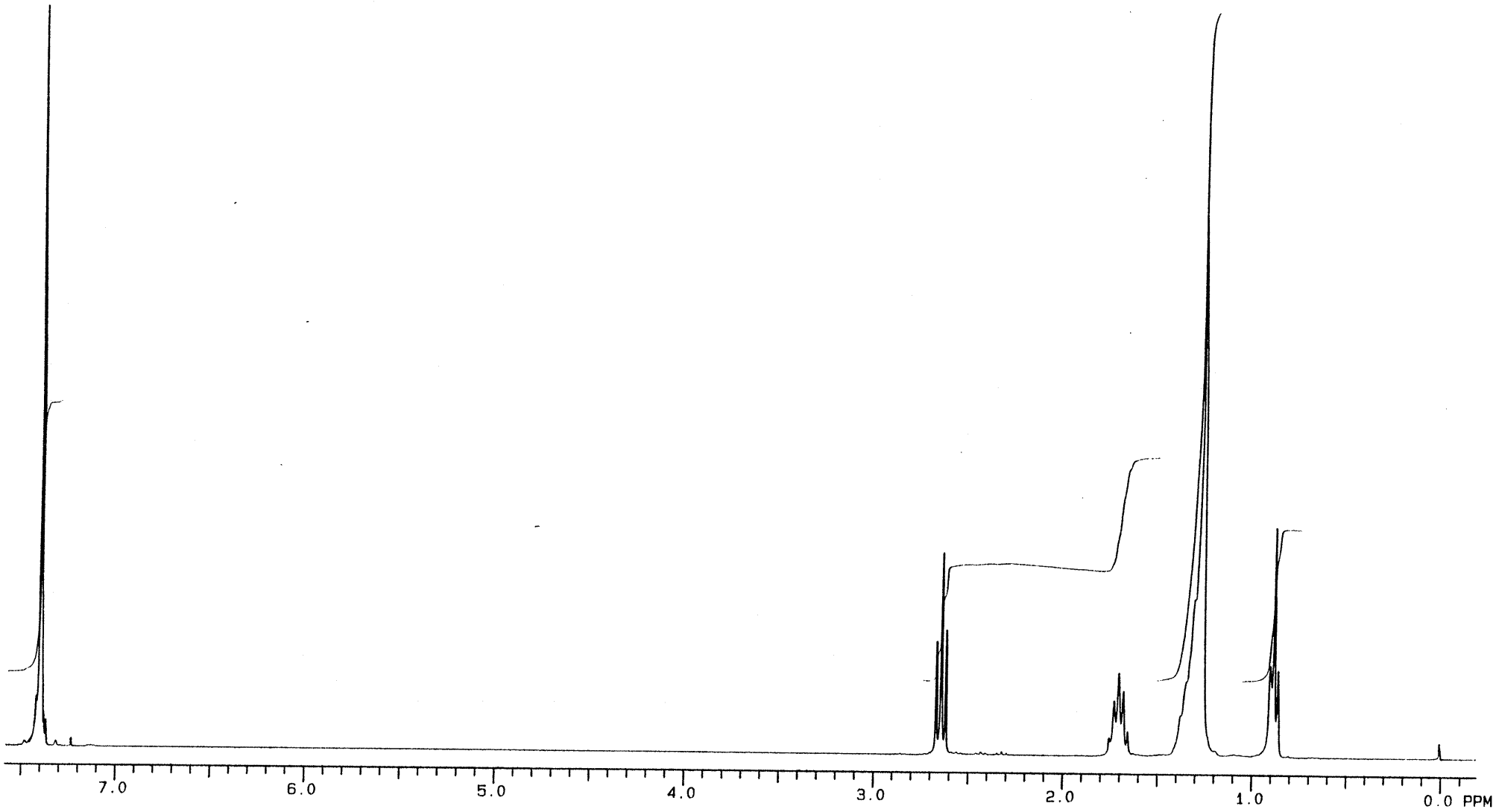


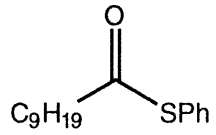


**3**

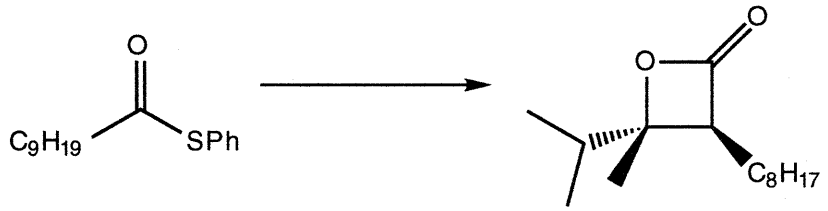


4

**4-Isopropyl-4-methyl-3-octyloxetan-2-one (4)**

A 500-mL, 3-necked, round-bottomed flask equipped with an argon inlet adapter, a 150-mL pressure-equalizing addition funnel fitted with a rubber septum, a magnetic stirring bar, and a rubber septum was charged with 200 mL of THF and diisopropylamine (17.5 mL, 0.125 mol), and then cooled in an ice-water bath. *n*-Butyllithium solution (2.10 M in hexanes, 56.2 mL, 0.118 mol) was added dropwise via syringe over the course of 10 min. After 10 min, the ice-water bath was replaced with a dry ice-acetone bath (-78 °C), and a solution of S-phenyl decanethioate (30.000 g, 0.113 mol) in 25 mL of THF was added dropwise via the addition funnel over the course of 15 min, rinsing with two 5-mL portions of THF. After 30 min, 3-methyl-2-butanone (12.1 mL, 0.113 mol) was added dropwise via syringe. The reaction mixture was stirred at -78 °C for 30 min and then allowed to warm gradually to 0 °C over the course of 1.5 h by adding room temperature acetone to the cooling bath. Half-saturated $NH_4Cl$ solution (150 mL) was then added, and the resulting mixture was partitioned between 200 mL of water and 200 mL of diethyl ether. The organic phase was washed with two 300-mL portions of 10% $Na_2CO_3$ solution, 300 mL of saturated NaCl solution, dried over $MgSO_4$, filtered, and concentrated to give 30.164 g of a yellow oil. A portion (29.841 g) of this material was distilled (43-80 °C, 0.25 mm Hg) to give 14.927 g of a liquid. A small portion of the distillate was further purified by column chromatography on silica gel (gradient elution with ethyl acetate-hexanes) to afford 0.046 g of **4** as a clear, colorless oil.

IR (neat) $cm^{-1}$: 2960, 2930, 2860, 1830, 1465, 1390, 1220, 1095, 1020, 810.

| | |
|---|---|
| $^1$H NMR (300 MHz, $CDCl_3$): | 3.13 (t, J = 8 Hz, 1 H), 1.99 (sept, J = 7 Hz, 1 H), 1.65-1.90 (m, 1 H), 1.50-1.65 (m, 1 H), 1.20-1.50 (m, 15 H), 1.02 (d, J = 7 Hz, 3 H), 0.93 (d, J = 7 Hz, 3 H), 0.88 (t, J = 7 Hz, 3 H). |
| $^1$H NMR NOE Experiment: | Irradiation of **4** at 3.13 ppm (ring CH) produces enhancement at 1.99 ppm (5.9%, isopropyl CH). |
| $^{13}$C NMR (75 MHz, $CDCl_3$): | 171.9, 85.0, 56.2, 37.5, 31.8, 29.4, 29.2, 29.1, 27.5, 25.0, 22.6, 17.5, 17.0, 14.9, 14.0. |
| Elemental Analysis: | Calculated for $C_{15}H_{28}O_2$: C, 74.95; H, 11.74.<br>Found: C, 75.17; H, 11.57. |

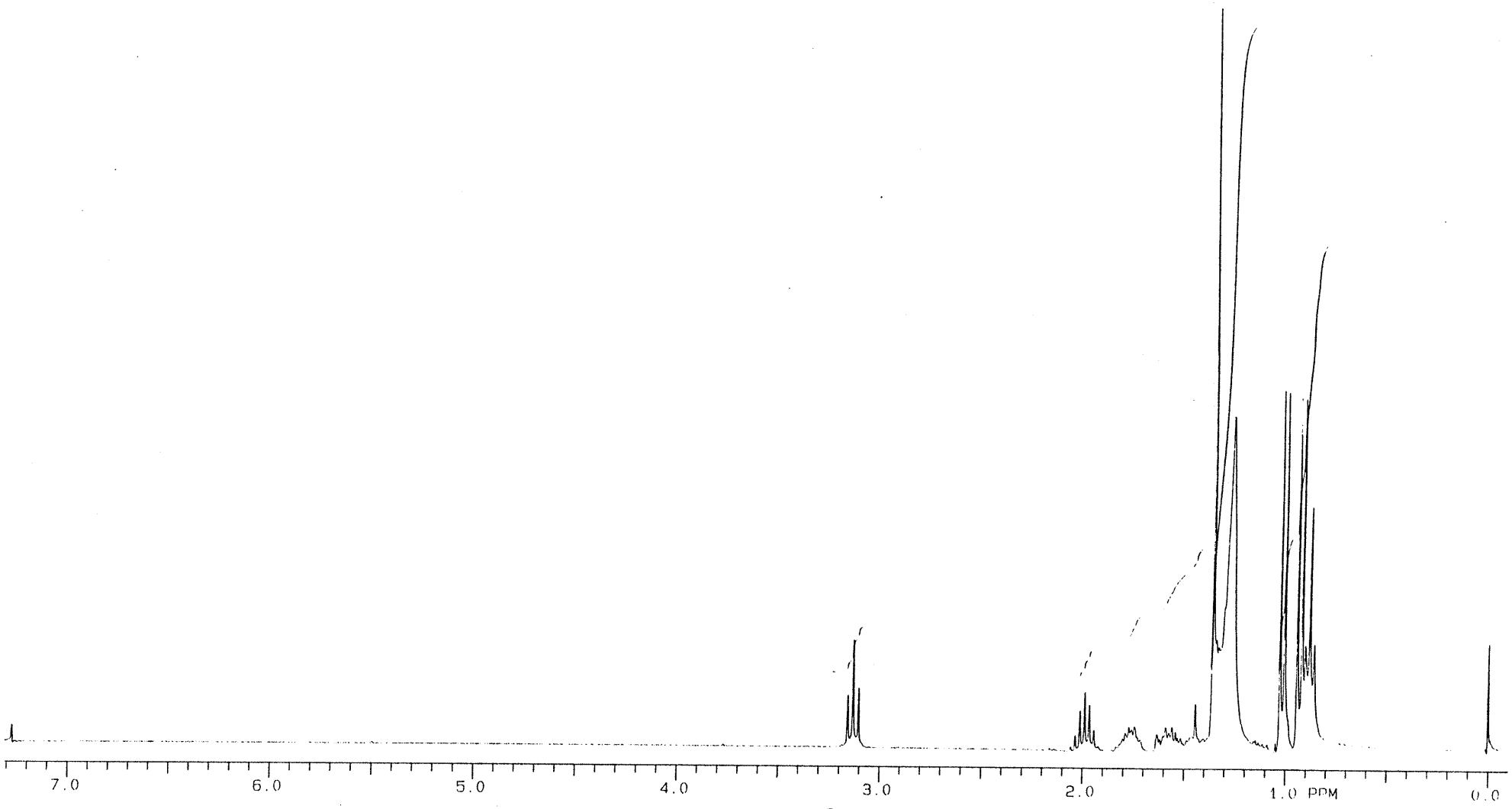


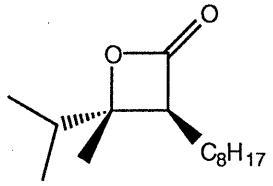


**4**

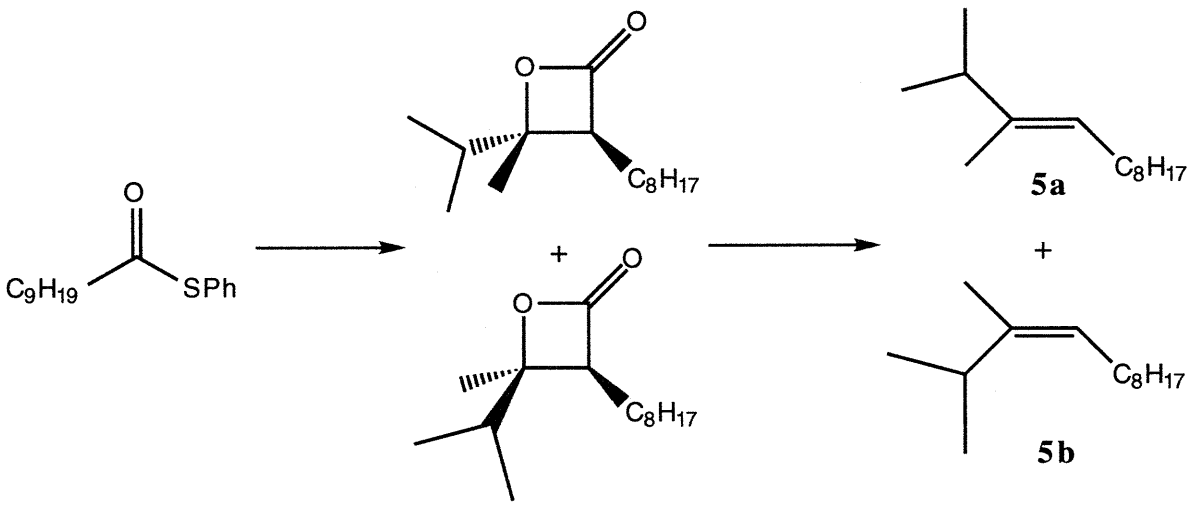


**(E)-2,3-dimethyl-3-dodecene (5a) and (Z)-2,3-dimethyl-3-dodecene (5b)**

A 500-mL, 3-necked, round-bottomed flask equipped with a nitrogen inlet adapter, a 150-mL pressure-equalizing addition funnel fitted with a rubber septum, a magnetic stirring bar, and a rubber septum was charged with 200 mL of THF and diisopropylamine (17.5 mL, 0.125 mol), and then cooled in an ice-water bath. *n*-Butyllithium solution (2.50 M in hexanes, 47.2 mL, 0.118 mol) was added dropwise via syringe over the course of 5-10 min. After 10 min, the ice-water bath was replaced with a dry ice-acetone bath (-78 °C), and a solution of S-phenyl decanethioate (30.000 g, 0.113 mol) in 25 mL of THF was added dropwise via the addition funnel over the course of 15 min. After 30 min, 3-methyl-2-butanone (12.1 mL, 0.113 mol) was added dropwise via syringe over the course of 5 min. The reaction mixture was stirred at -78 °C for 30 min and then allowed to warm gradually to 0 °C over the course of 1.5 h by adding room temperature acetone to the cooling bath. Half-saturated $NH_4Cl$ solution (150 mL) was then added, and the resulting mixture was partitioned between 200 mL of water and 200 mL of diethyl ether, The organic phase was washed with two 300-mL portions of 10% $Na_2CO_3$ solution, 300 mL of saturated NaCl solution, dried over $MgSO_4$, filtered, and concentrated to give 28.6 g of a yellow oil. This material was placed in a 500-mL, one-necked, round-bottomed flask equipped with a magnetic stirring bar and a reflux condenser fitted with a nitrogen inlet adapter. The flask was charged with 28.6 g of $SiO_2$ and 200 mL of cyclohexane. The reaction mixture was heated at

reflux for 1 h and then allowed to cool to room temperature and filtered to give 22.5 g of a clear orange oil. Distillation through an 8-cm Vigreux column (52 °C, 0.03 mm Hg) using shredded glass wool to reduce foaming afforded 13.02 g (59%) of a mixture of **5a** and **5b** as a colorless oil (96 : 4 mixture of isomers as determined by $^1$H NMR analysis).

| | |
|---|---|
| IR (neat) cm$^{-1}$: | 2970, 2940, 2870, 1465, 1380. |
| $^1$H NMR (300 MHz, $CDCl_3$): | For the *trans*-isomer **5a**:<br>5.15 (br t, J = 6.9 Hz, 1 H), 2.20 (m, 1 H), 1.95 (m, 2 H), 1.55 (s, 3 H), 1.25 (br s, 12 H), 0.98 (d, J = 6.5 Hz, 6 H), 0.87 (br t, 3H).<br><br>For the *cis*-isomer **5b** (partial data):<br>5.05 (appar t, J = 6.5 Hz), 2.80 (m), 1.60 (m), 0.94 (appar s). |
| $^1$H NMR NOE Experiment: | Irradiation of **5a** at 5.15 ppm (olefinic CH) produces enhancement at 2.20 ppm (6.7%, isopropyl CH). |
| $^{13}$C NMR (75 MHz, $CDCl_3$): | 140.6, 122.3, 36.8, 32.0, 30.0, 29.6, 29.4, 27.8, 22.7, 21.5, 20.9, 14.1. |
| Elemental Analysis: | Calculated for $C_{14}H_{28}$: C, 85.71; H, 14.29.<br>Found: C, 85.55; H, 14.38. |

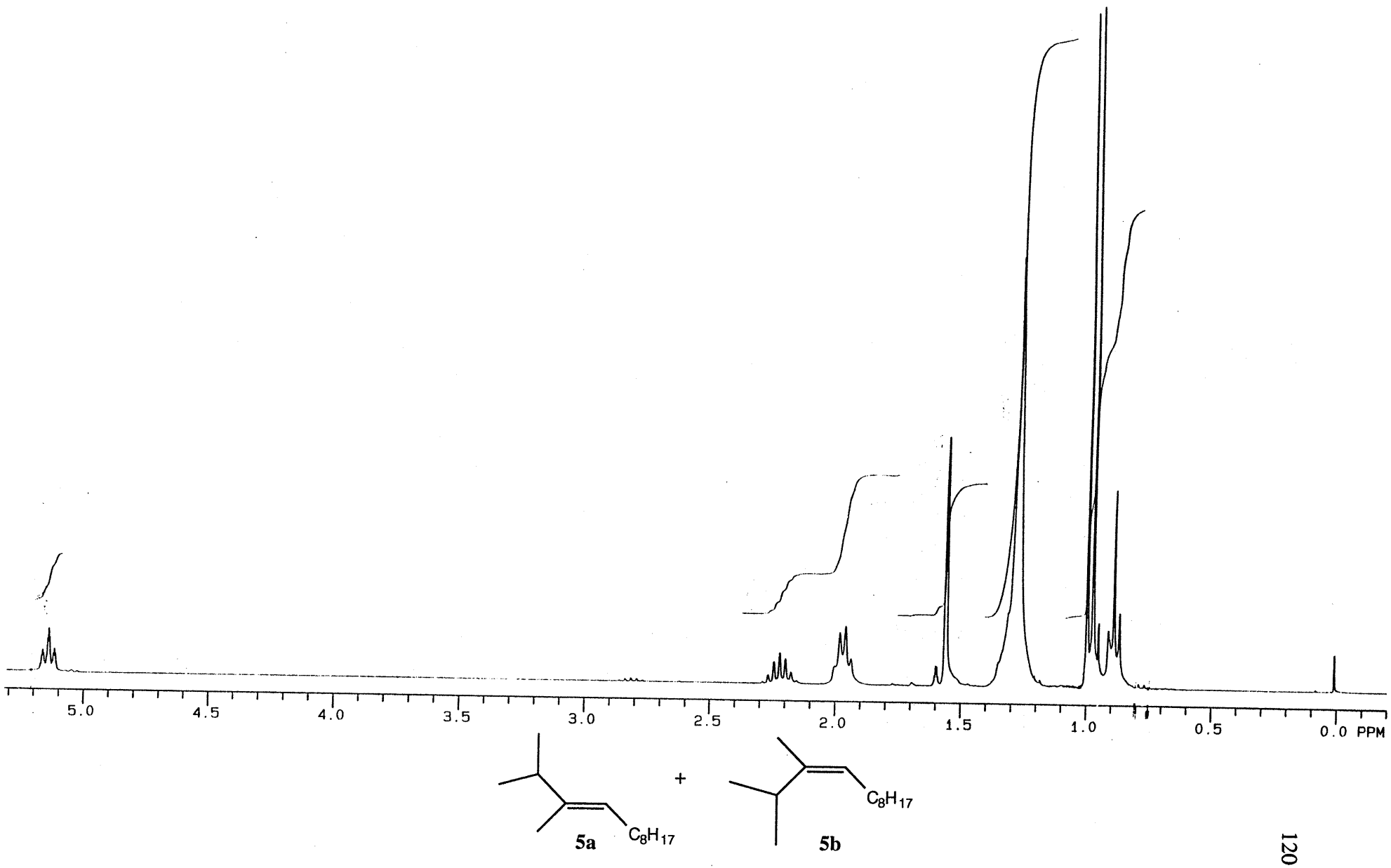


**5a** + **5b**

## Experimental Section for Part II

### Materials and Methods

#### Chromatography

For flash column chromatography silica gel (230-400 mesh) was purchased from EM Science. 5,5'-Dithiobis-(2-nitrobenzoic acid) was obtained from Aldrich and used for visualization of free thiols.

HPLC grade acetonitrile was purchased from J. T. Baker. Water was deionized and purified through a Millipore Milli-Q Plus filtration system. Trifluoroacetic acid (99+%) was purchased from Aldrich or Pierce Chemical Co. A binary solvent system was used consisting of acetonitrile and degassed 0.1% aqueous trifluoroacetic acid. Analytical HPLC was performed on a system consisting of either a) two Waters Model 501 pumps, a U6K injector, a Model 660 automated gradient controller, a Model 490 programmable multi-wavelength detector, a Model 730 data module, and a Vydec 0.46 x 25 cm (218TP54) $C_{18}$ reverse-phase column; a flow rate of 1 mL/min was used and absorbance was monitored at 214 nm; or b) two Waters Model 501 pumps, a U6K injector, a Model 660 automated gradient controller, a Model 990 programmable multi-wavelength detector, a Model 370 data module, and a Radial-Pak 8 X 10 RCM (2/17/95) $C_{18}$ column; a flow rate of 2 mL/min was used and absorbance was monitored simultaneously at 214 and 254 nm. Preparative HPLC purification was performed on a system consisting of a Waters Model 590 pump fitted with preparative heads, a Rheodyne injector, an Autochrome OPG/S solvent mixer, a Model 484 variable wavelength detector, a Vydec (GCH-101218GCC1210) guard column, and either a Vydec 2.2 X 25 cm (218TF1022) $C_{18}$ preparative column or a Waters Radial-Pak 25 X 10 RCM (2-9) preparative $C_{18}$ column; flow rates were typically 16 mL/min and absorbance was monitored at 214 nm. 0.45 μm Uniflo-25 disposable syringe filters were purchased from Schleicher & Scheull, Inc.

**IR**

Infrared spectra were taken on a Perkin-Elmer FT-IR Model 1600 using either NaCl salt plates or a horizontal trough attenuated total reflectance zinc selenide cell purchased from SpectroTech, Inc.

**NMR**

NMR spectra were taken on Varian VXR-500S and 501S spectrometers. Spectra were stored on disk and processed on a Silicon Graphics Iris Indigo workstation using Varian Instruments VNMR 4.3 software. Temperature was calibrated with methanol and maintained with a Varian VTC4 temperature control apparatus. For each temperature, probe and sample were allowed to equilibrate for 10 to 20 min.

$CDCl_3$ (99.8% D), $D_2O$ (99.9% and 99.96% D), and trifluoroethanol-$d_3$ (99% D) were purchased from Cambridge Isotope Laboratories. Trifluoroacetic acid-$d_1$ (99% D) and (2,2,3,3)-trimethylsilylpropionic acid-d4, sodium salt (TSP) were purchased from Aldrich. Aqueous NMR samples were prepared using 99.96% $D_2O$. Preparation of aqueous samples included lyophilization twice from 99.9% $D_2O$ followed by lyophilization from 99.96% $D_2O$ under high vacuum. Sample concentrations were typically 4 to 20 mM. The pD of resulting solutions of peptide amides were *ca.* 1 to 2 due to the trifluoroacetic acid salts of the peptides from reverse phase HPLC purification. All other samples were treated with 5 μL trifluoroacetic acid-$d_1$. Chemical shifts are expressed in parts per million (d) downfield from TSP for aqueous samples and TMS for organic samples.

The 90° pulse widths were obtained for each sample. Typical parameters for 1D $^1H$ NMR spectra of aqueous samples included acquisition times of 4 sec per transient and a delay time of 11 sec per transient to allow for sufficient relaxation of nuclei. The spectrum was phased to pure absorption. Level and tilt were adjusted for each set of peaks to be integrated. Three general areas

of integration were used. Region I encompasses *ca.* 3.7 to 4.2 ppm and contained the c and t states of the C12a, C12b, C11 and $C_\alpha$ protons of amino acid residues. In instances where this region was used, the c state of C11 proton is separated from the rest of the peaks in this region and used as an independent measure of the c state to calculate the t/c ratio for this region. Region II encompasses *ca.* 2.7 to 3.4 ppm and contains the c and t states of the C9b, C13b, and Lys-ε protons and the t state of the C9a proton. This region was always used since the c state of the C9b proton is well separated from other peaks. In some cases, the t state of the C9b proton is also well separated. Region III encompasses *ca.* 2.1 to 2.6 ppm and contains the c state of the C9a proton and the c and t states of the C13a, acetyl, C6b, and C7b protons. In instances where this region was used, the c state of the acetyl signal was separated from the rest of the peaks in this region. As many regions were used as possible. Integration resets were taken 8 to 10 Hz on either side of the outermost peaks depending on the proximity of nearby signals and the line shape. For spectra with good signal to noise and little or no baseline distortion, good agreement was found between the use of Region II and the use of multiple regions. Drift correction was not used. The error for integration is *ca.* 5% and slightly higher for t/c ratios greater than 6. (For a brief discussion of the identification of c and t state resonances, see p. 140.) Formulas for calculating t/c ratios from integrated areas can be found in the Allen thesis.[117]

**MS**

Mass spectra of peptides were acquired using a plasma desorption Applied Biosystems Bio-Ion 20 or by members of the Biemann laboratories using a Voyager Elite MALDI time of flight mass spectrometer. All other mass spectra were acquired by Ms. Li of the MIT Spectroscopy Lab using a Finnigan 8200 mass spectrometer.

---

[117] Allen, T. J., Ph. D. Thesis, Massachusetts Institute of Technology, 1993, p. 156.

### CD

Circular dichroism spectra were obtained on an Aviv Model 62-DS CD spectrometer equipped with a Neslab Coolflow CFT-33 refrigerated recirculator. Nitrogen to the spectrometer was from supplied from a GP-240 type liquid nitrogen tank equipped with a Model RGP-R1-3000 oxygen scrubber and an Oxisorb-W oxygen indicator cartridge. Calibration of wavelength was performed with benzene vapor at 266.7 nm. Calibration of CD detection was performed with a 1 mg/mL solution of (1S)-(+)-10-camphorsulfonic acid (CSA) in water. An exact concentration of the CSA solution was determined by absorption at 285 nm. Signal intensity was calibrated using a CSA solution of known concentration. Results of calibration tests fell within suggested operational parameter ranges. Quartz strain-free cells were supplied by Hellma, Inc. and were 0.1 cm in path length. A 0.2 M perchlorate solution consisting of 0.1 M sodium perchlorate and 0.1 M perchloric acid (pH of perchlorate solution = 1) was used as the solvent for all samples and for blanks. The same 0.1 cm quartz cell was used for the sample and the blank.

Each spectrum consisted of an average of 5 scans, each with a step size of 0.2 nm from 270 to 195 nm and an averaging time of 1 sec. A bandwidth of 0.06 nm was used. For each temperature, the sample was allowed to equilibrate for 15 min. One blank at 25 °C was taken per day of use using the same parameters. Spectra were corrected for blank and smoothed using Aviv 62 DS v4.0s software. For each spectrum, data for the region 250 to 270 nm were averaged and the spectrum corrected by that amount. Since the region 250 to 270 nm contain no signals for chromophores, the region was typically deleted.

### Concentration Determination

Concentrations were determined either by the MIT Biopolymers Laboratory (for all glycine containing peptides) or ninhydrin analysis of templated peptide hydrolysates developed by Dr. Oslick (for all other peptides).[118] For the latter method ninhydrin was purchased from Pierce

---

[118] Oslick, S. L., Ph. D. Thesis, Massachusetts Institute of Technology, 1996, pp. 122 - 153.

Chemical Co.; 2-methoxyethanol and sodium cyanide from Aldrich; acetic acid from Mallinckrodt. Solutions of 3% (w/v) ninhydrin in 2-methoxyethanol were tested for peroxides with 10% KI solution prior to use. Syringes were purchased from Hamilton Co. or Unimetrics Corp. Absorbance at 570 nm was measured using a Carl Zeiss UV/Vis spectrometer with a M4 QIII monochrometer, a 6V 30W tungsten lamp and a PI-2 detector.

Blanks consisted of the perchlorate solution used for CD studies. An alanine standard was used to reproduce the calibration curve for alanine. The following equations obtained by Dr. Oslick were used for each residue in the sample peptide:

| | |
|---|---|
| Ala: | absorbance = 0.0016294 + 21584 * molarity |
| Lys: | absorbance = 0.0040948 + 24175 * molarity |
| $NH_3$: | absorbance = 0.0155350 + 20286 * molarity |
| Ac-$Hel_1$: | absorbance = 0.0848650 + 1156.7 * molarity |

Microlitre pipets were not always reliable depending on whether they had ever been used for nonaqeous or volatile solvents. Refurbished microlitre pipets were not used. Hamilton and Unimetric syringes were deemed more reliable and used instead. The error of concentration determination by this method is *ca.* 5 %.

### Calculations

Calculations were performed using the software package Mathematica on Macintosh (v3.0), NeXT (v2.1), and PC (v3.0) platforms.

### Synthesis

Ammonia was supplied by Matheson Gas. Diethylazodicarboxylate, lithium borohydride, thiolacetic acid, trifluoroacetic acid, and triphenylphosphine were purchased from Aldrich. Methanol was purchased from Mallinckrodt. Tetrahydrofuran (THF) was distilled from sodium benzophenone ketyl prior to use.

**Solid Phase Peptide Synthesis**

Dimethylformamide was purchased from Burdick and Jackson. Reagent grade anhydrous methanol and methylene chloride were purchased from Fischer or Mallinckrodt. Anhydrous diethyl ether was purchased from Mallinkrodt and used within 2 to 3 months or if the containers were over half full. If there is doubt as to its quality, the ether should be checked for peroxides, which can oxidize the thioether bridge of Ac-Hel$_1$. All commercial solvents were used without further purification. Sigma-Cote was purchased from Aldrich. Reagent grade acetic acid was purchased from Mallinckrodt. Pyridine was purchased from Mallinckrodt and distilled from $CaH_2$ or ninhydrin. Trifluoroacetic acid (TFA) was purchased from Aldrich or Pierce Chemical Co. Thiophenol was purchased from Aldrich. Distilled water was purified through a Millipore Milli-Q filtration system. Fluorenylmethyl-2,4-dimethoxy-4'-(carbomethyloxy)-benzhydrylamine linked to aminomethyl resin (Knorr resin with a loading of 0.85 meq/g, 100 - 200 mesh) was purchased from Bachem Bioscience Inc. or Advanced Chemtech. Piperidine (99%), 1,3-diisopropylcarbodiimide (99%) (DIC) and 1-hydroxybenzotriazole (HOBt) were purchased from Aldrich. Fmoc-Ala-OH, Fmoc-Gly-OH, Fmoc-Lys(Boc)-OH were purchased from Bachem, Advanced Chemtech, or Novo Laboratories.

SPPS was performed using either a Thermolyne Type 500000 Maxi-Mix III or a Burrell Model 75 Wrist-Action shaker, with the latter giving better results; the maximum speed was used. Solid phase reaction vessels were custom made[119] using coarse (Grade C) fritted discs to avoid obstruction of pores by resin particles. The reaction vessels were prepared by silanizing with Sigma-Cote® for 5 to 20 min, flushed, and washed successively with methanol, water, methanol, and dichloromethane. Knorr resin (*ca.* 200 mg) was prepared by swelling in DMF for 1 to 4 h, then washed with DMF. The following protocol for Fmoc SPPS was used:

---

[119] Stewart, J. M.; Young, J. D., *Solid Phase Peptide Synthesis* 2nd ed.; Pierce Chemical Co.: Rockford, 1984; pp. 129-130. (A one-bore stopcock was used instead.)

Deprotection
5 min X 5 mL 30% piperidine in 1:1 DMF/dichloromethane (freshly prepared)
20 min X 5 mL 30% piperidine in 1:1 DMF/dichloromethane (freshly prepared). This was repeated for peptide chains 6 or more residues in length.
Washing: either
a) 10 X 1 min X 5 mL DMF
or b) 2 min X 5 mL DMF
2 min X 5 mL methanol
2 min X 5 mL dichloromethane
2 min X 5 mL methanol
2 min X 5 mL dichloromethane
Acylation
2 to 24 h X 5 mL 3 equiv Fmoc amino acid, 3 equiv DIC, and 3 equiv HOBt in *ca.* 5 mL 1:1 DMF/dichloromethane (freshly prepared)
Washing - same as above.
Capping
15 to 30 min X 5 mL 2 : 3 : 5 pyridine/acetic anhydride/dichloromethane (freshly prepared)
Washing - same as above.
Attachment of Ac-$Hel_1$
2 days X *ca.* 5 mL 10 mg Ac-$Hel_1$-OH, 10 equiv HOBt, 10 equiv DIC (measured by volume) in 5 mL 1:1 DMF/dichloromethane (freshly prepared). After 1 day, an additional 10 equiv DIC is added.

For acylation of growing peptide chains 4 or more residues in length, double acylations (excepting Ac-$Hel_1$) were performed, with each acylation performed overnight. Deprotections and acylations were monitored by the ninhydrin test.[120] Capping was performed after every residue except Ac-$Hel_1$. Towards the final stages of the syntheses, monitoring by analytical cleavage proceeded as follows. Several beads of resin were treated with 10 μL trifluoroacetic acid for 15-30 min in a vial, then subjected to vacuum to remove the acid; 10 to 20 μL acetonitrile and 10 to 20 μL water were added and mixed well; the solution was filtered through a plug of glass wool in a pipet and 20 μL of the filtrate was analyzed by HPLC to assess the purity of the peptide. If significant starting material (*ca.* 10 %) was observed, acylation or deprotection was repeated. Analytical cleavage was performed before and after attachment of Ac-$Hel_1$ and after difficult acylation and

---

[120] Sarin, V. K.; Kent, S. B. H.; Tam, J. P.; Merrifield, R. B. *Anal. Biochem.* **1981**, *117*, 147.

deprotection steps as determined by the qualitative ninhydrin test, for example after long alanine sequences (6 or more alanines). Prior to attachment of the template, *ca.* half of the peptidyl-resin was typically reserved. During acylation with Ac-$Hel_1$ additional diisopropylcarbodiimide should be added after 1 day, as noted in the protocol above.

Cleavage of templated peptide from the resin
3 X 45 min X *ca.* 5 mL 90 : 5 : 5 TFA/thioanisole/water (freshly prepared)

Final deprotection and cleavage of peptide from the resin was achieved by a mixture of trifluoroacetic acid, thiophenol, and water. The cleavage solution containing the free peptides was filtered from the resin through the sintered disk of the SPPS reaction vessel and flushed into a 40 mL plastic centrifuge tube filled with 25 mL diethyl ether, then centrifuged for 10 min at 3500 rpm and the ether layer discarded. The resin was treated with cleavage solution a total of three times for each peptide. The resulting white solid was removed of residual ether by house vacuum, then dissolved in water and filtered through a 0.45 μm Uniflo-25 low protein binding syringe filter and purified twice by preparative reverse-phase HPLC. Alternatively, the three cleavage mixtures were combined and concentrated by rotary evaporation under high vacuum; thiophenol was removed by repeated high vacuum evaporation from 1 to 2 mL water. Filtration and purification then proceeded as above. The product typically corresponds to the last major peak during HPLC (or the second to last major peak if residual thioanisole is present).

**Ac-$Hel_1$-OMe**

Ac-$Hel_1$-OMe was synthesized in 14 steps from L-proline and trans-4-hydroxy-L-proline according to the published procedure.[121] Ac-$Hel_1$-OH was obtained by saponification of Ac-$Hel_1$-OMe and prepared fresh before use.

**Ac-$Hel_1$-NHMe**

Ac-$Hel_1$-NHMe was available from Dr. Oslick.
IR ($CHCl_3$) $cm^{-1}$ (0.01 M): 3457, 3359, 3025, 1652

---

[121] McClure, K. F.; Renold, P.; Kemp, D. S. ***J. Org. Chem.*** **1995**, *60*, 454.

**(2S, 5S, 8S, 11S)-1-Acetyl-1,4-diaza-3-keto-5-methylenethiol-10-thiatricyclo[2.8.1.0$^{4,8}$]-tridecane (reduced template thiol, 7 X = S)**

The reduced template alcohol was synthesized by a procedure developed by Dr. McClure (unpublished): Ac-Hel$_1$-OMe (64 mg) was reduced with 2 equiv lithium borohydride in 1.8 mL THF for 1 h at room temperature. After reverse phase HPLC (0 to 100% $CH_3CN$ ($H_2O$ with 0.1% TFA/linear gradient)/120 min) and flash chromatography (9:1 ethyl acetate/methanol) 38 mg (65%) of the reduced template alcohol was obtained. To a solution of 43 mg triphenylphosphine in 1 mL THF cooled to 0 °C, 29 µL diisopropylazodicarboxylate was added and allowed to stir for 30 min. A solution of 38 mg of reduced template alcohol, 12 mL thiolacetic acid, and 2 mL THF was added and allowed to stir at 0°C for 2h, then at RT for 1 h. The crude thioacetate was purified by concentration by rotary evaporation followed by flash chromatography (ethyl acetate/hexanes, gradient elution, 5 to 10%) and preparative reverse phase HPLC (0 to 100% $CH_3CN$ ($H_2O$ with 0.1% TFA/linear gradient) / 120 min, RT 16 min). The thioacetate was cleaved with a methanolic solution of $NH_3$ at RT for 2.5 h, then concentrated by rotary evaporation, purified by preparative reverse phase HPLC (0 to 100% $CH_3CN$ ($H_2O$ with 0.1% TFE)/linear gradient)/120 min, RT 15 min) to afford 11 mg of a white solid (27% over 2 steps) which appeared as a single peak with analytical HPLC.

(2S, 5S, 8S, 11S)-1-Acetyl-1,4-diaza-3-keto-5-methylenethioacetate -10 - thiatricyclo[2.8.1.0$^{4,8}$]-tridecane (thioacetate) :

$^1$H NMR (300 MHz, $CDCl_3$): (2 conformations present, t/c = 0.2, c state = 1 H) 4.88 (m, 1.2 H), 4.39 (m, 1.2 H), 4.22 (m, 1.2 H), 3.89 (m, 2.4 H), 3.64 (m, 1.2 H), 3.27 (m, 2.4 H), 3.14 (dd, J = 6, 16 Hz, 1 H), 2.97 (m, 0.2 H), 2.91-2.68 (m, 2.4 H), 2.64 (d, J = 13 Hz, 1 H), 2.54-2.32 (m, 2.6 H), 2.37 (s, 3 H), 2.34 (s, 0.6 H), 2.21 (s, 0.6 H), 2.17 (s, 3 H), 1.77 (m, 3.6 H)

(2S, 5S, 8S, 11S) - 1 -Acetyl-1,4-diaza-3-keto-5-methylenethiol-10-thiatricyclo[2.8.1.$0^{4,8}$]-tridecane (reduced template thiol, 7) :

| | |
|---|---|
| $^1$H NMR (500 MHz, $CDCl_3$): | (2 conformations present, t/c = 0.5, c state = 1 H) 4.82 (d, J = 11 Hz, 0.5 H), 4.76 (d, J = 9 Hz, 1H), 4.32 (m, 1.5 H), 4.23 (m, 1.5 H), 3.96 (dd, J = 6, 11 Hz, 0.5 H), 3.83 (m, 2.5 H), 3.67 (t, J = 7 Hz, 0.5 H), 3.62 (t, J = 6 Hz, 1 H), 3.11 (dd, J = 6, 15 Hz, 1 H), 3.00 (ddd, J = 3, 8, 13 Hz, 1 H), 2.78 (m, 3 H), 2.59 (m, 2.5 H), 2.50 (d, J = 15 Hz, 0.5 H), 2.40 (dd, J = 9,15 Hz, 1 H), 2.34 (m, 1.5 H), 2.15 (s, 1.5 H), 2.13 (s, 3 H), 1.94 (m, 3 H), 1.76 (m, 1,5 H), H1.51 (appar t, J = 9 Hz, 0.5), 1.37 (dd, J = 8, 10 Hz, 1 H) |
| $^1$H NMR (500 MHz, $D_2O$): | (2 conformations present, t/c = 1.8, c state = 1 H) 4.80 (d, obscured by HDO signal), 4.65 (d, J = 10 Hz, 1.8 H), 4.21 (m, 5.6 H), 4.04 (m, 2.8 H), 3.96 (d, J = 12 Hz, 1H), 3.76 (m, 4.6 H), 3.48 (dd, J = 6, 16 Hz, 1 H), 3.13 (dd, J = , 5, 16 Hz, 1.8 H), 2.89 (dd, J = 2, 14 Hz), 2.80 (m, 4.6 H), 2.67 (m, 2.8 H), 2.52 (m, J = 3.8 Hz), 2.41 (d, J = 14 Hz, 1.8 H), 2.31 (m, 2.8 H), 2.12 (s, 5.4 H), 2.08 (s, 3 H), 1.93 (m, 5.6 H), 1.8 (dd, J = 6, 13 Hz, 2.8 H) |

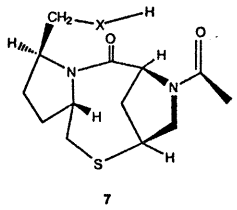


7




**7** in $CDCl_3$
X = S

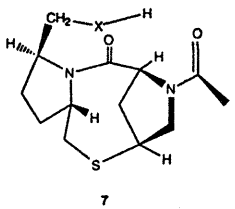


7




7 in $D_2O$
X = S

**Ac-Hel$_1$-Val-OH**

Ac-Hel$_1$-Val-OH was synthesized analogously to the published procedure for Ac-Hel$_1$-Ala-OH.[84a] Ac-Hel$_1$-OMe (50 mg) was treated with 0.1N NaOH (8.6 mL) for 6 h at room temperature, then quenched with 1N HCl (1.9 mL). The clear colorless solution was purified by preparative RP-HPLC (0% to 100% $CH_3CN$ ($H_2O$ with 0.1% TFA/linear gradient)/ 120 min, RT 15 min) to give 70 mg of a white solid. This was dissolved in $CH_2Cl_2$ (3 mL) and sequentially treated with benzotriazole-1-yl-oxy-tris-pyrrolidinophophonium hexafluorophosphate (PyBOP) (83 mg), HCl.$H_2$N-Val-O-*t*Bu (37 mg), and diisopropylethylamine (80 μL). The mixture was stirred for 4 h at room temperature, concentrated by rotary evaporation, and purified by preparative reverse phase HPLC (same conditions as above), and flash column chromatography (20:1 $CHCl_3$/MeOH) to give 91 mg of a white solid. This material was dissolved in $CH_2Cl_2$ (5 mL) and cooled to 0°C and a solution of 5 mL TFA in 1 mL $CH_2Cl_2$ was added. The reaction mixture was stirred at 0°C for 45 min, and at room temperature for 2.5 h, then concentrated by rotary evaporation and purified by preparative reverse phase HPLC to give 21 mg of a white powder (33% over 3 steps).

$^1$H NMR (500 MHz, $CDCl_3$): (2 conformations present, t/c = 1.2, c state = 1 H) 7.65 (d, J = 8 Hz, 1.2 H), 6.58 (d, J = 9 Hz, 1 H), 4.83 (d, J = 8 Hz, 1.2 H), 4.73 (m, 2.2 H), 4.56 (d, J = 9 Hz, 1 H), 4.52 (dd, J = 5, 9 Hz, 1 H), 4.37 (m, 1 H), 4.20 (m, 1.2 H), 4.16 (t, J = 8 Hz, 1.2 H), 3.90 (m, 1.2 H), 3.81 (m, 2 H), 3.66 (dd, J = 6, 7 Hz, 1.2 H), 3.60 (t, J = 5 Hz, 1 H), 3.19 (dd, J = 6, 15 Hz, 1 H), 2.88 (m, 2.2 H), 2.75 (m, 2.2 H), 2.59 (d, J = 13 Hz, 1 H), 2.52-1.80 (m, 17.8 H)

$^1$H NMR (500 MHz, $D_2O$): (2 conformations present, t/c = 0.8, c state = 1 H) 4.74 (m, obscured by HDO peak), 4.62 (d, J = 9 Hz, 1 H), 4.54 (d, J = 9 Hz, 0.8 H), 4.38 (m, 0.8 H), 4.31 (m, 1 H), 4.24 (d, J= 6 Hz, 1.8 H), 4.01 (m, 1.6 H), 3.31 (m, 1.8 H), 2.85 (m, 1 H), 2.75 (m, 0.8 H), 2.62 (dd, J = 9, 16 Hz, 0.8 H), 2.48 (m, 2 H), 2.39 (d, J = 14 Hz, 0.8 H), 2.20 (m, 10.8 H), 1.92 (m, 3.6 H), 0.98 (m, 10.8 H)

MS calc 397.167, obsd [M+H]+ 398.175

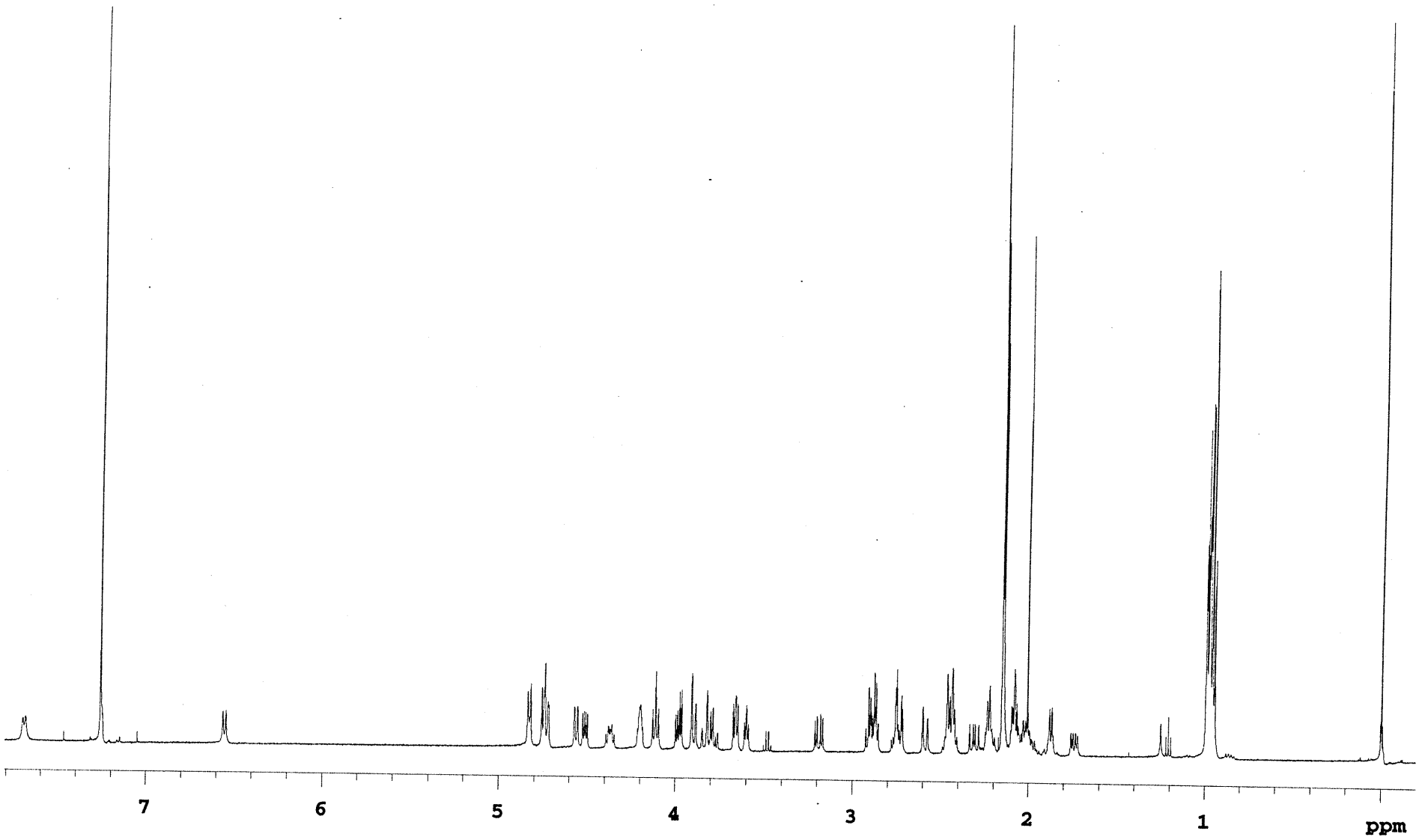


Ac-Hel$_1$-Val-OH in $CDCl_3$

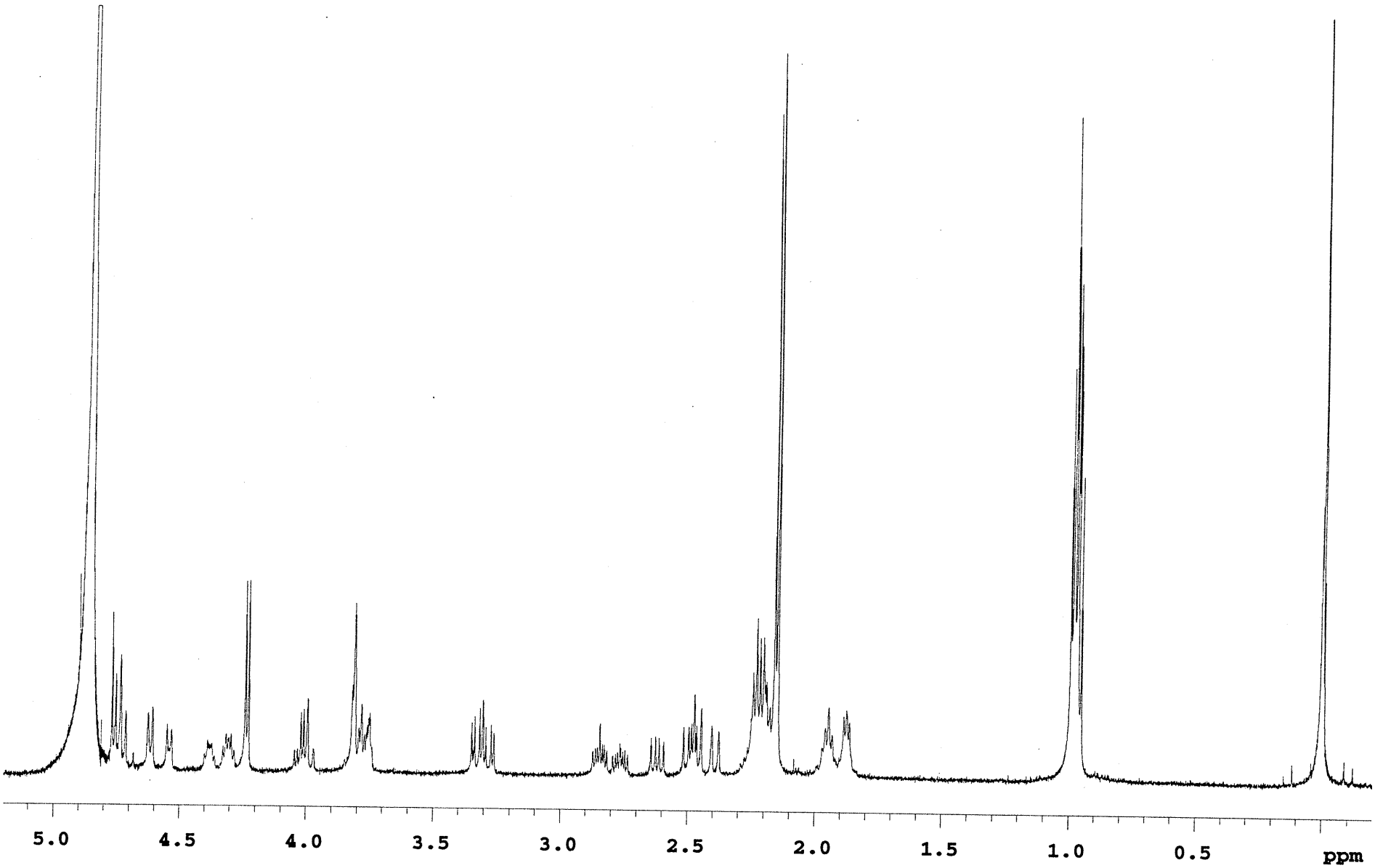


Ac-Hel$_1$-Val-OH in $D_2O$

**Templated polypeptides**

Templated polypeptides were synthesized and purified by preparative reverse phase HPLC at 0 to 60% $CH_3CN$ ($H_2O$ with 0.1% TFA/linear gradient) over 20 min, and at 0 to 65% $CH_3CN$ ($H_2O$ with 0.1% TFA/linear gradient) over *ca.* 40 min. The major side product is an alanine deletion. Purity was assessed by HPLC peak homogeneity and a mass spectrum showing the correct molecular ion. Alanine deletion or oxidation of the sulfur of the template are easily identified by this method. System A below refers to the preparative HPLC system indicated at the beginning of this section using the Radial-Pak and System B refers to the preparative HPLC system using the Vydec column.

| Compound<br>HPLC system, conditions, retention time | amount | calc [MH+] | obsd [MH+] |
|---|---|---|---|
| Ac-Hel$_1$-AAAAKAAAAKAAA-$NH_2$<br>System A, 0 to 65% $CH_3CN$/40 min, RT 16 min | 19 mg | 1335.73 | 1335.84 |
| Ac-Hel$_1$-AAAAKAAAAKAAAA-$NH_2$<br>System A, 0 to 65% $CH_3CN$/40 min, RT 16 min | 49 mg | 1407.68 | 1406.82 |
| Ac-Hel$_1$-AAAAAKAAAAKK-$NH_2$<br>System A, 0 to 65% $CH_3CN$/45 min, RT 17 min | 15 mg | 1322.62 | 1322.54 |
| Ac-Hel$_1$-AAAAAKAAAAKKK-$NH_2$<br>System A, 0 to 65% $CH_3CN$/45 min, RT 16 min | 33 mg | 1449.84 | 1450.43 |
| Ac-Hel$_1$-AAAAAKAAAAKKKK-$NH_2$<br>System A, 0 to 65% $CH_3CN$/40 min, RT 10 min | 11 mg | 1577.94 | 1579.05 |
| Ac-Hel$_1$-AGAAA-$NH_2$<br>System A, 0 to 60% $CH_3CN$/40 min, RT 11 min | 4 mg | 661.28 | 660.738 |
| Ac-Hel$_1$-AAGAA-$NH_2$<br>System A, 0 to 30% $CH_3CN$/30 min, RT 16 min | 2 mg | 661.28 | 660.566 |
| Ac-Hel$_1$-AAAGA-$NH_2$<br>System A, 0 to 60% $CH_3CN$/40 min, RT 12 min | 5 mg | 661.28 | 660.685 |
| Ac-Hel$_1$-AAAAG-$NH_2$<br>System A, 0 to 30% $CH_3CN$/30 min, RT 15 min | 3 mg | 661.28 | 660.590 |

| | | | |
|---|---|---|---|
| Ac-Hel$_1$-AAAAAAAK-NH$_2$<br>System B, 0 to 100% $CH_3CN$/120 min, RT 23 min | 58 mg | 923.12 | 923.8 |
| Ac-Hel$_1$-GAAAAAAK-NH$_2$<br>System A, 0 to 60% $CH_3CN$/40 min, RT 13 min | 34 mg | 909.46 | 909.529 |
| Ac-Hel$_1$-AGAAAAAK-NH$_2$<br>System A, 0 to 60% $CH_3CN$/40 min, RT 14 min | 14 mg | 909.46 | 909.508 |
| Ac-Hel$_1$-AAGAAAAK-NH$_2$<br>System A, 0 to 60% $CH_3CN$/40 min, RT 14 min | 8 mg | 909.46 | 909.546 |
| Ac-Hel$_1$-AAAGAAAK-NH$_2$<br>System A, 0 to 60% $CH_3CN$/40 min, RT 14 min | 19 mg | 909.46 | 909.486 |
| Ac-Hel$_1$-AAAAGAAK-NH$_2$<br>System A, 0 to 60% $CH_3CN$/40 min, RT 14 min | 9 mg | 909.46 | 909.481 |
| Ac-Hel$_1$-AAAAAGAK-NH$_2$<br>System A, 0 to 60% $CH_3CN$/40 min, RT 14 min | 17 mg | 909.46 | 909.355 |
| Ac-Hel$_1$-AAAAAAGK-NH$_2$<br>System A, 0 to 60% $CH_3CN$/40 min, RT 15 min | 10 mg | 909.46 | 909.384 |

$^1$H NMR spectra for Ac-Hel$_1$-AAAAKAAAAKAAA-NH$_2$, Ac-Hel$_1$-AAAAAKAAAAKK-NH$_2$, Ac-Hel$_1$-AAAGA-NH$_2$, and Ac-Hel$_1$-AAAGAAAK-NH$_2$ at 25 °C are shown on the following pages, one for each series of similar compounds. For Ac-Hel$_1$-AAAGAAAK-NH$_2$, spectra at 2, 25, and 60 °C are shown. The template region of the $^1$H NMR spectrum for Ac-Hel$_1$-GAAAAAAK-NH$_2$ is also shown.

Ac-Hel$_1$-AAAAKAAAAKAAA-NH$_2$ (500 MHz, D$_2$O, 25 °C):
(2 conformations present, t/c = 5.3, c state = 1 H) 4.50-4.83 (interference by HDO peak), 4.10-4.34 (m, 93.5 H), 3.52-3.90 (m, 8.3 H), 3.31 (dd, J = 6, 15 Hz, 1 H), 2.80-3.12 (m, 42.1 H), 2.20-2.54 (m, 35.8 H), 2.13 (s, 3 H), 1.64-2.10 (m, 63.0 H), 1.30-1.64 (m, 233 H)

Ac-Hel$_1$-AAAAKAAAAKAAAA-NH$_2$ (500 MHz, D$_2$O, 25 °C):
(2 conformations present, t/c = 5.8, c state = 1 H) 4.50-4.83 (interference by HDO peak), 4.07-4.39 (m, 107.8 H), 3.52-3.90 (m, 8.8 H), 3.31 (dd, J = 6, 15 Hz, 1 H), 2.80-3.12 (m, 45.6 H), 2.17-2.54 (m, 38.8 H), 2.13 (s, 3 H), 1.64-2.11 (m, 68.0 H), 1.30-1.64 (m, 272 H)

Ac-Hel$_1$-AAAAAKAAAAKK-NH$_2$ (500 MHz, D$_2$O, 25 °C):
(2 conformations present, t/c = 5.6, c state = 1 H) 4.50-4.80 (interference by HDO peak), 4.07-4.42 (m, 91.4 H), 3.53-3.90 (m, 8.6 H), 3.31 (dd, J = 6, 15 Hz, 1 H), 2.80-3.12 (m, 57.4 H), 2.16-2.53 (m, 37.6 H), 2.13 (s, 3 H), 1.62-2.10 (m, 92.4 H), 1.30-1.62 (m, 158 H)

Ac-Hel$_1$-AAAAAKAAAAKKK-NH$_2$ (500 MHz, D$_2$O, 25 °C):
(2 conformations present, t/c = 5.9, c state = 1 H) 4.50-4.82 (interference by HDO peak), 4.10-4.43 (m, 103 H), 3.53-3.90 (m, 7.9 H), 3.31 (dd, J = 6, 15 Hz, 1 H), 2.80-3.12 (m, 73.9 H), 2.17-2.53 (m, 39.4 H), 2.13 (s, 3 H), 1.62-2.10 (m, 124 H), 1.30-1.62 (m, 179 H)

Ac-Hel$_1$-AAAAAKAAAAKKKK-NH$_2$ (500 MHz, D$_2$O, 25 °C):
(2 conformations present, t/c = 5.9, c state = 1 H) 4.51-4.83 (interference by HDO peak), 4.10-4.43 (m, 109 H), 3.72-3.90 (m, 7.9 H), 3.31 (dd, J = 6, 15 Hz, 1 H), 2.80-3.14 (m, 87.7 H), 2.16-2.54 (m, 39.4 H), 2.13 (s, 3 H), 1.64-2.11 (m, 152 H), 1.32-1.64 (m, 193 H)

Ac-Hel$_1$-AGAAA-NH$_2$ (500 MHz, D$_2$O, 25 °C):
(2 conformations present, t/c = 1.3, c state = 1 H) 4.65-4.90 (interference by HDO peak), 4.57 (m, 2.3 H), 4.20-4.43 (m, 18.4 H), 3.75-3.92 (m, 12.5 H), 3.33 (dd, J = 6, 15 Hz, 1 H), 3.14 (dd, J = 5, 16 Hz, 1.3 H), 2.76-2.92 (m, 3.6 H), 2.41-2.54 (m, 3.3 H), 2.10-2.32 (m, 11.5 H), 1.74-2.04 (m, 4.6 H), 1.25-1.55 (m, 27.6 H)

Ac-Hel$_1$-AAGAA-NH$_2$ (500 MHz, D$_2$O, 25 °C):
(2 conformations present, t/c = 1.5, c state = 1 H) 4.68-4.80 (interference by HDO peak), 4.57 (m, 2.5 H), 4.22-4.44 (m, 20.0 H), 3.75-4.12 (m, 12.5 H), 3.33 (dd, J = 6, 15 Hz, 1 H), 3.12 (dd, J = 4, 16 Hz, 1.5 H), 2.80-2.92 (m, 4.0 H), 2.41-2.53 (m, 3.5 H), 2.10-2.30 (m, 12.5 H), 1.84-2.04 (m, 5.0 H), 1.45-1.55 (m, 30 H)

Ac-Hel$_1$-AAAGA-$NH_2$ (500 MHz, $D_2O$, 25 °C):
(2 conformations present, t/c = 1.6, c state = 1 H) 4.68-4.83 (interference by HDO peak), 4.58 (m, 2.6 H), 4.22-4.37 (m, 20.8 H), 4.03-4.12 (m, 3.2 H), 3.97 (m, 5.2 H), 3.70-3.90 (m, 3.6 H), 3.33 (dd, J = 6, 15 Hz, 1 H), 3.11 (dd, J = 4, 16 Hz, 1.6 H), 2.72-2.94 (m, 4.2 H), 2.43-2.54 (m, 3.6 H), 2.10-2.30 (m, 13 H), 1.84-2.03 (m, 5.2 H), 1.30-1.50 (m, 31.2 H)

Ac-Hel$_1$-AAAAG-$NH_2$ (500 MHz, $D_2O$, 25 °C):
(2 conformations present, t/c = 1.7, c state = 1 H) 4.68-4.82 (interference by HDO peak), 4.53-4.62 (m, 2.7 H), 4.41-4.47 (m, 1.7 H), 4.22-4.35 (m, 19.9 H), 3.74-4.12 (m, 13.5 H), 3.33 (dd, J = 6, 15 Hz, 1 H), 3.09 (dd, J = 4, 16 Hz, 1.7 H), 2.82-2.94 (m, 4.2 H), 2.42-2.54 (m, 3.7 H), 2.18-2.32 (m, 10.5 H), 2.16 (s, 3 H), 1.72-2.03 (m, 5.4 H), 1.30-1.50 (m, 31.4 H)

Ac-Hel$_1$-AAAAAAAK-$NH_2$ (500 MHz, $D_2O$, 25 °C):
(2 conformations present, t/c = 3.5, c state = 1 H) 4.48-4.82 (interference by HDO peak), 4.07-4.34 (m, 44 H), 4.25-4.40 (m, 6.5 H), 3.32 (dd, J = 6, 15 Hz, 1 H), 2.82-3.07 (m, 20.5 H), 2.27-2.54 (m, 24 H), 2.06 (s, 3 H), 1.62-2.07 (m, 27 H), 1.30-1.62 (m, 104 H)

Ac-Hel$_1$-GAAAAAAK-$NH_2$ (500 MHz, $D_2O$, 25 °C):
(2 conformations present, t/c = 2.9, c state = 1 H) 4.57-4.88 (interference by HDO peak), 4.20-4.46 (m, 31.2 H), 4.02-4.12 (m, 3.9 H), 3.87-4.12 (m, 7.8 H), 3.70-3.87 (m, 5.9 H), 3.32 (dd, J = 6, 15 Hz, 1 H), 2.80-3.10 (m, 17.4 H), 2.44-2.54 (m, 4.9 H), 2.16-2.33 (m, 16.5 H), 2.13 (s, 3 H), 1.64-2.04 (m, 23.4 H), 1.30-1.57 (m, 78 H)

Ac-Hel$_1$-AGAAAAAK-$NH_2$ (500 MHz, $D_2O$, 25 °C):
(2 conformations present, t/c = 1.7, c state = 1 H) 4.69-4.82 (interference by HDO peak), 4.54-4.58 (m, 2.7 H), 4.20-4.44 (m, 21.6 H), 3.70-4.10 (m, 13.5 H), 3.31 (dd, J = 6, 15 Hz, 1 H), 3.12 (dd, J = 4, 16 Hz, 1.7 H), 2.94-3.05 (m, 5.4 H), 2.78-2.94 (m, 4.4 H), 2.42-2.53 (m, 3.7 H), 2.17-2.30 (m, 10.5 H), 2.13 (s, 3 H), 1.64-2.04 (m, 16.2 H), 1.30-1.56 (m, 54 H)

Ac-Hel$_1$-AAGAAAAK-$NH_2$ (500 MHz, $D_2O$, 25 °C):
(2 conformations present, t/c = 1.7, c state = 1 H) 4.68-4.85 (interference by HDO peak), 4.53-4.60 (m, 2.7 H), 4.20-4.45 (m, 21.6 H), 3.70-4.12 (m, 13.5 H), 3.32 (dd, J = 6, 15 Hz, 1 H), 3.09 (dd, J = 4, 16 Hz, 1.7 H), 2.94-3.05 (m, 5.4 H), 2.80-2.94 (m, 4.4 H), 2.41-2.52 (m, 3.7 H), 2.10-2.30 (m, 13.5 H), 1.56-2.04 (m, 16.2 H), 1.30-1.56 (m, 54 H)

Ac-Hel$_1$-AAAGAAAK-$NH_2$ (500 MHz, $D_2O$, 25 °C):
(2 conformations present, t/c = 2.0, c state = 1 H) 4.68-4.83 (interference by HDO peak), 4.54-4.60 (m, 3.0 H), 4.20-4.46 (m, 24.0 H), 4.02-4.12 (m, 4.0 H), 3.89-3.98 (m, 6.0 H), 3.73-3.88 (m, 5.0 H), 3.31 (dd, J = 6, 15 Hz, 1 H), 3.07 (dd, J = 4, 16 Hz, 2.0 H), 2.95-3.03 (m, 6.0 H), 2.42-2.52 (m, 4.0 H), 2.27-2.80 (m, 12.0 H), 2.14 (s, 3 H), 1.62-2.03 (m, 18.0 H), 1.30-1.56 (m, 60 H)

Ac-Hel$_1$-AAAAGAAK-$NH_2$ (500 MHz, $D_2O$, 25 °C):
(2 conformations present, t/c = 2.1, c state = 1 H) 4.68-4.85 (interference by HDO peak), 4.54-4.60 (m, 3.1 H), 4.20-4.47 (m, 24.8 H), 4.03-4.12 (m, 4.2 H), 3.88-3.98 (m, 6.2 H), 3.74-3.88 (m, 5.1 H), 3.32 (dd, J = 6, 15 Hz, 1 H), 2.96-3.10 (m, 8.3 H), 2.40-2.53 (m, 4.1 H), 2.17-2.32 (m, 12.5 H), 2.14 (s, 3 H), 1.65-2.03 (m, 18.6 H), 1.30-1.57 (m, 62 H)

Ac-Hel$_1$-AAAAAGAK-$NH_2$ (500 MHz, $D_2O$, 25 °C):

(2 conformations present, t/c = 2.4, c state = 1 H) 4.68-4.85 (interference by HDO peak), 4.54-4.62 (m, 3.4 H), 4.20-4.48 (m, 27.2 H), 4.05-4.13 (m, 4.8 H), 3.89-3.98 (m, 7.8 H), 3.74-3.88 (m, 5.4 H), 3.32 (dd, J = 6, 15 Hz, 1 H), 2.80-3.07 (m, 15 H), 2.43-2.53 (m, 4.4 H), 2.18-2.34 (m, 14.0 H), 2.13 (s, 3 H), 1.65-2.03 (m, 20.4 H), 1.30-1.57 (m, 68 H)

Ac-Hel$_1$-AAAAAAGK-$NH_2$ (500 MHz, $D_2O$, 25 °C):
(2 conformations present, t/c = 2.8, c state = 1 H) 4.68-4.85 (interference by HDO peak), 4.54-4.64 (m, 3.8 H), 4.48 (m, 2.8 H), 4.19-4.35 (m, 27.6 H), 4.05-4.14 (m, 5.6 H), 3.70-3.90 (m, 5.8 H), 3.31 (dd, J = 6, 15 Hz, 1 H), 2.80-3.05 (m, 17 H), 2.43-2.53 (m, 4.8 H), 2.17-2.37 (m, 16.0 H), 2.13 (s, 3 H), 1.65-2.03 (m, 22.8 H), 1.28-1.60 (m, 76 H)

### Identification of t *vs.* cs state resonances[84ac,86a]

The invariance of the C9b proton is the key to the identification of t *vs.* cs state resonances. As a distinguishable doublet of doublets at *ca.* 3.2 to 3.3 ppm in water or at *ca.* 3.1 to 3.2 ppm in organic solvents, the C9b protons of the cs state are often isolated from nearby peaks. The template t state peaks shifts may change significantly upon temperature change or addition of TFE, particularly the C9a, C9b, C13a, and C13b protons, due to differing proportions of te and ts states within the t state manifold. The C12ab resonances for the t state are separated from the C12ab resonances for the cs state, with the latter appearing close to the C11 resonances. For templated peptides in water, alpha protons appear at *ca.* 4.2 ppm as overlapped peaks and cannot usually be distinguished between cs and t states. However, for peptides with glycine next to the template, alpha protons for t and cs states are distinguishable.[122] The two alpha protons are inequivalent for the t state and each proton appears as a doublet; the cs state alpha protons are equivalent and give rise to a singlet (see p. 147 for example). Side chain resonances for the beta, gamma, delta, and epsilon protons of lysine appear at *ca.* 1.7-1.9 ppm, 1.45 ppm, 1.70 ppm, and 2.99 ppm, respectively, and are not usually distinguishable for the cs *vs.* t states.[123] Though measurement of t/c ratios does not require use of 9:1 $H_2O$:$D_2O$ and water suppression, t and cs state amide proton resonances under these conditions are distinguishable by chemical shift.[124]

---

[122] Boyd, J. G., Ph.D. Thesis, Massachusetts Institute of Technology, 1989, p. 149-154.
[123] Chemical shifts for the side chains of other amino acid residues in the cs state can be found in *NMR of Proteins and Nucleic Acids*; Wüthrich, K.; Wiley and Sons, Inc.: New York, 1986; p. 17.
[124] Boyd, J. G., Ph.D. Thesis, Massachusetts Institute of Technology, 1989, p.103-106.

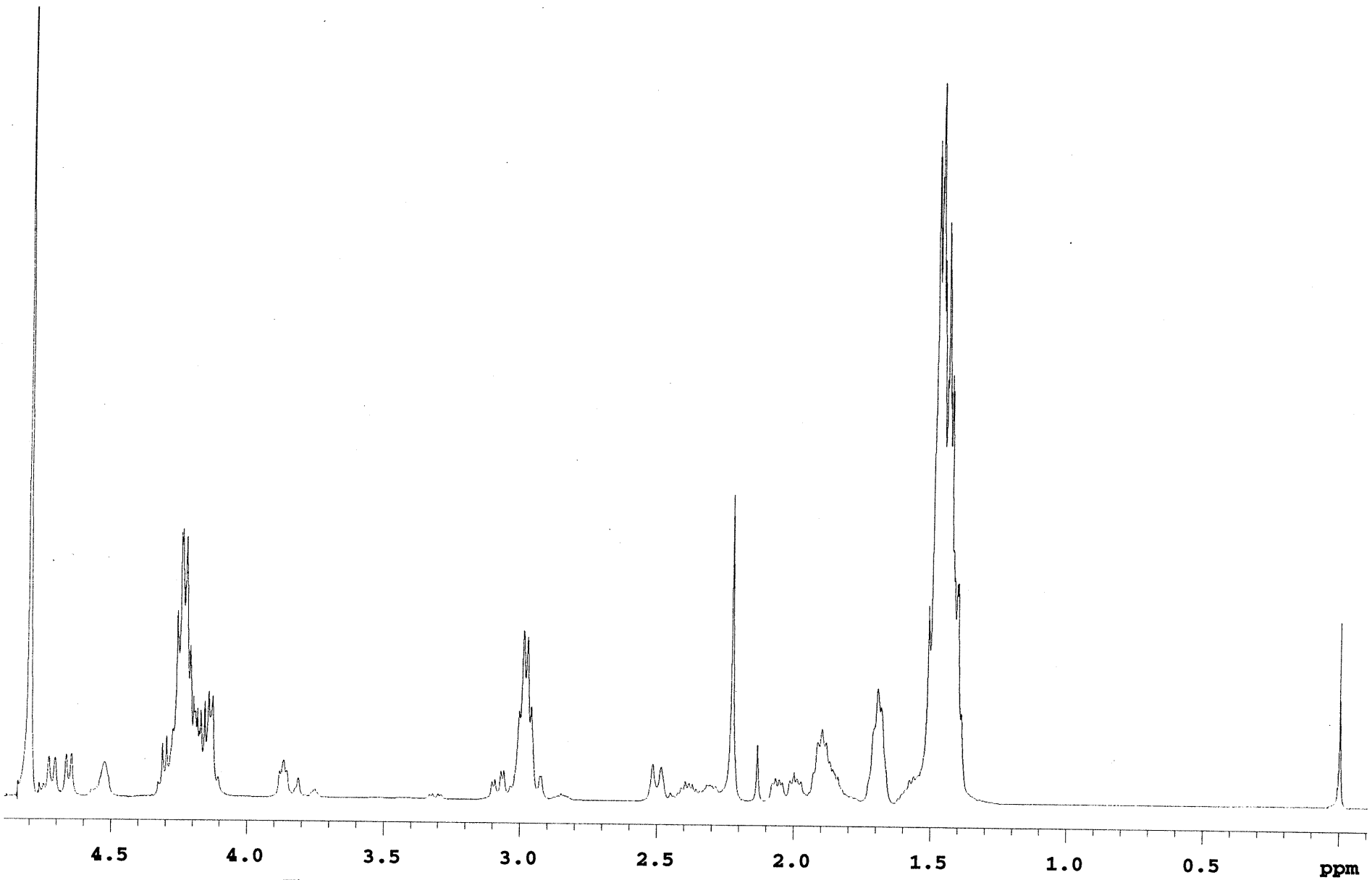


Fig. 1 $^{1}H$ NMR spectrum of Ac-$Hel_1$-AAAAKAAAAKAAA-$NH_2$ in $D_2O$ at 25 °C.

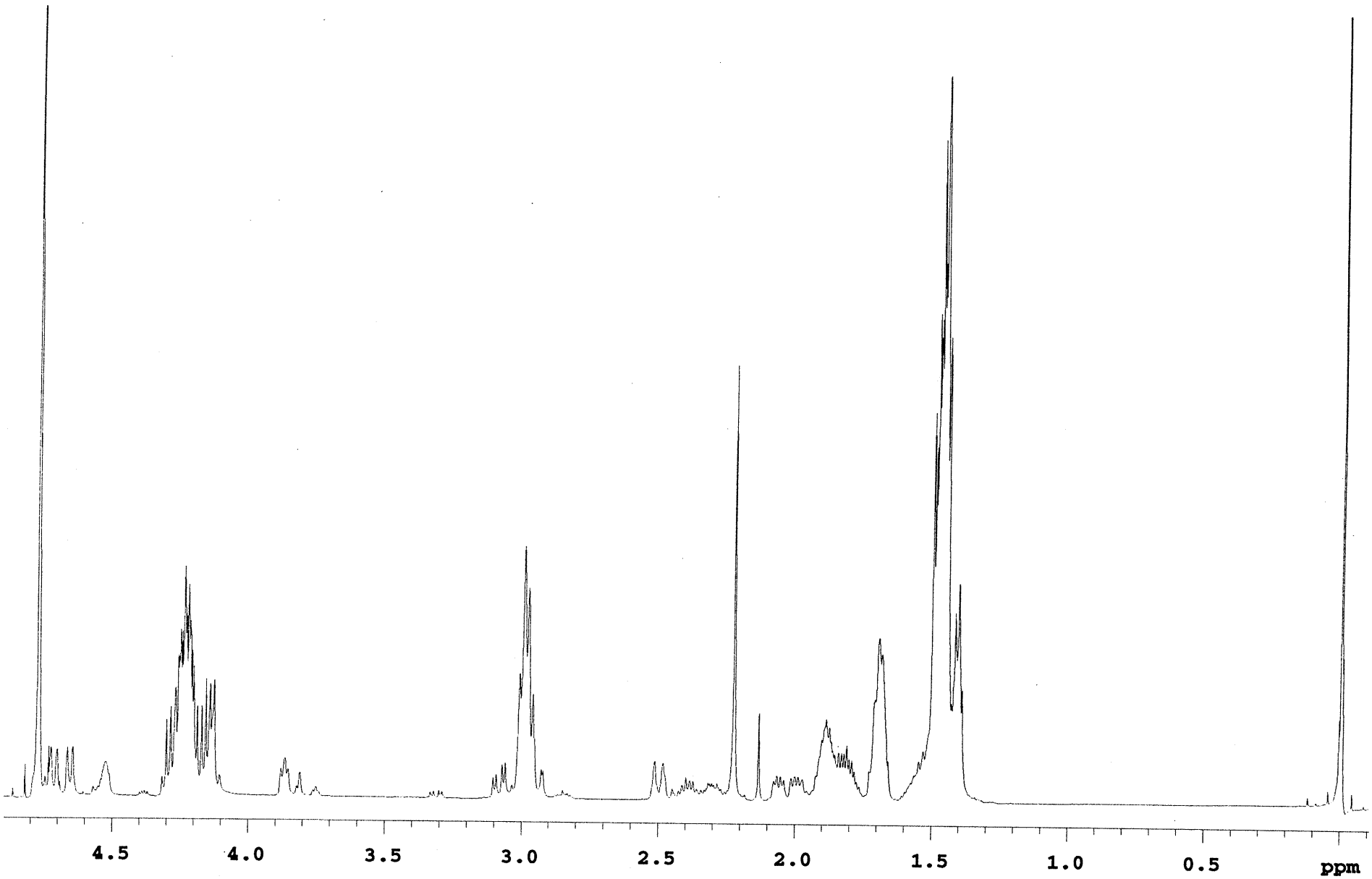


Fig. 2 $^{1}H$ NMR spectrum of Ac-$Hel_1$-AAAAAKAAAAKK-$NH_2$ in $D_2O$ at 25 °C.

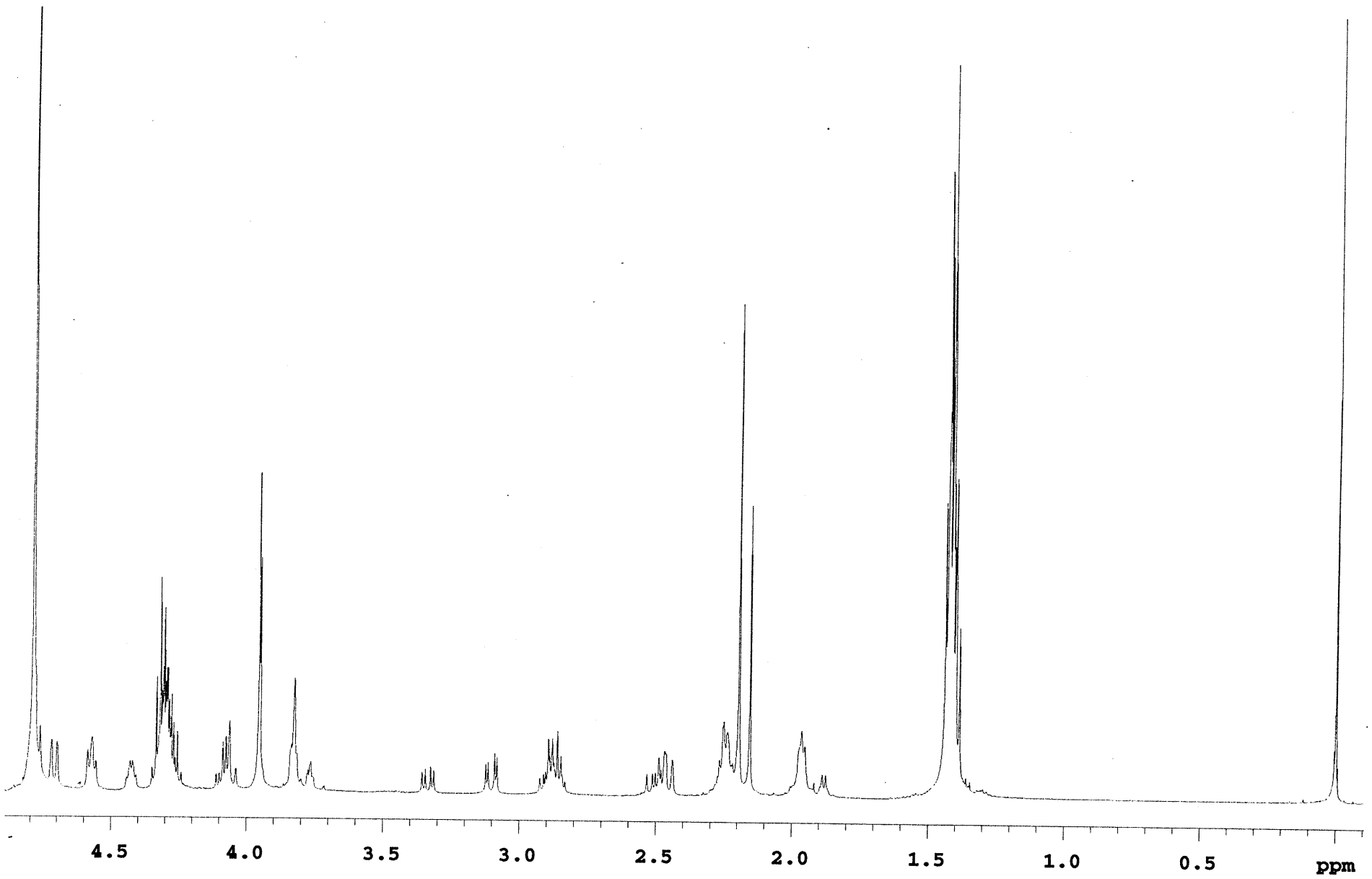


Fig. 3 $^{1}H$ NMR spectrum of Ac-$Hel_1$-AAAGA-$NH_2$ in $D_2O$ at 25 °C.

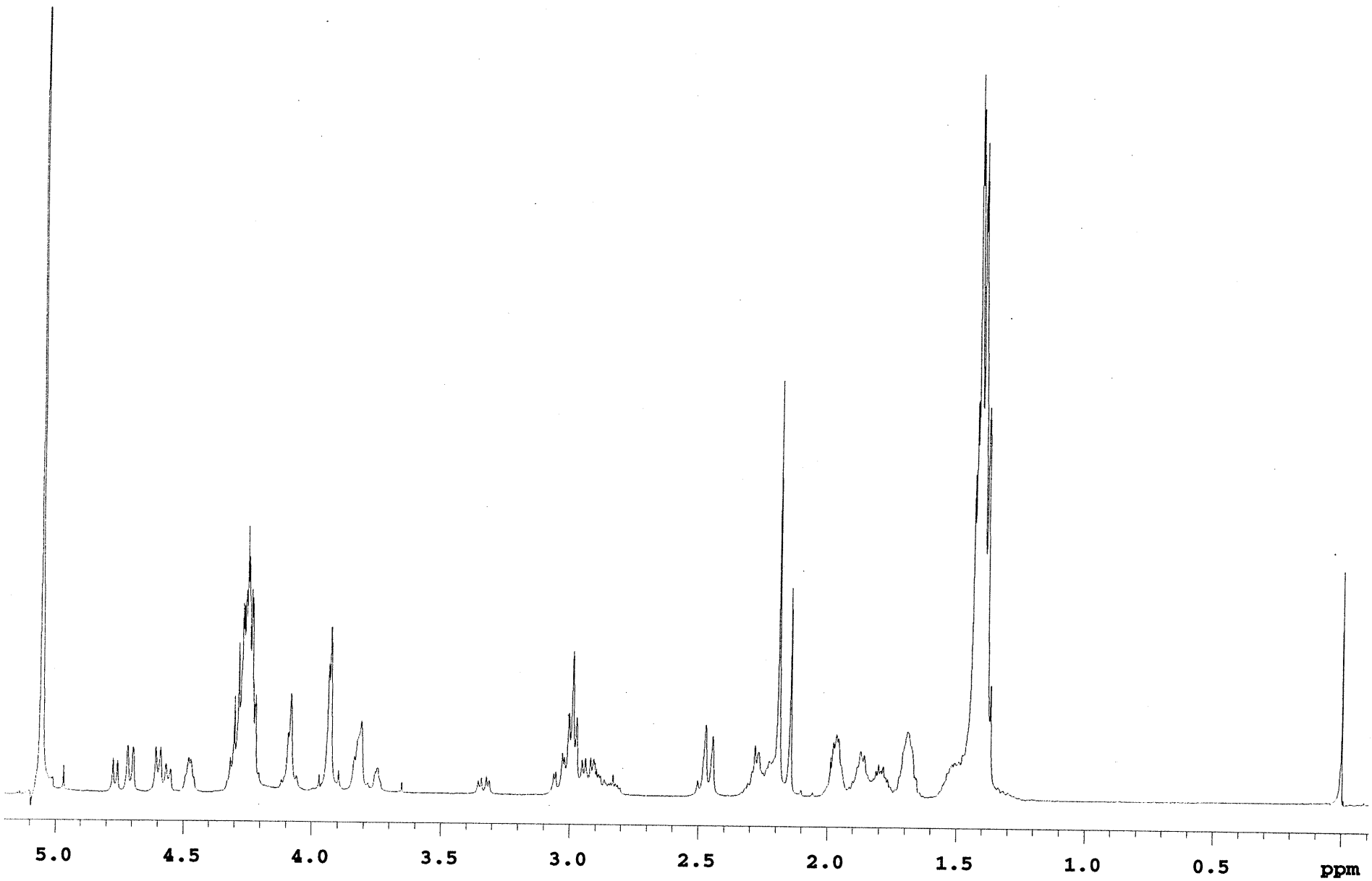


Fig. 4 $^1H$ NMR spectrum of Ac-$Hel_1$-AAAGAAAK-$NH_2$ in $D_2O$ at 2 °C.

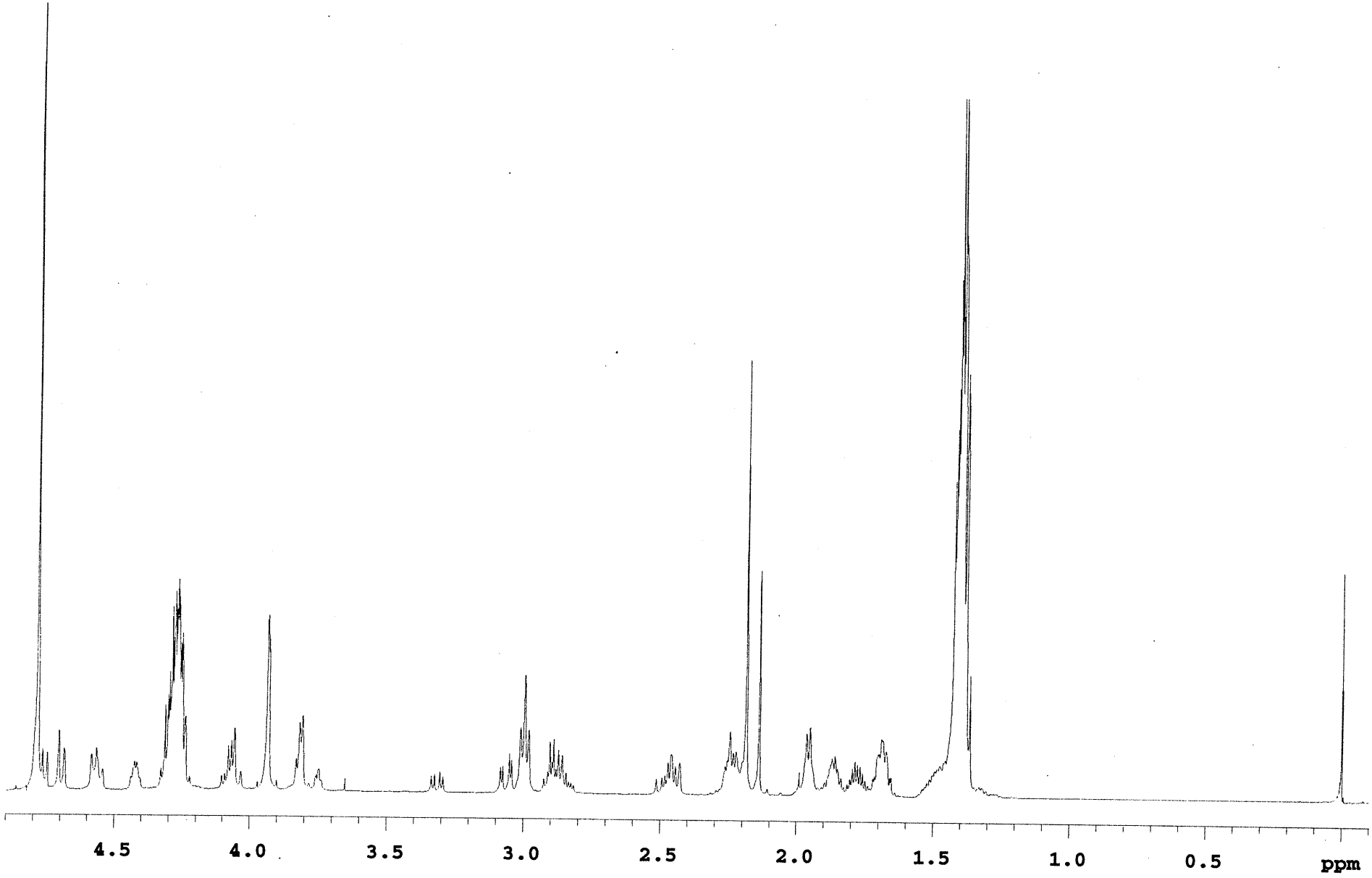


Fig. 5 $^{1}H$ NMR spectrum of Ac-$Hel_1$-AAAGAAAK-$NH_2$ in $D_2O$ at 25 °C

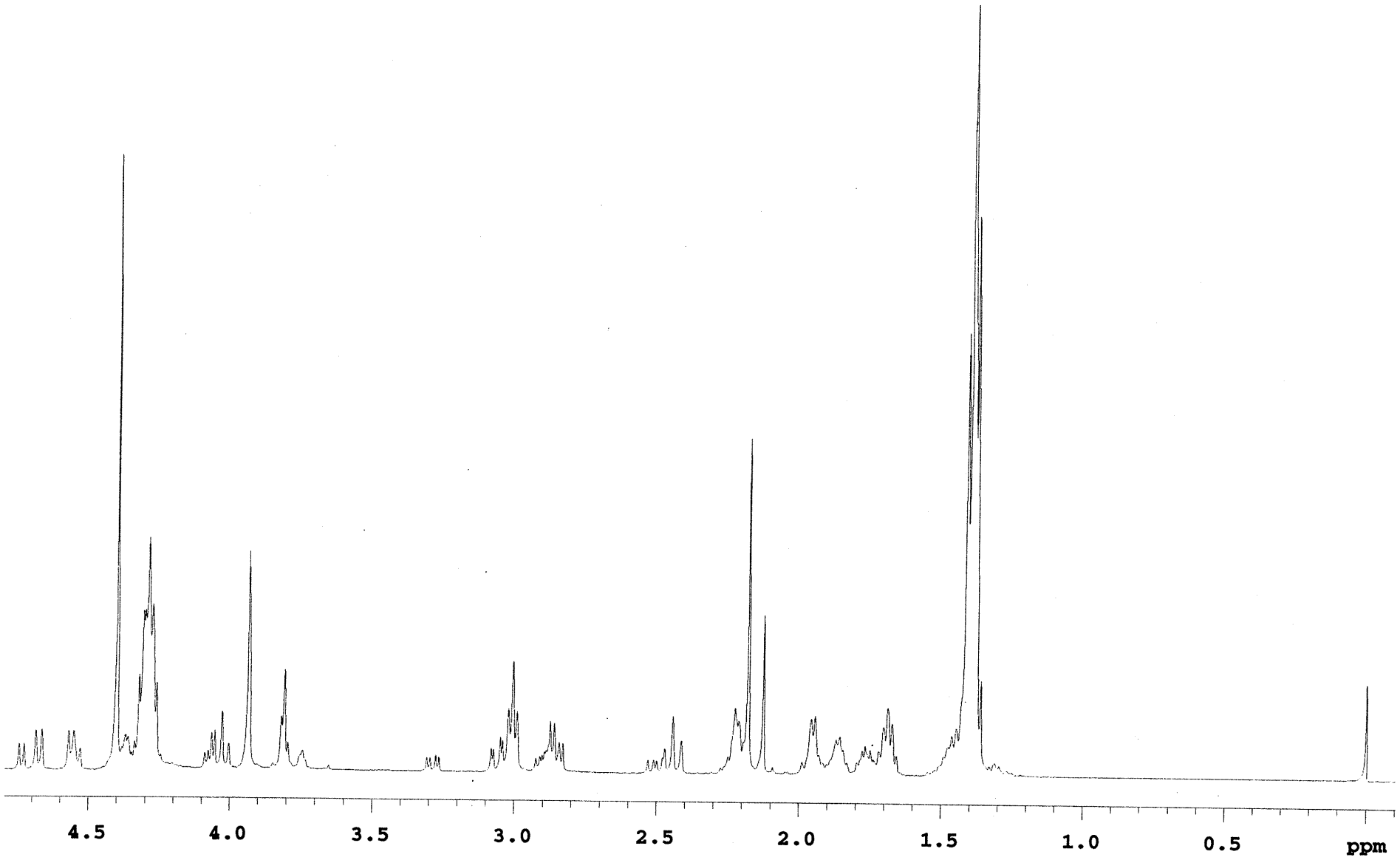


Fig. 6. $^{1}H$ NMR spectrum of Ac-$Hel_1$-AAAGAAAK-$NH_2$ in $D_2O$ at 60 °C.

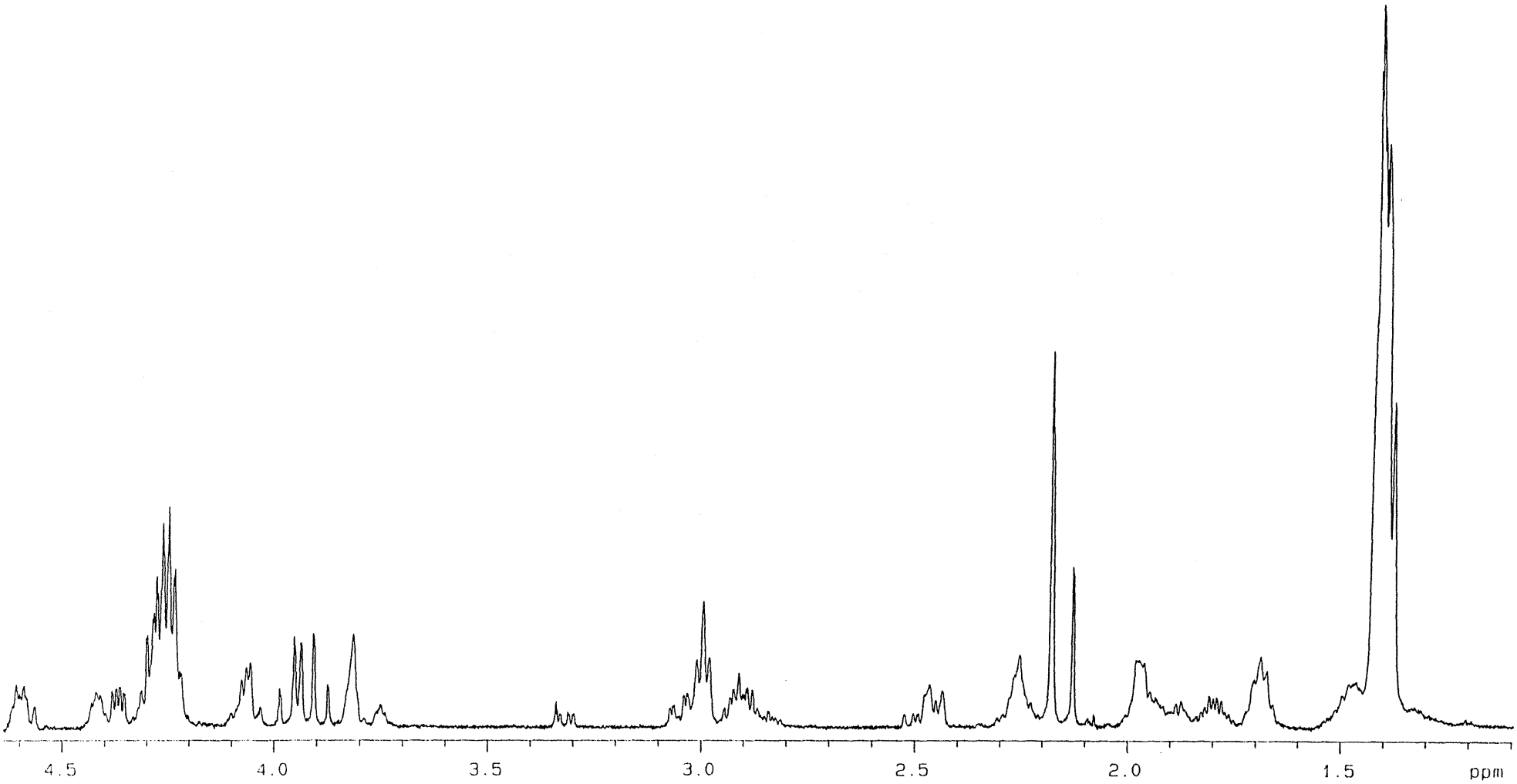


Template region of Ac-Hel$_1$-GAAAAAAK-NH$_2$ in $D_2O$ at 25 °C. The α-protons of the cs state glycine appear as a singlet at 3.94 ppm. Each α-proton of the t state glycine appears as a doublet, one centered at *ca.* 3.89 ppm, the other centered at *ca.* 3.97 ppm.